COMPONENT PART NOTICE

THIS PAPER IS A COMPONENT PART OF THE FOLLOWING COMPILATION REPORT:

TITLE: Special Course on Modern Theoretical and Experimental Approaches to Turbulent Flow Structure and its Modelling.

TO ORDER THE COMPLETE COMPILATION REPORT, USE AD-A198 872.

THE COMPONENT PART IS PROVIDED HERE TO ALLOW USERS ACCESS TO INDIVIDUALLY AUTHORED SECTIONS OF PROCEEDING, ANNALS, SYMPOSIA, ETC. HOWEVER, THE COMPONENT SHOULD BE CONSIDERED WITHIN THE CONTEXT OF THE OVERALL COMPILATION REPORT AND NOT AS A STAND-ALONE TECHNICAL REPORT.

THE FOLLOWING COMPONENT PART NUMBERS COMPRISE THE COMPILATION REPORT:

AD#: P005 794 thru AD-P005 800 AD#: P005 793

AD#: AD#:

AD#: AD#:

DTIC FORM 463 MAR 85

OPI: DTIC-TID

FUNDAMENTALS OF TURBULENCE FOR TURBULENCE MODELING AND SIMULATION

by

W.C.Reynolds
Department of Mechanical Engineering
Stanford University
Stanford, CA 93305
USA

1. FUNDAMENTALS OF FLUID MOTION

1.1 Introduction

This chapter presents a brief review of fluid flow fundamentals pertinent to turbulence. We expect them to be familiar to the reader, who may find our particular viewpoints, emphasis, and compact notation helpful and interesting.

We will make extensive use of the cartesian tensor summation convention, where repeated indices imply that the terms containing them must be summed over all possible coordinate indices. An overdot $\dot{()}$ will be used denote a partial derivative with respect to time, and a subscript after a comma will denote partial differentiation with respect to the indicated coordinate direction; for example,

$$\dot{\rho} = \frac{\partial \rho}{\partial t} \qquad P_{,i} = \frac{\partial P}{\partial x_i} \qquad u_{i,i} = u_{1,1} + u_{2,2} + u_{3,3} .$$

We will also use the isotropic tensors δ_{ij} and ϵ_{ijk} , defined by

$$\delta_{ij} = \begin{cases} 1 & \text{if } i = j \\ 0 & \text{otherwise.} \end{cases}$$

and

$$\epsilon_{ijk} = \begin{cases} 1 & \text{if } ijk \text{ is from the sequence } 123123 \\ -1 & \text{if } ijk \text{ is from the sequence } 321321 \\ 0 & \text{otherwise} \end{cases}$$

Various contractions will be used frequently, including

$$\delta_{ii} = 3 \qquad \epsilon_{ijk}\epsilon_{ipq} = \delta_{jp}\delta_{kq} - \delta_{jq}\delta_{kp}.$$

Tensors are entities that, in addition to being an array of elements identified by their subscripts, transform in a very special way when the coordinate system is transformed by rotation. A tensor that is totally unchanged by an arbitrary rotation of the coordinate system is called *isotropic*. Any second-order isotropic tensor must be a scalar times δ_{ij}, and any third-order isotropic tensor must be a scalar times ϵ_{ijk}. Moreover, any higher-order isotropic tensor must be expressible in terms of the various possible combinations of these two tensors, and hence they are fundamental building blocks in all sorts of physical modeling, including viscous flow and turbulence.

1.2 The basic equations

The basic equations are derived by application of basic principles to an elemental control volume (Fig. 1.2.1). The *conservation of mass* gives

$$\dot{\rho} + (\rho u_j)_{,j} = 0 \qquad (1.2.1)$$

where ρ is the fluid density, and u_j is the fluid velocity component in the j^{th} direction. This is also called the *continuity* equation.

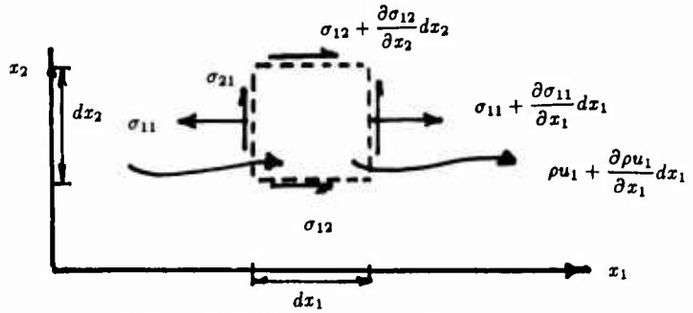

Figure 1.2.1 Control volume for basic equation derivation

The *momentum* equation is

$$(\dot{\rho u_i}) + (\rho u_j u_i)_{,j} = \sigma_{ji,j} + f_i \tag{1.2.2}$$

where σ_{ji} is the stress in the i^{th} direction on a control volume surface perpendicular to the j^{th} axis, and f_j is the body force (per unit volume) in the j^{th} direction.

The *conservation of energy* requires that

$$(\dot{\rho e_0}) + (\rho u_j e_0)_{,j} = (\sigma_{ji} u_i)_{,j} + f_i u_i - q_{j,j}. \tag{1.2.3}$$

Here $e_0 = e + \frac{1}{2}V^2$ is the total energy per unit mass, where e is the internal energy per unit mass and $V^2 = u_i u_i$, and q_j is the conduction heat *flux* (flow rate per unit area) in the j^{th} direction *outward* from the elemental control volume. The first term on the right represents the power input by the surface forces per unit volume, and the second that by the body forces.

The *entropy balance* is

$$(\dot{\rho s}) + (\rho u_j s)_{,j} = \varphi - (q_j/T)_{,j} \tag{1.2.4}$$

where s is the entropy per unit mass, T is the absolute temperature, and φ is the entropy production rate per unit volume. Here the term q_j/T represents the entropy flux associated with the heat flux q_j. The *second law of thermodynamics* requires that the entropy production be non-negative,

$$\varphi \geq 0. \tag{1.2.5}$$

These ideas are useful in assessing constitutive models for the stress tensor and heat flux vector, and in identifying the processes that produce entropy (*dissipate energy*) in viscous flows.

1.3 The stress tensor

The stress tensor σ_{ij} must be symmetric. This fact can be established by performing a *moment of momentum* analysis on the elemental control volume of Fig. 1.3.1. The torques of the stress terms are all of order $dx_1 dx_2$, and the moments of the momentum flows and body forces are all of higher order, hence $\sigma_{12} = \sigma_{21}$.

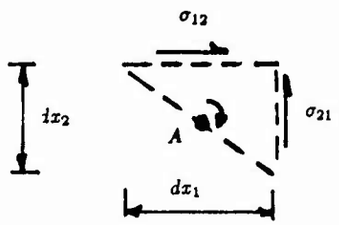

Figure 1.3.1 Control volume for stress tensor symmetry derivation

The tensor can be split into two parts:

$$\sigma_{ij} = -P\delta_{ij} + \tau_{ij}. \tag{1.3.1}$$

The P term represents the isotropic component of the (inward) normal stress; τ_{ij} is the deviations from this isotropic stress, attributed phenomenologically to *viscosity*. From a molecular point of view, σ_{ij} arises from molecular transport of momentum; the isotropic part P is determined by the average using the probability distribution for molecular velocities (e.g. Boltzmann), and τ_{ij} arises from anisotropy in the probability distribution.

1.4 Thermodynamic properties and concepts

The internal energy e reflects the randomly-oriented energy of molecular translation, rotation, vibration, and other microscopic energy modes (chemical bonds, etc.). In general, e depends upon the thermodynamic state (i.e. T and ρ), but for idealised gas and incompressible liquid models depends only on temperature. It is sometimes called the *thermal* energy, and is all too frequently confused with *heat* (q_j), which is the *transport* of energy by disordered molecular processes. The internal energy of an object can be increased by a transfer of energy as either heat or work, and the energy flowing as heat can come either from a source of internal energy or mechanical energy (kinetic, potential, or work). The internal energy is a thermodynamic property of matter, the heat transfer is not. The confusion between heat and internal energy is an infortunate remnant of the caloric theory of heat, but perhaps understandable since the theory was discarded only about a century ago.

The entropy can be thought of as a measure of the degree of randomness at the molecular level, and in modern thermodynamic treatments the temperature is interpreted as a measure of the sensitivity of this randomness to changes in energy at constant density. Orderly microscopic exchanges of energy (e.g. as work or as bulk kinetic energy) have no associated entropy transport. But heat, the microscopically disordered transport of energy, does carry entropy with it, and it may be shown that this entropy transfer flux is q_j/T. For more discussion of these important thermodynamic concepts from this viewpoint, see Reynolds and Perkins (1977).

It is usually assumed that as far as the thermodynamic properties are concerned the fluid is in a state of local equilibrium, and hence that the usual relations between thermodynamic properties are valid. Thus, the *Gibbs equation* is used to relate entropy changes to energy and density changes,

$$Tds = de + Pd(1/\rho). \tag{1.4.1}$$

The enthalpy h is defined as

$$h = e + P/\rho \tag{1.4.2}$$

and represents the sum of the convected internal energy and flow work associated with the transport of a unit mass of fluid across a control volume boundary. We emphasize that it is the *internal energy* that appears in the basic energy balance equation.

An alternative form of the energy equation is obtained using (1.3.1) in (1.2.3), moving the pressure term to the left hand side;

$$(\rho \dot{e}_0) + (\rho u_j h_0)_{,j} = (\tau_{ji} u_i)_{,j} + f_i u_i - q_{j,j}. \tag{1.4.3}$$

Here $h_0 = h + \frac{1}{2}V^2$ is the stagnation enthalpy. Note that the *enthalpy* appears as the *convected* energy per unit mass (internal energy e plus flow work P/ρ), but the *internal energy* e appears in the energy storage rate term. A common error is the use of enthalpy in *both* places.

1.5 Kinematics of motion

Any deformation rate $u_{i,j}$ can be decomposed into the sum of a strain rate S_{ij} and a rotation rate Ω_{ij},

$$u_{i,j} = \frac{1}{2}(u_{i,j} + u_{j,i}) + \frac{1}{2}(u_{i,j} - u_{j,i}) = S_{ij} + \Omega_{ij}. \tag{1.5.1}$$

Note that the strain rate is a symmetric tensor and the rotation rate is antisymmetric. They play quite different roles in fluid mechanics, particularly in turbulence, and for this reason we prefer forms of the equations that make their presence or absence very clear.

1.6 Mechanical and thermal energy equations

The fundamental equations may be combined to derive an equation describing the transport of macroscopic mechanical energy and another describing the transport of internal energy. The *mechanical energy equation* is derived by contracting the momentum equation with the velocity; multiplying $(1.2.2)_i$ by u_i,

$$(\rho \frac{1}{2}\dot{V^2}) + (\rho u_j \frac{1}{2}V^2)_{,j} = \sigma_{ji,j}\, u_i + f_i u_i. \tag{1.6.1}$$

The right hand side may be written as

$$(\sigma_{ij} u_i)_{,j} - \sigma_{ij} u_{i,j} + f_i u_i.$$

Then, using (1.3.1) to split the stress tensor and (1.5.1) in place of velocity gradients, and noting that $\tau_{ij}\Omega_{ij} = 0$ since τ_{ij} is symmetric and Ω_{ij} is antisymmetric (sum over both repeated indices is implied), (1.6.1) can be rewritten as

$$\dot{(\rho\frac{1}{2}V^2)} + (\rho u_j \frac{1}{2}V^2)_{,j} = PS_{jj} - (Pu_j)_{,j} + f_i u_i + (\tau_{ij}u_i)_{,j} - (\tau_{ij}S_{ij}). \tag{1.6.2}$$

The sum on the right represents the *input* of macroscopic mechanical energy to the control volume, which shows up as an increase in the kinetic energy of the flow. Two of these terms appear as power inputs in the thermal energy equation (1.6.4) but with opposite sign, and hence these terms represent exchanges between thermal and mechanical energy. The first is PS_{jj}, which is the rate of energy transfer, per unit volume, from thermal energy to mechanical energy due to expansion of the fluid. The second is $\tau_{ij}S_{ij}$, which represents the transfer of mechanical energy to thermal energy by viscous forces. This is the only viscous term involved in the entropy production equation (1.7.3), and hence this is the only viscous term properly termed *dissipation*. Since

$$\int (\tau_{ij}u_i)_{,j}\, d^3\mathbf{x} = 0 \tag{1.6.3}$$

if the integral is taken over a volume where either the velocity or stress is zero on the boundaries, this viscous term has no global effect; it represents *reversible* viscous power input to the control volume from surrounding fluid. The term containing f_i is the power input from body forces, and the $(Pu_j)_{,j}$ term represents power output by *flow work*.

The *thermal energy equation* is obtained by subtracting the mechanical energy equation (1.6.2) from the total energy equation (1.2.3), and is

$$\dot{(\rho e)} + (\rho u_j e)_{,j} = -PS_{jj} + (\tau_{ij}S_{ij}) - q_{j,j}\,. \tag{1.6.4}$$

Here PS_{jj} represents the power output from thermal energy due to expansion of the fluid, $\tau_{ij}S_{ij}$ is the power input to the thermal energy due to irreversible viscous effects, and $q_{j,j}$ is the net power output due to heat conduction, all per unit volume.

Note that the enthalpy, which appeared in the alternate form of the *total* energy equation (1.4.3), does *not* appear in the thermal energy equation. We have derived the thermal energy equation correctly from first principles. One must be wary in reading literature where the thermal energy equation is developed from a "heat balance", because there is no such principle as the conservation of heat.

1.7 Irreversibility rate equation

Using the conservation of mass equation (1.2.1) in the Gibbs equation (1.4.1),

$$\rho T Ds = \rho De + PS_{ii} \tag{1.7.1}$$

where D denotes the substantial derivative

$$D() = \dot{()} + u_j()_{,j}\,. \tag{1.7.2}$$

Using the thermal energy equation (1.6.4) and the entropy balance (1.2.4), this yields an expression for the *irreversibility rate*,

$$T\varphi = -\frac{1}{T}q_j T_{,j} + \tau_{ij}S_{ij} \geq 0. \tag{1.7.3}$$

This clearly identifies the viscous dissipation term as discussed above, and provides a neat framework for evaluation of consitutive models for the heat flux or viscous stresses.

1.8 Constitutive equations

The theory of linear algebra is extremely helpful in developing constitutive models for the heat flux and viscous stresses, and also for developing turbulence models. We will use these ideas to review the constitutive equations so as to set the stage for later use of these ideas in developing turbulence models.

The most general vector f_i that is a function of *only one other* vector v_i is

$$f_i = Cv_i \tag{1.8.1}$$

where the coefficient C can be a function of scalars, including the invariant of the vector (its magnitude $v_k v_k$). Higher-order terms, such as $v_i v_k v_k$, need not be added since they are represented by allowing the coefficient to depend on the invariant of $\mathbf{v}$. Thus, if one assumes that the heat flux vector q_i is a function of the temperature gradient vector $T_{,i}$, the most general form is the familiar Fourier heat conduction law,

$$q_j = -kT_{,j} \tag{1.8.2}$$

where k is the *thermal conductivity*, which depends to first approximation on the temperature and may, in higher approximations, also depend on the scalar $T_{,k}T_{,k}$. It is generally believed that (1.8.2) describes heat conduction in fluids, except perhaps in regions of very strong temperature gradient such shock waves or combustion fronts.

The most general tensor a_{ij} that is a function of *only one other* tensor b_{ij} is, in three dimensions,

$$a_{ij} = A\delta_{ij} + Bb_{ij} + Cb_{ij}^2 \tag{1.8.3}$$

where $b_{ij}^2 = b_{ik}b_{kj}$. The coefficients A, B and C may depend on relevant scalars, including the three scalar invariants of the tensor $\mathbf{b}$. Higher-order terms such as $b_{ij}^3 = b_{ik}^2 b_{kj}$ need not be added since, by the Cayley-Hamilton theorem, they can be expressed in terms of lower-order terms and the invariants of $\mathbf{b}$ and hence are already included in (1.8.3). Therefore, if it is assumed that the viscous stress tensor τ_{ij} is a function of the local strain-rate tensor S_{ij}, this functional dependence must be of the form

$$\tau_{ij} = A\delta_{ij} + BS_{ij} + CS_{ij}^2 \tag{1.8.4}$$

where the coefficients may depend on scalars, such as temperature, density, or the invariants of $\mathbf{S}$. This is called the *Stokes* model for viscous stresses.

The rms strain-rate $S = (S_{ij}S_{ji})^{1/2}$ is a reciprocal time scale for the fluid deformation. If this time is long compared to molecular collision times, then the strain is considered weak and only linear terms in (1.8.4) are used. This leads to

$$\tau_{ij} = A\delta_{ij} + BS_{ij} \tag{1.8.5}$$

where A can depend at most linearly on the invariants of $\mathbf{S}$, and B must be independent of $\mathbf{S}$. If it further assumed that $P = -\frac{1}{3}\sigma_{ii}$, then by (1.3.1)

$$\tau_{kk} = 0 = 3A + BS_{kk}$$

so

$$A = -\frac{1}{3}BS_{kk}. \tag{1.8.6}$$

For a simple shearing flow where the only non-zero strain-rate elements are

$$S_{12} = S_{21} = \frac{1}{2}\frac{\partial u_1}{\partial x_2}$$

one defines the fluid viscosity μ by

$$\tau_{12} = 2\mu S_{12} \tag{1.8.7}$$

from which, using (1.8.5), it follows that $B = 2\mu$. The resulting *Newtonian constitutive equation* is

$$\tau_{ij} = 2\mu S_{ij} - \frac{2}{3}\mu S_{kk}\delta_{ij}. \tag{1.8.8}$$

Note that the Newtonian constitutive equation assumes *only* that the viscous stress tensor is a trace-free linear function of the local strain rate; this assumption is believed to be quite adequate for many continuum fluid flows. The model fails in strong shock waves (normal stresses are incorrect) and in flow of polymers (rotation rates are also important).

Using (1.8.2) and (1.8.8) in (1.7.3), the irreversibility rate becomes

$$T\varphi = \frac{k}{T}T_{,i}\,T_{,i} + 2\mu(S_{ij}S_{ij} - \frac{1}{3}S_{ii}S_{kk}) \geq 0. \tag{1.8.9}$$

It is clear that the heat flux term is positive-definite. It is left as an exercise to demonstrate that the strain-rate term is also positive-definite (Hint: evaluate in the principal coordinates of S_{ij} by expressing the diagonal elements as the components of a vector in polar coordinates).

1.9 Vorticity

Vorticity is one of the most fundamental concepts in fluid mechanics, and probably *the* most important concept in turbulence. The vorticity vector $\underline{\omega}$ is defined by

$$\omega_i = \epsilon_{ijk}u_{k,j}. \tag{1.9.1}$$

Note that $\epsilon_{ijk}u_{k,ji}=0$ and hence the vorticity, by definition, is *divergence free*,

$$\omega_{i,i}=0. \tag{1.9.2}$$

By the definitions, the vorticity is related to the rotation rate,

$$\omega_i=\epsilon_{ijk}\Omega_{kj}. \tag{1.9.3}$$

Taking $\epsilon_{pqi}\times(1.9.3)_i$, one finds

$$\Omega_{qp}=\frac{1}{2}\epsilon_{pqi}\omega_i. \tag{1.9.4}$$

The vorticity field can be thought of as contributing to the velocity field. Forming $\epsilon_{pqi}\times(1.9.1)_{i,q}$, one finds

$$\epsilon_{pqi}\omega_{i,q}=\epsilon_{pqi}\epsilon_{ijk}u_{k,jq}=u_{q,pq}-u_{p,qq}$$

or

$$u_{i,kk}=-\epsilon_{ikj}\omega_{j,k}+(u_{k,k})_{,i}. \tag{1.9.5}$$

This is a *Poisson equation* for the velocity, analogus to the equation for temperature in a heat conducting medium with distributed sources. Eqn. (1.9.5) displays two "sources" of velocity, namely vorticity (more specifically vorticity *gradients*) and flow divergence (expansion or compression). In addition to the velocity generated by these sources, one can also have an additional component of velocity satisfying the *Laplace* equation $u_{i,kk}=0$. From (1.9.5) we see that this component could be thought of as arising from *uniform vorticity* (a solid-body rotation) and *uniform irrotational expansion*, of which irrotational flow at constant density is a special case.

The part of the velocity field due to the vorticity gradients may be found using the general solution to the Poisson equation; at any instant in time, this solution is

$$u_i(\mathbf{x})=-\int G(\mathbf{x},\mathbf{x}')\epsilon_{ikj}\omega_{j,k}(\mathbf{x}')d^3\mathbf{x}' \tag{1.9.6}$$

where $G(\mathbf{x},\mathbf{x}')$ is the *Green's function* for the Poisson solution in the flow domain, and $d^3\mathbf{x}'$ represents an element of volume for the interation over the flow domain. The Green's function for an infinite domain is

$$G(\mathbf{x},\mathbf{x}')=\frac{-1}{4\pi\sqrt{(x_n-x_n')(x_n-x_n')}}. \tag{1.9.7}$$

Using this Green's function in (1.9.6), and integrating by parts to transfer the k differentiation from the vorticity to the Green's function, one finds

$$u_i(\mathbf{x})=\int\epsilon_{ijk}\frac{(x_k-x_k')}{4\pi[(x_n-x_n')(x_n-x_n')]^{3/2}}\omega_j d^3\mathbf{x}'. \tag{1.9.8}$$

This is called the *Biot-Savart* equation. It gives that portion of the velocity field arising from vorticity, for an *infinite* flow domain. Computational methods in which markers track the motion of vorticity-bearing fluid use the Biot-Savart equation to compute the velocity field; this is an efficient calculation if the vorticity is highly concentrated and most of the fluid has negligible vorticity, and there are many interesting problems in turbulence that can be addressed in this manner.

We emphasize that all of the features of vorticity discussed thus far are *kinematic* in nature, and apply in either compressible or incompressible flows. In the next section we will adress the *dynamics* of the vorticity.

1.10 Vorticity dynamics

Using the continuity equation (1.2.1) and the stress tensor split (1.3.1), the momentum equation (1.2.2) can be written as

$$\dot{u_k}+u_q u_{k,q}=\frac{1}{\rho}(\tau_{kq,q}-P_{,k}+f_k). \tag{1.10.1}$$

Taking $\epsilon_{ijk}\times$ $(1.10.1)_{k,j}$ one obtains

$$\dot{\omega_i}+u_j\omega_{i,j}=-\epsilon_{ijk}u_{q,j}\,u_{k,q}+\epsilon_{ijk}\left[\frac{1}{\rho}(\tau_{kq,q}-P_{,k}+f_k)\right]_{,j}.$$

Using (1.5.1) and (1.9.4), the first term on the right is exactly

$$\omega_q S_{iq}-S_{qq}\omega_i.$$

The pressure term can be expanded into two terms, one of which vanishes, and the vorticity equation becomes

$$\dot{\omega}_i + u_j \omega_{i,j} = \omega_j S_{ij} - S_{jj}\omega_i + \epsilon_{ijk}\left[\left(\frac{1}{\rho}\tau_{kq,q}\right)_{,j} + \frac{1}{\rho^2} P_{,k}\,\rho_{,j} + \left(\frac{f_k}{\rho}\right)_{,j}\right] . \tag{1.10.2}$$

Note that the left-hand side of (1.10.2) represents the rate of change of vorticity following a fluid particle. Thus, the terms on the right display the processes that can give rise to changes in vorticity of a fluid particle. The first term represents the straining of vortex filaments, and is a crucial term in turbulence; in a two-dimensional flow, this strain is always in planes perpendicular to the vorticity, and hence there is no vortex stretching in two-dimensional flow. The second term shows that fluid compression ($S_{kk} < 0$) tends to amplify the vorticity, and expansion to attenuate it. The term containing τ_{kq} represents viscous effects, including diffusion. The term containing pressure gradients and density gradients shows that these may combine to act as a source for vorticity, if these gradient vectors have a non-zero cross product; this term is important in the atmosphere. Body force gradients can also generate vorticity; but body forces are often *conservative*, i.e. of the form

$$f_k = \rho\phi_{,k} \tag{1.10.3}$$

where ϕ is a scalar potential, and (1.10.2) shows that such forces do not generate vorticity.

In a Newtonian flow where $\rho = \rho(t)$, μ is constant, and $f_k = \rho\phi_{,k}$, the vorticity equation becomes

$$\dot{\omega}_i + u_j \omega_{i,j} = \omega_j S_{ij} - \omega_i S_{jj} + \nu\omega_{i,jj} . \tag{1.10.4}$$

This is the form to which we will refer most often in our studies of turbulence; it emphasizes the interaction between strain-rate and vorticity that is so important in turbulence.

One usually sees the vorticity equation with the first term on the right in (1.10.4) replaced using an identity derived from (1.5.1) and (1.9.4),

$$\omega_j S_{ij} = \omega_j u_{i,j} . \tag{1.10.5}$$

We prefer (1.10.4) because it makes the interaction between vorticity and strain-rate very clear.

1.11 Vortex lines and tubes

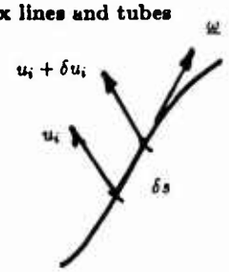

Figure 1.11.1 Velocities along a vortex line

A vortex line is a line everywhere tangent to the $\underline{\omega}$ vector. Along a vortex line (see Figure 1.11.1)

$$\frac{\delta x_i}{\delta s} = \frac{\omega_i}{|\underline{\omega}|} . \tag{1.11.1}$$

Vortex lines move as the fluid moves. For *inviscid, incompressible flow*, the vortex lines move with the fluid. This fact is extremely helpful in understanding fluid flows in general and turbulence in particular, and forms the basis for an important class of numerical methods for simulating turbulent flow.

We will now prove this important fact about vortex lines. Let $\tilde{\underline{\omega}}$ be the vorticity at the center of an elemental segment δs of a line marked in the fluid along a vortex line at time t. The rate of change of the vorticity following the fluid particle attached to the center of this line given by (1.10.4). Neglecting the viscous term, and assuming constant density (so that $S_{kk} = 0$), and using (1.10.5), the rate of change of the vorticity of this fluid particle is

$$\dot{\tilde{\omega}}_i = \tilde{\omega}_j u_{i,j} . \tag{1.11.2}$$

The right hand side of (1.11.2) is evaluated at time t using (1.11.1) to express δx_i in terms of δs, yielding

$$\dot{\tilde{\omega}}_i = |\tilde{\underline{\omega}}| \frac{\delta u_i}{\delta s} . \tag{1.11.3}$$

Since each end of the line moves with its own velocity,

$$\frac{d(\delta x_i)}{dt} = \delta u_i. \tag{1.11.4}$$

We now examine the changes in $\delta x_1/\omega_1$:

$$\frac{d}{dt}\left(\frac{\delta x_1}{\tilde{\omega}_1}\right) = \frac{1}{\tilde{\omega}_1}\frac{d(\delta x_1)}{dt} - \frac{\delta x_1}{\tilde{\omega}^2}\frac{d\tilde{\omega}_1}{dt}\ . \tag{1.11.5}$$

Using (1.11.4) for the first term on the right and (1.11.3) for the second, the right hand side is zero, and hence $\delta x_1/\tilde{\omega}_1$ is constant in time. The same is true for the other two components. Hence, if the line was originally a vortex line, it will remain a vortex line, as we have claimed. Moreover, since $\delta x_1 = \tilde{\omega}_1 C$, it follows that $|\underline{\omega}|$ will be proportional to the line length.

We can form a vortex tube from a set of nearby vortex lines. In inviscid, incompressible flow, this tube will move with the fluid, and can be stretched by strain along its length. This strain will intensify the vorticity in the tube. Since the fluid is incompressible, and the tube is imbedded in the fluid, stretching the tube reduces its diameter. The increase in vorticity can be though of in terms of the increased rotational rate necessary to maintain conserved angular momentum as the tube decreases in diameter. These processes of vortex convection and stretching by the flow are central in turbulence.

It is left as an exericise to show that, in inviscid, *compressible* flow, lines everywhere tangent to $\underline{\omega}/\rho$ move with the fluid. This fact may be useful in simulations of compressible turbulence.

2. TURBULENCE EQUATIONS

2.1 Averaging concepts

Different kinds of averaging procedures are appropriate for different situations. In situations that are statistically steady, the *time average* is useful. Denoting a random field by $f(\mathbf{x},t)$, its time average is

$$\overline{f}(\mathbf{x}) = \lim_{T\to\infty}\frac{1}{T}\int_0^T f(\mathbf{x},t)dt. \tag{2.1.1}$$

The time average can not be used in fields that are statistically developing in time. But if the field is statistically *homogeneous*, i.e. statistically the same at all space points, then a *volume average* can be used,

$$\overline{f}(t) = \lim_{L\to\infty}\frac{1}{L^3}\int_0^L\int_0^L\int_0^L f(\mathbf{x},t)d^3\mathbf{x}. \tag{2.1.2}$$

If the field is not statistically steady or homogeneous in space, but is homogeneous on planes or along lines, averages on the planes or lines can be used. But if the field is not statistically the same in time or any space dimension, one has to resort to the concept of *ensemble averaging*, i.e. averaging over a large set of (usually hypothetical) similiar experiments:

$$\overline{f}(\mathbf{x},t) = \lim_{N\to\infty}\frac{1}{N}\sum_{n=1}^{N} f_n(\mathbf{x},t). \tag{2.1.3}$$

One must always be careful to choose an averaging concept appropriate to the situation. It will be assumed that an averaging process has been chosen that commutes with differentiations with respect to both time and space; the ensemble average always has this property.

2.2 Turbulence decomposition

Each variable in a random field is represented as the sum of its average and its fluctuation,

$$f = \overline{f} + f'. \tag{2.2.1}$$

The averaging processes defined above are all such that

$$\overline{f'} = 0. \tag{2.2.2}$$

It follows that

$$\overline{\overline{f}\,\overline{h}} = \overline{f}\,\overline{h} \tag{2.2.3}$$

and

$$\overline{\overline{f}h'} = 0. \tag{2.2.4}$$

In compressible flows, mass-weighted averaging is often employed. The methods for doing this averaging are simple extensions of those given above.

Most turbulence literature concerns incompressible flows. However, there is a class of compressible flows that can be handled as a very modest extension of incompressible flows, namely flows where $\rho = \rho(t)$ (*uniform density flows*). Many practical flows fall in this class, including flow in an internal combustion engine cylinder. The equations for uniform density flow are much simpler than those of full compressible flow, and so in the interest of simplicity much of what follows will be limited to uniform density flows with constant viscosity μ.

2.3 Governing equations

If $\rho = \rho(t)$, the continuity equation reduces to

$$\dot{\rho} + \rho u_{i,i} = 0. \tag{2.3.1}$$

We will write the turbulence decomposition with capital letters for mean quantities and lower case letters for the fluctuations,

$$p = P + p' \tag{2.3.2a}$$

$$u_i = U_i + u_i'. \tag{2.3.2b}$$

Inserting these decompositions into the continuity equation (2.3.1), and averaging, we obtain the *mean continuity equation*

$$\dot{\rho} + \rho U_{i,i} = 0. \tag{2.3.3}$$

Subtracting this result from (2.3.1) we obtain the *fluctuating continuity equation*,

$$u_{i,i}' = 0 \tag{2.3.4}.$$

Note that, for *uniform denity flow*, the *fluctuation* velocity field is divergence-free, as would be the mean velocity field if the flow were incompressible.

For uniform density flow with μ =constant and $f_k = 0$, the momentum equation (1.2.2) reduces to

$$\dot{u}_i + u_j u_{i,j} = -\frac{1}{\rho} p_{,i} + \nu u_{i,jj}. \tag{2.3.5}$$

Introducing the turbulence decomposition, averaging, and making use of (2.3.4), the *mean momentum equation* is found as

$$\dot{U}_i + U_j U_{i,j} = -\frac{1}{\rho} P_{,i} + \nu U_{i,jj} - R_{ij,j} \tag{2.3.6}$$

where

$$R_{ij} = \overline{u_i' u_j'}. \tag{2.3.7}$$

The quantity $-\rho R_{ij}$ appears in (2.3.6) like a stress, and so is called the *Reynolds stress* after O. Reynolds, who introduced the basic decomposition.

Equations (2.3.3) and (2.3.6) would permit calculation of the mean density and velocity field *if* the Reynolds stresses were all known. Since they are not known, we have a closure problem, which can be addressed, but not solved, by further development of the equations for the Reynolds stresses.

An alternative way of thinking about the turbulence "forces" has some physical appeal. From (1.9.1) it follows that

$$\overline{\omega_i' u_p'} = \epsilon_{ijk} \overline{u_{k,j}' u_p'} \tag{2.3.8}$$

Multiplying by ϵ_{qip}

$$\epsilon_{qip} \overline{\omega_i' u_p'} = \epsilon_{qip} \epsilon_{ijk} \overline{u_{k,j}' u_p'} = (\delta_{pj}\delta_{qk} - \delta_{pk}\delta_{qj}) \overline{u_{k,j}' u_p'} = \overline{u_{q,p}' u_p'} - \overline{u_{p,q}' u_p'}.$$

Using (2.3.4), this produces

$$\epsilon_{qip} \overline{\omega_i' u_p'} = (\overline{u_q' u_p'})_{,p} - \frac{1}{2} (\overline{u_p' u_p'})_{,q}$$

or equivalently

$$(\overline{u_i' u_j'})_{,j} = \frac{1}{2} (\overline{u_j' u_j'})_{,i} + \epsilon_{ijk} \overline{\omega_j' u_k'}. \tag{2.3.9}$$

We define

$$P^* = P + \frac{1}{2}\rho q^2 \tag{2.3.10}$$

where the mean square fluctuation velocity is

$$q^2 = \overline{u_i' u_i'}. \tag{2.3.11}$$

It is convenient to denote the *mean-convection substantial derivative* by

$$\overline{D}() = \dot{()} + U_j()_{,j}. \tag{2.3.12}$$

Then, using (2.3.9) in (2.3.6), the mean momentum equation becomes

$$\overline{D}U_i = -\frac{1}{\rho}P^*_{,i} + \nu U_{i,jj} - \epsilon_{ijk}\overline{\omega_j' u_k'}. \tag{2.3.13}$$

In this alternative representation the turbulence provides a contribution to the *normal* stress in P^* and a *turbulent body force*, but no shear stress. The potential of this alternative view of turbulence forces remains to be investigated.

2.4.1 Mean vorticity equation

The turbulence decomposition of the vorticity is

$$\omega_i = \Omega_i + \omega_i'. \tag{2.4.1}$$

The mean strain rate and rotation rate are denoted by S_{ij} and Ω_{ij}, respectively, and the fluctuation strain rate by s_{ij}'. By continuity for uniform density flow, $s_{ii}' = 0$. Introducing the turbulence decomposition into (1.10.4), and averaging, the *mean vorticity equation* is found to be

$$\overline{D}\Omega_i = \Omega_j S_{ij} - \Omega_i S_{jj} + \nu\Omega_{i,jj} - (\overline{\omega_i' u_j'})_{,j} + \overline{\omega_j' s_{ij}'}. \tag{2.4.2}$$

Note the appearance of the turbulence body force term $\overline{\omega_i' u_j'}$ in the equation.

2.5 Turbulent fluctuation equations

The fluctuating continuity equation is (2.3.4). Subtraction of the mean momentum equation (2.3.6) from the full equation (2.3.5) gives the *fluctuating momentum equation*,

$$\overline{D}u_i' = -u_j' U_{i,j} - (u_i' u_j' - \overline{u_i' u_j'})_{,j} - \frac{1}{\rho}p'_{,i} + \nu u_{i,jj}'. \tag{2.5.1}$$

Subtraction of (2.4.2) from (1.10.4) gives the *fluctuating vorticity equation*

$$\overline{D}\omega_i' = +\omega_j' S_{ij} - \omega_i' S_{jj} + \Omega_j s_{ij}'$$

$$-u_j'\Omega_{i,j} - (u_j'\omega_i' - \overline{u_j'\omega_i'})_{,j} + (\omega_j' s_{ij}' - \overline{\omega_j' s_{ij}'}) + \nu\omega_{i,jj}'. \tag{2.5.2}$$

By taking $(2.5.1)_{,i}$ one obtains an equation for the fluctuating pressure,

$$\frac{1}{\rho}p'_{,ii} = -2u_{i,j}' U_{j,i} - (u_{i,j}' u_{j,i}' - \overline{u_{i,j}' u_{j,i}'}) \tag{2.5.3}$$

These equations are useful for deriving equations relating statistical properties of the turbulence and in the study of the dynamics of turbulent fluctuations.

2.6 Kinetic energy equations

The transport equation for the *turbulent kinetic energy*

$$\frac{1}{2}q^2 = \frac{1}{2}\overline{u_i' u_i'} \tag{2.6.1}$$

is derived by multiplying $(2.5.1)_i$ by u_i' and averaging. After some rearranging, one obtains

$$\overline{D}(\frac{1}{2}q^2) = P - \mathcal{D} - J_{j,j}. \tag{2.6.2}$$

Here

$$P = -\overline{u_i' u_j'} S_{ij} \tag{2.6.3}$$

is the rate of turbulent energy *production*,

$$\mathcal{D} = \nu\overline{u'_{i,j}u'_{i,j}} \tag{2.6.4}$$

is the (*homogeneous*) rate of turbulent energy dissipation, and

$$J_j = \frac{1}{\rho}\overline{p'u'_j} + \frac{1}{2}\overline{u'_j u'_i u'_i} - \nu(\frac{1}{2}q^2)_{,j} \tag{2.6.5}$$

is the *turbulent kinetic energy flux* in the j^{th} direction.

Note that $\mathcal{P}$ involves the product of turbulent stresses and mean strain rates, and that the mean rotation rate does not appear explicitly in the turbulent kinetic energy equation (though it may influence the turbulent kinetic energy by altering terms in the equation). $\mathcal{P}$ arises from the stretching of the tangle of vortex filaments that make up the turbulence by the mean deformation. $\mathcal{P}$ is almost always found to be positive, although there are situations in which it is negative.

Since the source of turbulent kinetic energy is the mean flow, the production term should appear with opposite sign in the evolution equation of the mean kinetic energy. Multiplying (2.3.6)$_i$ by U_i, and rearranging, the *mean kinetic energy equation* is

$$\overline{D}(\frac{1}{2}U_iU_i) = -(\frac{1}{\rho}PU_i)_{,i} + \frac{1}{\rho}PS_{ii} - 2\nu S_{ij}S_{ij} + 2\nu(U_iS_{ij})_{,j} - \mathcal{P} - (U_i\overline{u'_iu'_j})_{,j} \tag{2.6.6}$$

Indeed, $-\mathcal{P}$ does appear on the right, indicating a drain from the mean kinetic energy. The two pressure terms represent the power associated with flow work and the power transfer from internal energy due to expansion of the flow. The first viscous term is the rate of dissipation of mean kinetic energy by viscous effects (see 1.8.9), and the second is the reversible viscous power transfer. The last term, which integrates to zero over a large volume of flow bounded by non-turbulent fluid, represents an internally conservative transfer of mean kinetic energy within this volume.

We have been careful to call $\mathcal{D}$ the *homogeneous* dissipation, because (as shown in the next chapter) only in homogeneous turbulence does it represent the true rate of energy dissipation. From (1.8.9) the true dissipation rate is

$$\varepsilon = \nu\overline{\tau'_{ij}s'_{ij}} = 2\nu\overline{s'_{ij}s'_{ij}} = \nu\overline{u'_{i,j}\,(u'_{i,j}+u'_{j,i})}. \tag{2.6.7}$$

The right hand side of the turbulent kinetic energy equation can be modified to replace $\mathcal{D}$ by ε, with a concurrent modification in the definition of the flux. This is left as an exercise.

2.7 Reynolds stress evolution equation

The evolution equation for R_{ij} is derived by multiplying the i^{th} fluctuation momentum equation by u'_j and the j^{th} equation by u'_i, adding the resulting equations, and averaging. The result may be written as

$$\overline{D}R_{ij} = P_{ij} + O_{ij} + T_{ij} - D_{ij} - J_{ijk,k}\,. \tag{2.7.1}$$

Here the *production* term

$$P_{ij} = -(R_{ik}S_{kj} + R_{jk}S_{ki}) \tag{2.7.2}$$

is the source of Reynolds stress; note that its trace is

$$P_{ii} = 2\mathcal{P}. \tag{2.7.3}$$

The *kinematic rotation* term

$$O_{ij} = R_{ik}\Omega_{kj} + R_{jk}\Omega_{ki} \tag{2.7.4}$$

is trace free ($O_{ii} = 0$) and hence this term does *not* contribute to production of new turbulence energy, but simply rotates the turbulence structure. The *pressure strain* term

$$T_{ij} = +\frac{1}{\rho}\overline{p'(u'_{i,j}+u'_{j,i})} \tag{2.7.5}$$

is also trace-free and provides intercomponent energy transfer. The *dissipation* term

$$D_{ij} = 2\nu\overline{u'_{i,k}\,u'_{j,k}} \tag{2.7.6}$$

has a trace

$$D_{ij} = 2\mathcal{D}. \tag{2.7.7}$$

Finally, the *flux* of R_{ij} in the k^{th} direction is

$$J_{ijk} = \frac{1}{\rho}(\overline{p'u_j'}\delta_{ik} + \overline{p'u_i'}\delta_{jk}) + \overline{u_i'u_j'u_k'} - \nu R_{ij,k}\,. \tag{2.7.8}$$

Again we have used the mean strain-rate and rotation-rate instead of just the mean velocity gradients to bring out the different roles played by strain and rotation. Most previous workers have included the mean rotation term in with the production. But it is trace-free it does not add new energy (it is absent from the turbulent kinetic energy equation), and therefore is different than production. The rotation term provides exactly the changes that would be seen if the R_{ij} structure were to be rotated as a solid body without change. Only strain, acting on the Reynolds stresses, can act as a new source for additional Reynolds stress.

The R_{ij} equation is sometimes rewritten so that the trace of the dissipation term is 2ε instead of $2\mathcal{D}$. with an associated modification in the flux. This is left as an exercise.

The R_{ij} evolution equation forms the basis for many of the current types of turbulence models. It is very useful in exploring the general nature of the changes that occur in turbulent flows subjected to strain.

2.8 Vorticity equation

The mean-square turbulent vorticity, sometimes called the *enstrophy*, is an important quantity in turbulence. Its evolution equation, derived by multiplying $(2.5.2)_i$ by ω_i' and averaging, is useful in studying the small scales of turbulence. Denoting

$$\omega^2 = \overline{\omega_i'\omega_i'} \tag{2.8.1}$$

one finds

$$\overline{D}(\frac{1}{2}\omega^2) = \overline{\omega_i'\omega_j'}S_{ij} - \omega^2 S_{jj} - \overline{\omega_i'u_j'}\Omega_{i,j} + \Omega_j\overline{s_{ij}'\omega_i'}$$

$$+\overline{\omega_i'\omega_j's_{ij}'} - \nu\overline{\omega_{i,j}'\omega_{i,j}'} + \left[-\frac{1}{2}\overline{u_j'\omega_i'\omega_i'} + \nu\left(\frac{1}{2}\omega^2\right)_{,j}\right]_{,j}. \tag{2.8.2}$$

3. STATISTICAL DESCRIPTIONS OF HOMOGENEOUS TURBULENCE

3.1 Introduction

A field in which all statistical properties are independent of position is called *homogeneous*. If the statistical properties are independent of the orientation of the coordinate frame, the field is called *isotropic*. Turbulence may be approximated as homogeneous and/or isotropic, although turbulence is usually homogeneous if it is isotropic. Few practical flows are either homogeneous or isotropic. Nevertheless, regions of practical flows often are essentially homogeneous, and homogeneous flows provide a very important point of departure for models and theories of turbulence. Therefore, development of good understanding of homogeneous turbulence is an important first step in the study of turbulence.

In order for the turbulence to be homogeneous, the terms in the equations for statistical properties of turbulence must be independent of position. Since the production term (2.7.2) involves mean velocity gradients, these must be independent of position if homogeneity is to be achieved. Therefore, a necessary condition for homogeneity is that the mean velocity be a *linear function of the coordinates*. Since there are no Reynolds stress gradients in homogeneous turbulence, the mean momentum equation (2.3.6) shows that the mean velocity field is unaffected by the turbulence.

Since the mean field is decoupled from the turbulence in homogeneous turbulence, almost any mean velocity history can be imposed on homogeneous turbulence. Any mean strain-rate history can be imposed, but the mean rotation history is determined by the imposed strain-rate history. From (1.10.5) it follows that the last term on the right in the mean vorticity equation (2.4.2) is $(\overline{\omega_j'u_i'})_{,j}$ which vanishes in homogeneous turbulence. Hence, the mean vorticity equation in homogeneous turbulence is

$$\dot{\Omega}_i = \Omega_j S_{ij} - \Omega_i S_{jj}. \tag{3.1.1}$$

Thus, while an initial arbitrary mean rotation can be imposed, any subsequent changes in the mean rotation are governed by (3.1.1). This restriction is important in the analysis and simulation of turbulence distortion by mean strain and rotation.

The statistics of homogeneous turbulence will depend upon time. Experiments on homogeneous turbulence generally involve passing flow through a grid, which generates turbulence, and then through a flow passage of varying cross section. The flow is approximately homogeneous as seen by an observer moving downstream with the mean flow, and the evolution of this turbulence as seen by the observer is interpreted as the time evolution of the turbulence. The behavior of turbulence under imposed mean strain can be studied by changing the cross-sectional geometry of the flow channel. Ingeneous experiments permit great flexibility in such experiments (Gence and Mathieu 1980). Homogeneous shear flow, in which the mean

streamwise velocity gradient is uniform across the flow, can be produced using upstream grids of special geometry (Tavoularis and Corrsin 1981).

Grid turbulence is not quite isotropic. However, by placing a contraction in the flow stream downstream of the grid, essentially isotropic turbulence can be obtained (Comte-Bellot and Corrsin 1966) for study in a subsequent constant cross-section duct downstream. One can also study the relaxation of homogeneous turbulence after strain in such a duct.

In the period 1960-1980, a number of basic experiments on homogeneous turbulence provided a sound data base on these flows. Since then numerical simulations of homogeneous turbulence have added considerably to this data base. The insight gleaned from these experiment and simulations now allow us to paint a useful picture of the structure of homogeneous turbulence. The next section presents this picture and discusses the important scales of turbulent motion.

3.2 Structure and scales in homogeneous turbulence

One can think of homogeneous turbulence as a complex tangle of vortex filaments, each acting as a "Biot-Savart source" in moving, distorting, and and straining all the filaments (Fig.3.2.1). This continual vortex stretching concentrates the vorticity, and so the volume of vortical fluid tends to be a small fraction of the total. Vortex filaments of the same sign tend to collect, and this provides a mechanism for the creation of larger eddies. This is counterbalanced by the three-dimensional straining of filaments, which tend to twist and tangle themselves to produce smaller eddies. The imposition of mean strain distort the tangle of vortex filaments, much as the fibres in a ball of steel-wool are distored when it is stretched. This alters the structure of the filaments, and hence the structure of the turbulence. Upon removal of the mean strain-rate, interactions between filaments randomize their orientation, bring about a *return to isotropy*.

This tangle of vorticity produces a very broad range of turbulent motions. The larger scales are more efficient in generating the Reynolds stress required to extranct energy from the mean field flow, and and new turbulent energy appears initially at large scales. Through the complex non-linear interactions, which are *inviscid* processes, turbulence energy is cascaded successively to smaller and smaller eddies, ultimately to be dissipated by viscous straining in the smallest eddies, where the local strain rates are the greatest.

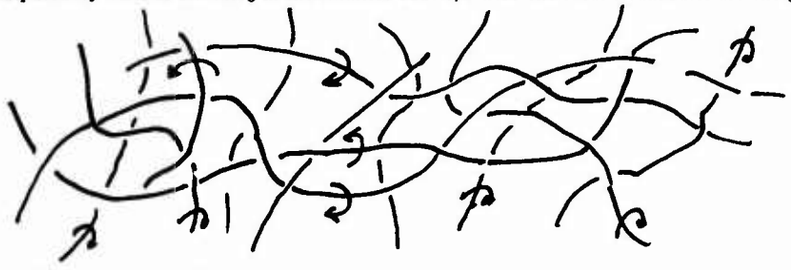

Figure 3.2.1 Homogeneous turbulence as a tangle of vortex filaments

The scale of the largest eddies is set by whatever object produced them. In grid turbulence the grid mesh determines the largest eddies, in wakes the large eddies scale on the diameter of the object, and in pipes they scale on the pipe diameter. The scale of the smallest eddies is set by the rate at which they must dissipate energy, provided to them by the large eddies through the cascade, through viscous stresses. The role of viscosity in turbulence is to set the scale of the smallest eddies.

These ideas suggest that the dissipation rate is determined by the scale of the energetic large-scale turbulence which starts the energy cascade. If we assume that q^2 and ε characterize these large scales, then by dimensional analysis the length scale of these eddies is

$$\ell = q^3/\varepsilon \tag{3.2.1a}$$

and the time scale is

$$\tau = q^2/\varepsilon. \tag{3.2.1b}$$

The velocity scale is of course just q. These scales tell us how the statistical properties of large eddies should be non-dimensionalised to collapse data from similar flows at different scales.

The Reynolds number of the turbulence, defined in terms of the velocity and length scales for the large eddies, is

$$R_T = \frac{q^4}{\varepsilon\nu}. \tag{3.2.2}$$

In practical flows, q is generally proportional to the velocity difference driving the flow (velocity at the center of a pipe or the velocity defect in a wake), and ℓ is proportional to the object dimension. Thus, R_T is usually proportional to (but smaller than by a factor of 20-100) the flow Revnolds number.

The scales of the smallest eddies are determined by the ϵ and ν. By dimensional analysis, the length scale must be

$$\ell_K = (\nu^3/\epsilon)^{1/4} \tag{3.2.3a}$$

and the time scale

$$\tau_K = (\nu/\epsilon)^{1/2}. \tag{3.2.3b}$$

These *Kolmogorov scales* characterize the vortex filaments in turbulence, with the cores of the vortex being of order ℓ_K and rotation time for the core scaling on τ_K. The corresponding velocity scale, characterizing the velocity difference developed locally around a vortex filament, is

$$v_K = (\nu\epsilon)^{1/4}. \tag{3.2.3c}$$

Using these scales, the ratio of the largest scales to the smallest scales is

$$\frac{\ell}{\ell_K} = R_T^{3/4} \tag{3.2.4}$$

Thus, the range of turbulence eddies broadens as the Reynolds number increases. This wide range limits direct numerical simulations of turbulence to low Reynolds numbers. *Large eddy simulations* of turbulence, in which turbulence of smaller scale than the computational mesh is modeled and the larger scales are computed, depends heavily on models for the small scales. It is tempting to approximate this sub-grid scale turbulence as homogeneous, and therefore a firm understanding of homogeneous turbulence is important to progress in large eddy simulation.

The remainder of this chapter is devoted to the mathematics used to describe the statistical properties of homogeneous turbulence. Subsequent chapters deal with the dynamic evolution of these statistical properties in response to imposed mean strain.

3.3 Correlations and spectra

The statistical properties of homogeneous random fields are most often described in terms of correlations and spectra. for example, if f and g are two random field variables, the *two-point correlation* of f and g is defined as

$$Q_{fg}(\mathbf{x}, \mathbf{x}', t) = < \overline{f(\mathbf{x}, t) g(\mathbf{x}', t)} > \tag{3.3.1a}$$

where the overline denotes a volume average and the brackets denote an ensemble average. Ensemble and volume averages are usually assumed to be the same for homogeneous fields (*ergodic hypothesis*); the dual averaging is therefore redundant but useful in the analysis that follows.

For homogeneous fields Q_{fg} depends only on the separation of the two points $\mathbf{r} = (\mathbf{x}' - \mathbf{x})$ and t,

$$Q_{fg}(\mathbf{r}, t) = < \overline{f(\mathbf{x}, t) g(\mathbf{x} + \mathbf{r}, t)} > . \tag{3.3.1b}$$

Often the time dependence of the correlation is not expressed explicitly, but it must not be forgotten.

There is an infinite set of other correlations of possible interest, for example the two-point correlation with time delay, three-point correlations, etc. A complete statistical description requires knowledge of the *probability density function* for all variables of interest at all space points and time, an impossible goal to achieve. Therefore, statistical descriptions are always limited in what they can provide, and the challengs is to provide what is really essential, with minimum effort and maximum accuracy.

In homogeneous fields, Fourier expansions can be used to represent individual realizations of the fields. Suppose that f and g are defined within a box of interest (Fig. 3.3.1). In order to give them Fourier expansions we have to imagine that they are periodic functions, so let

$$\tilde{f}(\mathbf{x}) = \begin{cases} f(\mathbf{x}) & \text{inside the box} \\ & \text{periodic repetition outside.} \end{cases}$$

The Fourier representation of $\tilde{f}$ at any instant of time is

$$\tilde{f}(\mathbf{x}) = \sum_{\mathbf{k}'} \hat{f}(\mathbf{k}') e^{-i\mathbf{k}'\cdot\mathbf{x}} \tag{3.3.2a}$$

where $\mathbf{k} = (k_1, k_2, k_3)$ is the three-dimensional *wavenumber vector*, and $\mathbf{k}\cdot\mathbf{x} = k_n x_n$. Since the Fourier modes must fit into the box with integer periods,

$$k_i = 2\pi n_i / L. \tag{3.3.2b}$$

The summation is a triple sum over all Fourier modes,

$$\sum_{\mathbf{k}'} = \sum_{k_1}^{\infty}\sum_{k_2}^{\infty}\sum_{k_3}^{\infty}. \tag{3.3.2c}$$

Note that the Fourier coefficients may vary with time; we do not show this explicitly here.

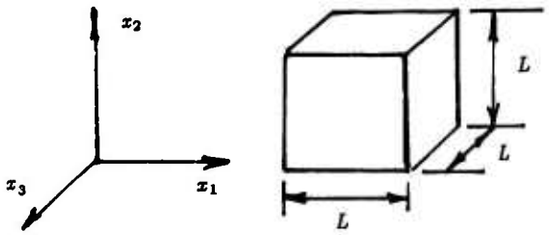

Figure 3.3.1 Box for Fourier representation

There is an important relationship between the Fourier coefficients of positive and negative wavenumbers *for a real field*. Taking the complex conjugate of (3.3.2a), replacing $\mathbf{k}'$ by $\mathbf{k}''$,

$$\tilde{f}^*(\mathbf{x}) = \sum_{\mathbf{k}''} \hat{f}^*(\mathbf{k}'')e^{+i\mathbf{k}''\cdot\mathbf{x}}$$

where the $*$ denotes a complex conjugate. Letting $\mathbf{k}'' = -\mathbf{k}'$,

$$\tilde{f}^*(\mathbf{x}) = \sum_{\mathbf{k}'} \hat{f}^*(-\mathbf{k}')e^{-i\mathbf{k}'\cdot\mathbf{x}}. \tag{3.3.3}$$

Now, if $\tilde{f}$ is real it is equal to its complex conjugate. Equating the Fourier coefficients of like exponentials in (3.3.2a) and(3.3.2),

$$\hat{f}(\mathbf{k}') = \hat{f}^*(-\mathbf{k}')$$

or alternatively (for *real* f)

$$\hat{f}(-\mathbf{k}) = \hat{f}^*(\mathbf{k}). \tag{3.3.4}$$

The Fourier coefficients are evaluated using the orthogonality property of the Fourier modes, using integrals over the domain. In what follows $\int()d^3\mathbf{x}$ denotes an integral over the box in Fig. 3.3.1. Then, multiplying (3.3.2a) by $e^{i\mathbf{k}\cdot\mathbf{x}}$ and integrating over the box,

$$\int e^{i\mathbf{k}\cdot\mathbf{x}}\tilde{f}(\mathbf{x})d^3\mathbf{x} = \sum_{\mathbf{k}'} \hat{f}(\mathbf{k}')\int e^{i(\mathbf{k}-\mathbf{k}')\cdot\mathbf{x}}d^3\mathbf{x}. \tag{3.3.5}$$

Since each Fourier mode that fits the box contains an integer number of cycles,

$$\int e^{i(\mathbf{k}-\mathbf{k}')\cdot\mathbf{x}}d^3\mathbf{x} = \begin{cases} 0 & \text{if } \mathbf{k} \neq \mathbf{k}' \\ L^3 & \text{if } \mathbf{k} = \mathbf{k}'. \end{cases} \tag{3.3.6}$$

Hence all terms in the summation of (3.3.4) drop out except for the one where $\mathbf{k}' = \mathbf{k}$. Thus, the Fourier coefficients can be evaluated as

$$\hat{f}(\mathbf{k}) = \frac{1}{L^3}\int \tilde{f}(\mathbf{x})e^{i\mathbf{k}\cdot\mathbf{x}}d^3\mathbf{x}. \tag{3.3.7}$$

The two-point correlation of f and g can be expressed in terms of the Fourier representations. Consider the correlation of f and g within the box of Fig. (3.3.1),

$$< \tilde{f}(\mathbf{x})\tilde{g}(\mathbf{x}') >= \sum_{\mathbf{k}}\sum_{\mathbf{k}'} < \hat{f}(\mathbf{k})\hat{g}(\mathbf{k}') > e^{-i(\mathbf{k}\cdot\mathbf{x}+\mathbf{k}'\cdot\mathbf{x}')}.$$

The brackets indicate that the Fourier coefficients are random variables that will differ from from realisation to realisation. Let $\mathbf{k}'' = -\mathbf{k}'$ and $\mathbf{r} = \mathbf{x}' - \mathbf{x}$. Then, using (3.3.4),

$$< \tilde{f}(\mathbf{x})\tilde{g}(\mathbf{x}+\mathbf{r}) >= \sum_{\mathbf{k}}\sum_{\mathbf{k}''} < \hat{f}(\mathbf{k})\hat{g}^*(\mathbf{k}'') > e^{-i\mathbf{x}\cdot(\mathbf{k}-\mathbf{k}'')+i\mathbf{k}''\cdot\mathbf{r}}. \tag{3.3.8}$$

Now we average by integrating over the box and dividing by L^3, denoting this average by an overline. Using (3.3.6), all the terms in the sum drop out except the terms where $\mathbf{k}'' = \mathbf{k}$. The result is then

$$\tilde{Q}_{fg}(\mathbf{r}) = < \overline{\tilde{f}(\mathbf{x})\tilde{g}(\mathbf{x}+\mathbf{r})} > = \sum_{\mathbf{k}} < \hat{f}(\mathbf{k})\hat{g}^*(\mathbf{k}) > e^{i\mathbf{k}\cdot\mathbf{r}}. \tag{3.3.9}$$

In computational simulations in which the evolution of the Fourier coefficients is calculated for finite-series approximations to the fields, (3.3.9) is used to calculate the the two-point correlation.

Theoretical treatments take the limit as $L \to \infty$, in which case the sums become integrals. To pass to this limit, we note that the difference between consecutive wavenumbers in the summation is $\Delta k_\alpha = 2\pi/L$ for each direction, so $\Delta k_i L/2\pi = 1$. We can multiply each term in the summation by unity three times to obtain

$$\tilde{Q}_{fg}(\mathbf{r}) = \sum_{\mathbf{k}} < \hat{f}(\mathbf{k})\hat{g}^*(\mathbf{k}) > \left(\frac{L}{2\pi}\right)^3 \Delta k_1 \Delta k_2 \Delta k_3 e^{i\mathbf{k}\cdot\mathbf{r}}. \tag{3.3.10}$$

We define the *cospectrum* of $\tilde{f}$ and $\tilde{g}$ as

$$\tilde{E}_{fg}(\mathbf{k}) = \left(\frac{L}{2\pi}\right)^3 < \hat{f}(\mathbf{k})\hat{g}^*(\mathbf{k}) > . \tag{3.3.11}$$

This is the equation used to calculate the co-spectrum in discrete spectral simulations of random fields. Then,

$$\tilde{Q}_{fg}(\mathbf{r}) = \sum_{\mathbf{k}} \tilde{E}_{fg}(\mathbf{k}) e^{i\mathbf{k}\cdot\mathbf{r}} \Delta k_1 \Delta k_2 \Delta k_3. \tag{3.3.12}$$

Taking the limit as $L \to \infty$, we define the cospectrum of f and g by

$$E_{fg}(\mathbf{k}) = \lim_{x\to\infty} \tilde{E}_{fg}(\mathbf{k}). \tag{3.3.13}$$

E_{fg} does not become infinite as $L \to \infty$ because the Fourier coefficients of individual modes become very small as the number of significant modes increases. As $L \to \infty$, $\Delta k_1 \Delta k_2 \Delta k_3$ becomes an elemental volume in wavenumber space $dk_1 dk_2 dk_3 = d^3\mathbf{k}$. Therefore, in (3.3.12) the two-point correlation

$$Q_{fg}(\mathbf{r}) = \lim_{x\to\infty} \tilde{Q}_{fg}(\mathbf{r}) \tag{3.3.14}$$

becomes the *three-dimensional Fourier transform* of the cospectrum,

$$Q_{fg}(\mathbf{r}) = \int E_{fg}(\mathbf{k}) e^{i\mathbf{k}\cdot\mathbf{x}} d^3\mathbf{k}. \tag{3.3.15}$$

Here the triple integration is to be carried out over all wavenumbers.

There is an inverse of the transform (3.3.15). Multiplying (3.3.9) by $e^{-i\mathbf{k}'\cdot\mathbf{r}}$ and integrating over a box of size L in r space,

$$\int \tilde{Q}_{fg}(\mathbf{r}) e^{-i\mathbf{k}'\cdot\mathbf{r}} d^3\mathbf{r} = \sum_{\mathbf{k}} \int < \hat{f}(\mathbf{k})\hat{g}^*(\mathbf{k}) > e^{i\mathbf{r}\cdot(\mathbf{k}-\mathbf{k}')} \tag{3.3.16}$$

Each exponential in the summation will execute an integer number of cycles in each direction and hence integrate to zero, except for the term where $\mathbf{k} = \mathbf{k}'$. Hence,

$$\int \tilde{Q}_{fg}(\mathbf{r}) e^{-i\mathbf{k}'\cdot\mathbf{r}} d^3\mathbf{r} = L^3 < \hat{f}(\mathbf{k})\hat{g}^*(\mathbf{k}) > = (2\pi)^3 \tilde{E}_{fg}(\mathbf{k}). \tag{3.3.17}$$

In computational simulations based on finite-difference methods, this equation is used to calculate the cospectrum from the two-point correlation. Taking the limit as $L \to \infty$, and replacing $\mathbf{k}'$ by $\mathbf{k}$,

$$E_{fg}(\mathbf{k}) = \left(\frac{1}{2\pi}\right)^3 \int Q_{fg}(\mathbf{r}) e^{-i\mathbf{k}\cdot\mathbf{r}} d^3\mathbf{r}. \tag{3.3.18}$$

Note that E_{fg} and Q_{fg} are *Fourier tranform pairs*.

We could have obtained the cospectrum simply by Fourier transformation of the two-point correlation. We started with a finite box so that the relationships between the Fourier coefficients and the cospectrum would be made clear, and also to derive results useful to persons engaged in discrete-representation simulations of homogeneous turbulence in finite computational domains. It should be understood that the Fourier transforms of f and g defined over an infinite region do not exist. However, because events at distant separations are uncorrelated, $Q_{fg} \to 0$ as $|\mathbf{r}| \to \infty$, and hence the Fourier transform of Q_{fg} does exist.

3.4 Velocity correlations and spectra

The velocity field in homogeneous turbulence can be represented in the terms outlined above. Let $f = u_i$ and $g = u_j$. Then, dropping the redundant ensemble average,

$$Q_{ij}(\mathbf{r}) = \overline{u_i'(\mathbf{x})u_j'(\mathbf{x}+\mathbf{r})}. \tag{3.4.1}$$

Q_{ij} is the *two-point velocity correlation tensor*. Note that

$$Q_{ii}(0) = \overline{u_i'(\mathbf{x})u_i'(\mathbf{x})} = q^2. \tag{3.4.2}$$

$Q_{ij}(\mathbf{r})$ expresses the average relationship between two velocity components measured at two locations separated by a distance $\mathbf{x}$. $Q_{\alpha\alpha}$ (*repeated Greek indices are not summed*) will be largest for zero separation, fall to a fraction of this value for separations comparable with the large eddies in the turbulence, and become zero for infinite separation. If the eddies tend to be long in one direction and short in another, this will be reflected in the different rate at which the correlation falls off with different r_α. Thus, the two-point correlation tensor can tell one quite a bit about the structure of the turbulence.

Using (3.3.18), the *velocity spectrum tensor* is

$$E_{ij}(\mathbf{k}) = \left(\frac{1}{2\pi}\right)^3 \int Q_{ij}(\mathbf{r})e^{-i\mathbf{k}\cdot\mathbf{r}}d^3\mathbf{r} \tag{3.4.3}$$

where the integrations are over all $\mathbf{r}$. It is related to the two-point velocity correlation tensor by (3.3.15),

$$Q_{ij}(\mathbf{r}) = \int E_{ij}(\mathbf{k})e^{i\mathbf{k}\cdot\mathbf{r}}d^3\mathbf{k} \tag{3.4.4}$$

where the integrations are over all $\mathbf{k}$.

The Reynolds stresses $R_{ij} = \overline{u_i'u_j'}$ are given by

$$R_{ij} = Q_{ij}(0) \tag{3.4.5}$$

for which (3.4.4) gives

$$R_{ij} = \int E_{ij}(\mathbf{k})d^3\mathbf{k}. \tag{3.4.6}$$

Reviewing the developments of the previous section, one sees that $E_{ij}(\mathbf{k})d^3\mathbf{k}$ represents the contributions to R_{ij} coming from an element of $\mathbf{k}$ space of volume $d^3\mathbf{k}$ positioned at $\mathbf{k}$.

For uniform density flow, the continuity equation (2.3.4) provides important constraints on $Q_{ij}(\mathbf{r})$. From (3.4.1)

$$\frac{\partial Q_{ij}}{\partial r_j} = \overline{u_i'(\mathbf{x})u_j'(\mathbf{x}+\mathbf{r})}_{,j} = 0. \tag{3.4.7a}$$

Replacing $\mathbf{x}$ by $\mathbf{x}' - \mathbf{r}$ in (3.4.1), then differentiating with respect to r_i, (2.3.4) also requires that

$$\frac{\partial Q_{ij}}{\partial r_i} = 0. \tag{3.4.7b}$$

The continuity equation (2.3.4) also constrains E_{ij}. In terms of the Fourier expansion, continuity requires

$$-\sum_{\mathbf{k}} ik_j\hat{u}_j(\mathbf{k})e^{-i\mathbf{k}\cdot\mathbf{x}} = 0. \tag{3.4.8}$$

This must hold for all $\mathbf{x}$, which requires that the coefficient of each and every exponential must vanish. Hence, for each wavenumber vector $\mathbf{k}$,

$$k_j\hat{u}_j(\mathbf{k}) = 0. \tag{3.4.9}$$

Equation (3.4.9) is the continuity equation in Fourier form. It says that, for each $\mathbf{k}$, the Fourier coefficient vector $\hat{\mathbf{u}}$ must be orthogonal to $\mathbf{k}$ in order for the velocity field to be divergence-free. This condition is used very often in analysis and simulation of homogeneous turbulence. From (3.4.9), it follows (most obviously using the the discrete Fourier representations) that

$$k_iE_{ij} = 0 \tag{3.4.10a}$$

and

$$k_j E_{ij} = 0. \tag{3.4.10b}$$

The correlation tensor Q_{ij} has an important symmetry property. Noting that

$$Q_{ij}(-\mathbf{r}) = \overline{u_i'(\mathbf{x})u_j'(\mathbf{x}-\mathbf{r})}$$

we let $\mathbf{x} = \mathbf{x}' + \mathbf{r}$ and rewrite this as

$$Q_{ij}(-\mathbf{r}) = \overline{u_i'(\mathbf{x}'+\mathbf{r})u_j'(\mathbf{x}')}.$$

The right hand side is just $Q_{ji}(\mathbf{r})$. Hence

$$Q_{ij}(-\mathbf{r}) = Q_{ji}(\mathbf{r}). \tag{3.4.11}$$

The spectrum tensor E_{ij} also has a symmetry property. Since the Fourier coefficients for real fields obey (3.3.3), It follows (most obviously from the discrete Fourier representations) that

$$\tilde{E}_{ij}(-\mathbf{k}) = \left(\frac{L}{2\pi}\right)^3 < \hat{u}_i(-\mathbf{k})\hat{u}_j^*(-\mathbf{k}) >$$

$$= \left(\frac{L}{2\pi}\right)^3 < \hat{u}_i^*(\mathbf{k})\hat{u}_j(\mathbf{k}) >= \tilde{E}_{ji}(\mathbf{k}). \tag{3.4.12}$$

In the limit $L \to \infty$ this becomes

$$E_{ij}(-\mathbf{k}) = E_{ji}(\mathbf{k}). \tag{3.4.13}$$

The turbulence kinetic energy may be expressed as

$$\frac{1}{2}q^2 = \frac{1}{2}Q_{ii}(0) = \frac{1}{2}\int E_{ii}(\mathbf{k})d^3\mathbf{k}. \tag{3.4.14}$$

Integral scales of motion may be defined in terms of Q_{ij}. For example,

$$L_{11} = \frac{\int_0^\infty Q_{11}(r_1,0,0)dr_1}{Q_{11}(0,0,0)} \tag{3.4.15}$$

is useful as a measure of the x_1 scale of the turbulence. Here the arguments display the three components of the separation vector,

Q_{ij} and E_{ij} are the classical quantities used to describe homogeneous turbulence. They are less useful for inhomogeneous turbulence because expansion functions other than Fourier modes really should be used in directions of inhomogeneity. They are used for inhomogeneous flows when the turbulence can be approximated as locally homogeneous over regions large compared to the integral scale.

3.5 Other statistical quantities

There are many other statistical quantities of interest in turbulence. Those that involve only quadratic forms in the velocity are termed *second-order*. Any second-order statistical property of the velocity field can be derived from the two-point correlation tensor or the velocity spectrum tensor. For example, a tensor of interest is

$$D_{ijpq} = \overline{u_{i,p}' u_{j,q}'}. \tag{3.5.1}$$

From (3.4.1),

$$\frac{\partial Q_{ij}(\mathbf{r})}{\partial r_q} = \overline{u_i'(\mathbf{x})u_{j,q}'(\mathbf{x}+\mathbf{r})}. \tag{3.5.2}$$

Replacing $\mathbf{x}$ by $\mathbf{x}' - \mathbf{r}$ in (§ 5.2), then differentiating with respect to r_p, one has

$$\frac{\partial^2 Q_{ij}(\mathbf{r})}{\partial r_p r_q} = -\overline{u_{i,p}'(\mathbf{x}'-\mathbf{r})u_{j,q}'(\mathbf{x}')}. \tag{3.5.3}$$

Now letting $\mathbf{r} = 0$,

$$D_{ijpq} = -\left(\frac{\partial^2 Q_{ij}(\mathbf{r})}{\partial r_p \partial r_q}\right)_{|\mathbf{r}|=0}. \tag{3.5.4}$$

The corresponding result in terms of the spectrum tensor can be derived directly by taking the derivatives of the discrete Fourier series for the velocities, and proceding as in section 3.2 above, or by applying (3.5.4) to (3.4.4). Either approach gives

$$D_{ijpq} = \int k_p k_q E_{ij}(\mathbf{k}) d^3\mathbf{k}. \tag{3.5.5}$$

Since gradients of all statistical quantities vanish in homogeneous turbulence,

$$\overline{(u_i' u_j')}_{,ij} = 0. \tag{3.5.6}$$

Expanding the differentiation using the continuity equation (2.3.4),

$$D_{ijji} = \overline{u_{i,j}' u_{j,i}'} = 0. \tag{3.5 7}$$

Note that this is consistent with (3.5.4) and (3.5.5) if the continuity constraints (3.4.7) or (3.4.10) are applied. The dissipation rate ε may be expressed in general as

$$\varepsilon = \nu(D_{iijj} + D_{ijji}). \tag{3.5.8}$$

From (3.5.7), the second term does not contribute, and in homogeneous turbulence the true dissipation rate ε is the same as the homogeneous dissipation rate D defined by (2.6.4).

Using (3.5.8), (3.5.7), and (3.5.5), we find that the dissipation rate is related to the velocity spectrum tensor by

$$\varepsilon = \nu \int k^2 E_{ii}(\mathbf{k}) d^3\mathbf{k}. \tag{3.5.9}$$

The factor k^2 means that the main contributions to the dissipation come from higher wavenumbers (smaller eddies) than those that provide the major contribution to the kinetic energy.

3.6 Vorticity

The *two-point vorticity correlation tensor* is

$$W_{ij}(\mathbf{r}) = \overline{\omega_i'(\mathbf{x})\omega_j'(\mathbf{x}+\mathbf{r})}. \tag{3.6.1}$$

Note that

$$W_{ii}(0) = \overline{\omega_i'\omega_i'} = \omega^2. \tag{3.6.2}$$

From the definition of vorticity (1.9.1),

$$\omega^2 = D_{iijj} - D_{ijji} \tag{3.6.3}$$

so it follows from (3.5.7) and (3.5.8) that in homogeneous turbulence the dissipation is directly related to the mean-square vorticity,

$$\varepsilon = \nu\omega^2. \tag{3.6.4}$$

The enstrophy equation (2.8.1) is therefore sometimes used as a guide in developing model equations for the dissipation.

The vorticity can also be expanded in a Fourier representation; for the box of section 3.2,

$$\tilde{\omega}_i'(\mathbf{x}) = \sum_{\mathbf{k}} \hat{\omega}_i(\mathbf{k}) e^{-i\mathbf{k}\cdot\mathbf{x}} \tag{3.6.5}$$

Because the vorticity is by definition divergence-free,

$$k_i \hat{\omega}_i(\mathbf{k}) = 0 \tag{3.6.6}$$

and because the vorticity is real

$$\hat{\omega}_i(\mathbf{k}) = \hat{\omega}_i^*(-\mathbf{k}). \tag{3.6.7}$$

The *vorticity spectrum tensor* $H_{ij}(\mathbf{k})$ can be developed following the approach above. It is of course the Fourier transform of the two-point vorticity correlation tensor, and can be related to the velocity tensor. Because the vorticity is divergence-free,

$$k_i H_{ij}(\mathbf{k}) = 0 \tag{3.6.8a}$$

and

$$k_j H_{ij}(\mathbf{k}) = 0 \tag{3.6.8b}$$

and because it is real

$$H_{ij}(-\mathbf{k}) = H_{ji}(\mathbf{k}). \tag{3.6.9}$$

The Fourier coefficients of the vorticity are related to those of the velocity. Using (1.9.1),

$$\tilde{\omega}_i'(\mathbf{x}) = \sum_{\mathbf{k}} \epsilon_{ipq}(-ik_q)\hat{u}_q(\mathbf{k})e^{-i\mathbf{k}\cdot\mathbf{x}}. \tag{3.6.10}$$

Equating coefficients of like exponentials, the vorticity coefficients are found to be

$$\hat{\omega}_i(\mathbf{k}) = -ik_p\epsilon_{ipq}\hat{c}_q(\mathbf{k}). \tag{3.6.11}$$

From this it follows that

$$H_{ij}(\mathbf{k}) = \epsilon_{ipq}\epsilon_{jrs}k_pk_rE_{qs}(\mathbf{k}) \tag{3.6.12}$$

One can express Q_{ij} in terms of the vorticity correlation tensor and E_{ij} in terms of the vorticity spectrum tensor. This requires the solution of the Poisson equation (1.9.5), which is easily accomplished using the Fourier representations. Alternatively, one can multiply (3.6.10) by $\epsilon_{rsi}k_s$. The result is

$$\hat{u}_i(\mathbf{k}) = \epsilon_{ipq}\frac{ik_p}{k^2}\hat{\omega}_q(\mathbf{k}). \tag{3.6.13}$$

where $k^2 = k_ik_i$. Substituting in the discrete representation of $\tilde{E}_{ij}$ and taking the limit, one finds

$$E_{ij}(\mathbf{k}) = \epsilon_{ipq}\epsilon_{jrs}\frac{k_pk_r}{k^4}H_{qs}(\mathbf{k}). \tag{3.6.14}$$

This result finds important use in *rapid distortion theory*, where it is used to estimate the anisotropy in the Reynolds stresses produced by distortion of the vorticity field due to imposed mean strain. It is also useful in constructing models of E_{ij} for anisotropic turbulence using models for the anisotropic H_{ij}.

3.7 Correlations and spectra in isotropic turbulence

If the statistics are independent of the coordinate system orientation, only two types of correlations completely characterize the velocity correlation tensor (Fig. 3.7.1). The *longitudinal correlation function*

$$f(r) = \frac{3}{q^2}Q_{11}(r_1,0,0) \tag{3.7.1}$$

describes the coherence of the velocity fluctuations aligned with the separation of the two points. The *lateral correlation function*

$$g(r) = \frac{3}{q^2}Q_{22}(r_1,0,0) \tag{3.7.2}$$

relates to the coherence of fluctuation velocities perpendicular to the separation axis.

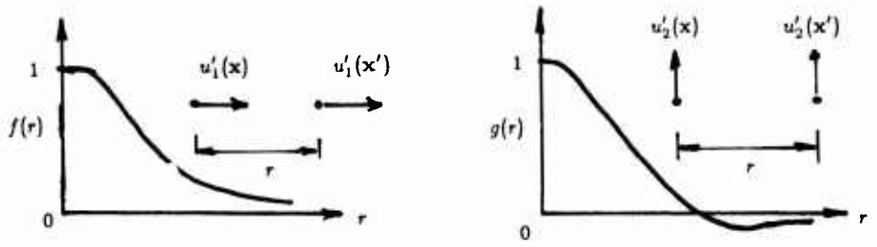

Figure 3.7.1 Longitudinal and lateral correlation functions

The complete tensor $Q_{ij}(\mathbf{r})$ can expressed in terms of these two scalar functions. The tensor must be a function of the separation vector $\mathbf{r}$. The most general such function is

$$Q_{ij}(\mathbf{r}) = C_1\delta_{ij} + C_2r_ir_j \tag{3.7.3}$$

where the coefficients C_1 and C_2 may be functions of the scalar invariant of the vector, $r = \sqrt{r_ir_i}$. The coefficients can be identified by expressing the longitudinal and lateral correlations:

$$Q_{22}(r_1,0,0) = \frac{q^2}{3}g(r) = C_1 \tag{3.7.4}$$

$$Q_{11}(r_1,0,0) = \frac{q^2}{3} f(r) = C_1 + C_2 r^2. \tag{3.7.5}$$

Solving for C_1 and C_2, one finds

$$Q_{ij}(\mathbf{r}) = \frac{q^2}{3}\left[\frac{f(r)-g(r)}{r^2} r_i r_j + g(r)\delta_{ij}\right]. \tag{3.7.6}$$

Note that f and g are scalar functions of the scalar separation magnitude r (and of time, not shown explicitly).

The continuity equation provides a relationship between f and g. Since $r = \sqrt{r_i r_i}$,

$$\frac{\partial r}{\partial r_k} = \frac{r_k}{r}. \tag{3.7.6}$$

Differentiating (3.7.6) with repect to r_k,

$$Q_{ij,k} = \frac{q^2}{3}\left[\left(\frac{f-g}{r^2}\right)' r_i r_j \frac{r_k}{r} + \left(\frac{f-g}{r^2}\right)(r_i\delta_{jk} + r_j\delta_{ik}) + g'\frac{r_k}{r}\right] \tag{3.7.8}$$

where the primes denotes differentiation with respect to r. Setting $k = j$ and using the continuity condition(3.4.7), one finds

$$f' + \frac{2}{r}(f-g) = 0 \tag{3.7.9}$$

This integrates readily to give

$$f(r) = \frac{2}{r^2}\int_0^r \tilde{r} g(\tilde{r}) d\tilde{r}. \tag{3.7.10}$$

E_{ij} for isotropic turbulence can be obtained by Fourier transform of Q_{ij} as outlined in section 3.3. Alternatively, we can construct its general form directly since, for isotropic turbulence the E_{ij} tensor must be a function only the vector k. The most general form is

$$E_{ij}(\mathbf{k}) = C_1\delta_{ij} + C_2 k_i k_j \tag{3.7.11}$$

where the coefficients can depend on the scalar invariant of the vector, $k = \sqrt{(k_i k_i)}$. Using the continuity condition (3.4.10),

$$C_1 k_j + C_2 k^2 k_j = 0 \tag{3.7.12}$$

hence

$$C_2 = -C_1/k^2 \tag{3.7.13}$$

Redefining C_1 as $4\pi k^2 E(k)$, we have

$$E_{ij}(\mathbf{k}) = \frac{E(k)}{4\pi k^2}\left(\delta_{ij} - \frac{k_i k_j}{k^2}\right). \tag{3.7.14}$$

$E(k)$ is called the *energy spectrum function*. Note that it is a scalar function of the scalar k (and of time, not shown explicitly).

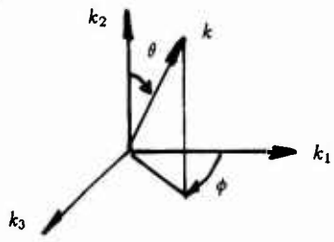

Figure 3.7.2 Coordinate system for k-space integration

The turbulence energy is, using (3.4.14),

$$\frac{1}{2}q^2 = \int \frac{1}{4\pi k^2} E(k) d^3\mathbf{k} \tag{3.7.15}$$

The integration of integrals of this type , in which the unknown function depends only on the magnitude of the vector, can best be carried out in spherical coordinates (Fig. 3.7.2). We have

$$\frac{1}{2}q^2 = \frac{1}{4\pi}\int_{k=0}^{\infty}\int_{\theta=0}^{\pi}\int_{\phi=0}^{2\pi}\frac{E(k)}{k^2}k^2\sin\theta\, d\theta\, d\phi\, dk. \tag{3.7.16}$$

Carrying out the integrations over ϕ and θ,

$$\frac{1}{2}q^2 = \int_0^{\infty} E(k)dk. \tag{3.7.17}$$

We see that $E(k)dk$ represents the contribution to the kinetic energy per unit mass arising from all the Fourier modes in a spherical shell in k-space of radius k and thickness dk. Once $E(k)$ is known, the entire velocity spectrum tensor E_{ij} is known from (3.7.14).

In theory, homogeneous isotropic turbulence evolves in time, and one should measure the spectrum tensor by making measurements at many space points. In reality this is very difficult (but it is what is in fact done in a numerical simulation). Instead, laboratory experiments make use of *Taylor's hypothesis*, which assumes that the velocity pattern measured as a function of time at one point is frozen in the fluid and being swept over the probe. The probe measurement is thereby interpreted as providing $Q_{11}(r_1,0,0)$. Using (3.7.14) in (3.4.4),

$$Q_{11}(r_1,0,0) = \int \frac{E(k)}{4\pi k^2}\left(1-\frac{k_1^2}{k^2}\right)e^{ik_1r_1}d^3\mathbf{k} \tag{3.7.18}$$

This integration is conveniently carried out in the coordinates of Fig. 3.7.3. We sort the Fourier contributions according to those with the same wavenumber $|k_1|$. Terms from both sides of the k_1 axis contribute, with opposite signs in their exponentials; these are combined into a cosine:

$$Q_{11}(r_1,0,0) = \int_{k_1=0}^{\infty}\int_{k=k_1}^{\infty}\int_{\phi=0}^{2\pi}\frac{E(k)}{4\pi k^2}\left(1-\frac{k_1^2}{k^2}\right)2\cos(k_1r_1)k\, d\phi\, dk\, dk_1 \tag{3.7.19}$$

We carrying out the ϕ integration, and define the *one dimensional spectrum function* E_1 by

$$E_1(k_1) = \int_{k=k_1}^{\infty}\frac{E(k)}{k}\left(1-\frac{k_1^2}{k^2}\right)dk. \tag{3.7.20}$$

Then,

$$Q_{11}(r_1,0,0) = \int_{k_1=0}^{\infty}E_1(k)\cos(k_1r_1)dk_1 \tag{3.7.21}$$

One can taking the Fourier cosine transformation of the measured $Q_{11}(r_1,0,0)$ to get $E_1(k_1)$. Then, differentiating (3.7.18) twice (a courageous step with laboratory data!),

$$E(k_1) = \frac{k_1^2}{2}\frac{\partial^2 E_1(k_1)}{\partial k_1^2} - \frac{k_1}{2}\frac{\partial E_1(k_1)}{\partial k_1} \tag{3.7.22}$$

This allows $E(k)$ to be determined. It also shows that if $E(k)$ varies as a power of k in some range then $E_1(k_1)$ will vary with the same power of k_1.

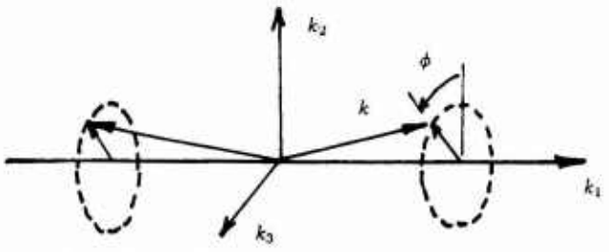

Figure 3.7.3 Coordinates for one-dimensional spectrum integration

Eqn. (3.7.21) in essence defines Q_{11} as a one-dimensional Fourier cosine transform of E_1. The inverse transform is

$$E_1(k_1) = \frac{2}{\pi}\int_0^{\infty}Q_{11}(r_1,0,0)\cos(k_1r_1)dr_1. \tag{3.7.23}$$

Noting that $Q_{11}(0) = q^2/3$ in isotropic turbulence, the integral scale defined by (3.4.15) is given by (3.7.23) as

$$L_{11} = \Lambda_f = \frac{3\pi}{2q^2}E_1(0) \tag{3.7.24}$$

Λ_f is the integral scale derived from the longitudinal correlation function $f(r)$, and hence it is called the called the *longitudinal integral scale.* Since it is non-zero, $E_1(0) > 0$, in contrast to $E(0) = 0$.

3.8 Dissipation in isotropic turbulence

Using the isotropic spectrum (3.7.14) in (3.5.9), carrying out the integrations using polar coordinates as above, the dissipation rate is found as

$$\varepsilon = \nu \int_0^\infty k^2 E(k) dk \tag{3.8.1}$$

The factor k^2 means that higher wave numbers (smaller scales) make more contribution to the dissipation (and vorticity) than they do to the energy (compare 3.7.17).

Since the small-scale component of turbulence is generally throught to be very nearly isotropic at high Reynolds numbers, isotropic turbulence theory is used as an aid in estimating ε from laboratory data. This approach makes use of the tensor D_{ijpq} defined by (3.5.1). In an isotropic field, the only tensors upon which D_{ijpq} can depend are the isotropic numerical tensors, hence it must be of the form

$$D_{ijpq} = C_1 \delta_{ij}\delta_{pq} + C_2 \delta_{ip}\delta_{jq} + C_3 \delta_{iq}\delta_{jp} \tag{3.8.2}$$

where the coefficients must be scalars. The coefficients can be evaluated from three known constraints. First, the definition forces a symmetry,

$$D_{ijpq} = D_{jiqp}. \tag{3.8.3a}$$

Second, continuity requires that

$$D_{ijiq} = 0. \tag{3.8.3b}$$

Finally, we know that

$$\varepsilon = \nu D_{iipp}. \tag{3.8.3c}$$

Using these considition, one finds

$$D_{ijpq} = \frac{2\varepsilon}{15\nu}\left[\delta_{ij}\delta_{pq} - \frac{1}{4}(\delta_{ip}\delta_{jq} + \delta_{jp}\delta_{iq})\right]. \tag{3.8.4}$$

The pertinent quantity most easily measured in an experiment (again using Taylor's hypothesis) is

$$\overline{(u'_{1,1})^2} = \frac{\varepsilon}{15\nu}. \tag{3.8.5}$$

This is usually the way that ε is estimated in laboratory experiments.

Another important turblence scale defined in terms of the dissipation is the *microscale.* It can be approached through the longitudinal correlation function $f(r)$. The symmetry property (3.4.11) indicates that $f(r)$ must be an even function of r, so its expansion is

$$f(r) = 1 - \frac{1}{2}ar^2 + O(r^4) \tag{3.8.6}$$

The interception of this osculating parabola (Fig. 3.8.1) with $f = 0$ defines a scale $\lambda_f = \sqrt{2/a}$, called the *longitudinal Taylor microscale.* From (3.5.4), using (3.7.5) and then (3.8.4),

$$a = \frac{3}{q^2} D_{1111} = \frac{\varepsilon}{5\nu q^2}$$

so

$$\lambda_f^2 = 10\nu q^2/\varepsilon. \tag{3.8.7}$$

Alternatively, the dissipation rate can be expressed as

$$\varepsilon = 10\nu \frac{q^2}{\lambda_f^2}. \tag{3.8.8}$$

This equation is sometimes used to determine ε from measurements of the longitudinal correlation.

Using (3.2.3) and (3.2.2), the ratio of the Taylor microscale to the Kolmogorov scale is

$$\frac{\lambda_f}{\ell_K} = \sqrt{10} R_T^{1/4} \tag{3.8.9}$$

Using (3.2.1), the ratio of the energy-containing scale to the Taylor scale is

$$\frac{\ell}{\lambda_f} = \frac{1}{\sqrt{10}} R_T^{1/2} \tag{3.8.10}$$

Thus the microscale falls between the smallest and largest scales. Although it is the most commonly reported turbulence scale, it is the least well understood. It has been suggested that it is a measure of the size of the loops in the vortex filaments, but this is not at all certain.

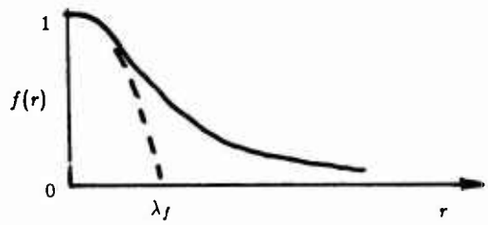

Figure 3.8.1 The osculating parabola defines the Taylor microscale

3.9 Scaling of the spectrum in isotropic turbulence

The general form of $E(k)$ deduced from measurements in isotropic turbulence is shown in Fig. 3.7.1. By (3.7.17), the area under the curve is the turbulent kinetic energy, to which then greatest contributions come from wavenumbers around the peak. The vorticity and dissipation occur predominantly at high wavenumbers.

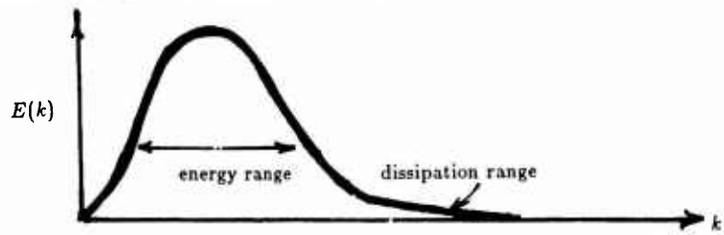

Figure 3.9.1 Form of the spectrum in isotropic turbulence

It is generally thought that the small-scale motions in *any* turbulent flow become isotropic at high Reynolds numbers, and therefore that the Kolmogorov scales characterize the high wavenumber region of *any* turbulent flow. Moreover, if one assumes that there is a *universal small-scale spectrum*, then by dimensional analysis it must be of the form

$$\frac{E(k)}{\nu^{5/4}\varepsilon^{1/4}} = F\left(\frac{k\nu^{3/4}}{\varepsilon^{1/4}}\right). \tag{3.9.1}$$

The one-dimensional spectrum $E_1(k_1)$ would have to scale in the same manner. Figure 3.9.2 shows that the data from a wide variety of flows do indeed collapse when plotted in these Kolmogorov variables. The data flatten at low wavenumbers because they are one-dimensional spectra where $E_1(0)$ is given by (3.7.24).

STREAMWISE ENERGY SPECTRA FOR VARIOUS TURBULENT FLOWS
(CHAPMAN, 1979)

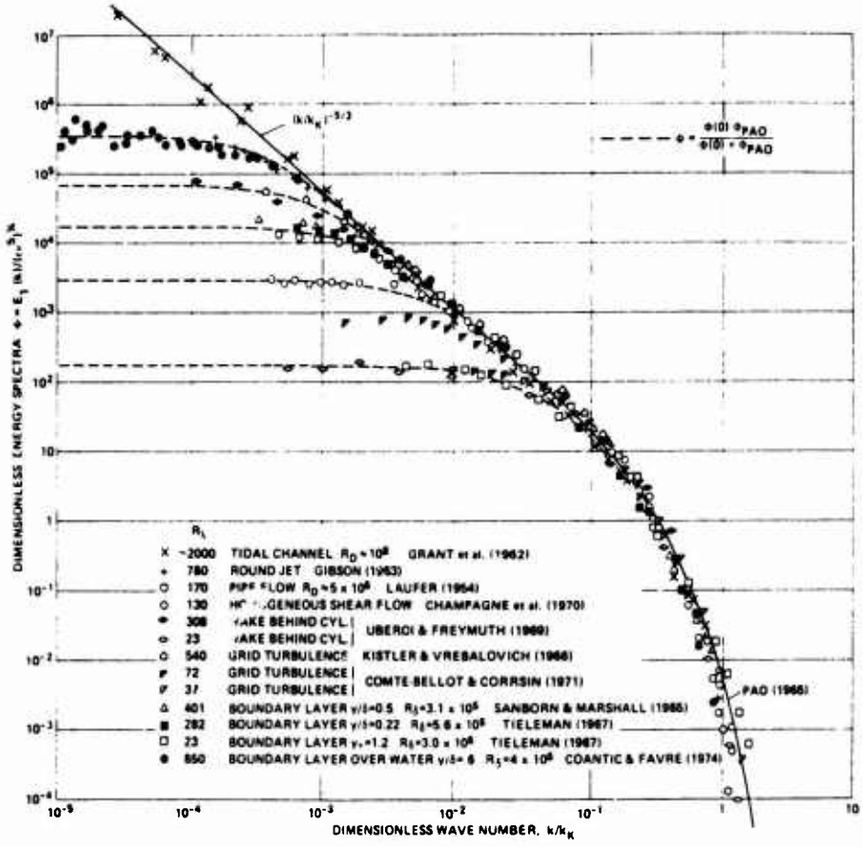

Figure 3.9.2 Spectra in Kolmogorov variables

Kolmogorov suggested that there should be a range of wavenumbers in which the main process is the passing of energy from larger eddies to smaller eddies (the *cascade* of turbulence energy), and that the structure of this region should depend only on the rate of energy cascade. Since this cascade ultimately ends with dissipation at the small scales, the rate of energy cascade must be ε. If one assumes that $E(k)$ depends

only on ϵ (and of course k) in this range, by dimensional analysis

$$E(k)k^{5/3}\epsilon^{-2/3} = \text{constant} = \alpha$$

or

$$E(k) = \alpha\epsilon^{2/3}k^{-5/3}. \tag{3.9.2}$$

This is the *Komogorov spectrum*, a cornerstone of turbulence. Measurements give a *Kolmogorov constant* α of about 1.5. The data of Figure 3.9.2 show the $-5/3$ range, with longer runs of $-5/3$ behavior at larger Reynolds numbers, consistent with the broadening of scales as $R_T^{3/4}$.

In the vicinity of the peak in $E(k)$, the spectrum should scale on the large-scale variables (see section 3.1), and hence should collapse when plotted as

$$\frac{\epsilon E(k)}{q^5} = G\left(\frac{k\epsilon}{q^3}\right). \tag{3.9.3}$$

Where this form overlaps with the Kolmogorov spectrum the function G must be such that q drops out, and this again establishes the $-5/3$ law for the asymptotic overlap range between low and high wavenumbers.

Figure 3.9.1 indicates that $E(k) \to 0$ as $k \to 0$, but there is controversy as to just how. There are good arguments supporting both k^2 (*Saffman*) and k^4 (*Loitskianski*) variation as $k \to 0$. The k^4 behavior is required if E_{ij} is to be analytic at $k = 0$. The k^2 behavior implies some residual preferential directions at zero wavenumbers, which may be more characteristic of physical experiments. Numerical simulations with delta spectra at mid-range fill-out as k^4 as the turbulence develops, but simulations initiated with k^2 behavior at low wavenumbers persist as k^2. Simple models of turbulence show that the rate of energy decay in isotropic turbulence depends on the low wavenumber portion of the spectrum, and with the experimental decay rates support the k^2.

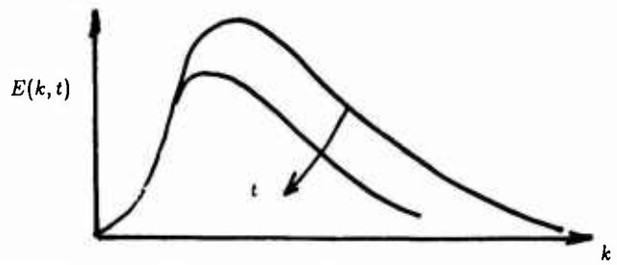

Figure 3.9.3 Evolution of the spectrum in decaying isotropic turbulence

Turbulence not subjected to mean deformation will decay as time passes. The larger eddies take more time to change, and the smallest scales of motion adjust most rapidly. Figure 3.9.3 depicts the nature of the evolution of $E(k,t)$ (we now include the time variable heretofore suppressed). Note that the peak moves to larger scales (small wavenumbers) because the smaller eddies die out faster. Thus as time progresses the integral scale will grow.

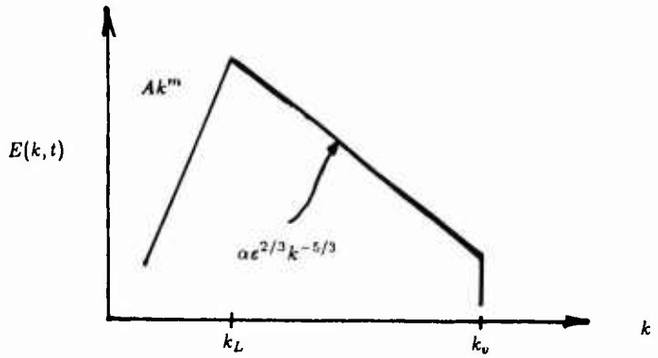

Figure 3.9.4 Model spectrum for isotropic turbulence

A simple model spectrum for isotropic turbulence is shown in Fig. 3.9.4. It assumes a power law behavior at low wavenumbers, a $-5/3$ inertial range, and a sharp cutoff at the Kolmogorov scale:

$$E(k) = \begin{cases} Ak^m & \text{for } k \le k_L \\ \alpha\epsilon^{2/3}k^{-5/3} & \text{for } k_L \le k \le k_v \\ 0 & \text{for } k > k_v \end{cases}. \tag{3.9.4}$$

Matching the spectrum at k_L gives

$$k_L = \left(\frac{\alpha\epsilon^{2/3}}{A}\right)^{3/(3m+5)}. \tag{3.9.5}$$

Assuming $k_v \gg k_L$,

$$\frac{1}{2}q^2 = \int_0^\infty E(k)dk = \alpha\left(\frac{1}{m+1} + \frac{3}{2}\right)k_L^{-2/3}\epsilon^{2/3}$$

from which an estimate of the peak wavenumber is obtained,

$$\frac{k_L q^3}{\epsilon} = \left[2\alpha\left(\frac{1}{m+1} + \frac{3}{2}\right)\right]^{3/2}. \tag{3.9.6}$$

Again assuming $k_v \gg k_L$, the viscous cutoff wavenumber is estimated

$$\epsilon = \nu\int_0^\infty k^2 E(k)dk = \nu\frac{3}{4}\alpha\epsilon^{2/3}k_v^{4/3} \tag{3.9.7}$$

from which

$$\frac{k_v\nu^{3/4}}{\epsilon^{1/4}} = \left(\frac{4}{3\alpha}\right)^{3/4} \tag{3.9.8}$$

It is left as an exercise to work out the one-dimensional spectrum E_1 for this model spectrum, and from that to determine the integral scale. For $m = 2$ and $\alpha = 1.5$, one finds

$$\Lambda_f\epsilon/q^3 \approx 0.11. \tag{3.9.9}$$

This model spectrum exhibits the proper scaling for isoropic turbulence, and gives values of the scales within about a factor of two of those found from actual spectra. It is very useful in constructing simple turbulence models, in setting up initial fields for turbulence simulations, and in addressing other aspects of homogeneous turbulence.

3.10 Third-order statistics in isotropic turbulence

Correlations involving products of three quantities are called *third order* statistics. These depend on the relative phases of the Fourier modes, information not contained in the spectrum tensor E_{ij}. Of particular interest in turbulence modeling are one-point third-order statistics. For isotropic turbulence these tensors can be worked out using the methods used previously. For example,

$$\overline{u_i' u_j' u_k'} = C q^{3/2} \epsilon_{ijk}. \tag{3.10.1}$$

In dealing with the vorticity and dissipation equations, one encounters the tensor

$$\psi_{ijkpqr} = \overline{u_{i,p}' u_{j,q}' u_{k,r}'}. \tag{3.10.2}$$

This is evaluated for isotropic turbulence by first writing the general tensor

$$\begin{aligned}\psi_{ijkpqr} = \delta_{ip}(C_1\delta_{jq}\delta_{kr} + C_2\delta_{jk}\delta_{qr} + C_3\delta_{jr}\delta_{kq}) + \delta_{ij}(C_4\delta_{pq}\delta_{kr} + C_5\delta_{pk}\delta_{qr} + C_6\delta_{pr}\delta_{qk}) \\ +\delta_{iq}(C_7\delta_{pj}\delta_{kr} + C_8\delta_{pk}\delta_{jr} + C_9\delta_{pr}\delta_{jk}) + \delta_{ik}(C_{10}\delta_{pj}\delta_{qr} + C_{11}\delta_{pq}\delta_{jr} + C_{12}\delta_{pr}\delta_{jq}) \\ +\delta_{ir}(C_{13}\delta_{pj}\delta_{qk} + C_{14}\delta_{pq}\delta_{jk} + C_{15}\delta_{pk}\delta_{qj}).\end{aligned} \tag{3.10.3}$$

There are three are three symmetry constraints,

$$\psi_{ijkpqr} = \psi_{jipqkr} \tag{3.10.4a}$$

$$\psi_{ijkpqr} = \psi_{kjirqp} \tag{3.10.4b}$$

$$\psi_{ijkpqr} = \psi_{ikjprq}. \tag{3.10.4c}$$

Continuity also provides some constraints, but with the symmetries enforced only one is required,

$$\psi_{ijkipq} = 0. \tag{3.10.5}$$

Forming $(\overline{u_i' u_j' u_k'})_{,ijk}$ and using homogeneity conditions, one can show that

$$\psi_{ijkjki} = 0. \tag{3.10.6}$$

With these constraints, (3.10.3) can be reduced to a form containing only one unknown coefficient. With $C_5 = A$, one finds

$$\begin{aligned}\psi_{ijkpqr} = A\big[(\delta_{ip}\delta_{jq}\delta_{kr} + \delta_{ij}\delta_{pk}\delta_{qr} + \delta_{iq}\delta_{pr}\delta_{jk} + \delta_{ik}\delta_{pj}\delta_{qr} + \delta_{ik}\delta_{pq}\delta_{jr} + \delta_{ir}\delta_{pq}\delta_{jk}) \\ -\frac{4}{3}(\delta_{ip}\delta_{jk}\delta_{qr} + \delta_{ij}\delta_{pq}\delta_{kr} + \delta_{ik}\delta_{pr}\delta_{jq}) - \frac{3}{4}(\delta_{iq}\delta_{pk}\delta_{jr} + \delta_{ir}\delta_{pj}\delta_{qk}) - \frac{1}{6}(\delta_{ip}\delta_{jr}\delta_{kq} + \delta_{iq}\delta_{pj}\delta_{kr} + \delta_{ir}\delta_{pk}\delta_{jq})\big].\end{aligned} \tag{3.10.7}$$

For example,

$$\overline{(u_{1,1}')^3} = A \tag{3.10.8}$$

$$\overline{\omega_i' \omega_j' s_{ij}'} = -\frac{35}{2} A. \tag{3.10.9}$$

The *derivative skewness* γ is related to A; using (3.8.5) and (3.10.8),

$$\gamma = \overline{(u_{1,1}')^3} / \left[\overline{(u_{1,1}')^2}\right]^{3/2} = A\left(\frac{15\nu}{\varepsilon}\right)^{3/2}. \tag{3.10.10}$$

The skewness is measured to be negative, the term given by (3.10.9) is positive. This is the turbulent vortex stretching source term in the equation for mean-square vorticity (2.8.2), by which the turbulence tends to enhance its own mean-square vorticity.

4. RAPID DISTORTION OF HOMOGENEOUS TURBULENCE

4.1 Introduction

The state of homogeneous turbulence changes significantly when it is subjected to mean strain. This occurs in practice whenever turbulence passes through a duct of variable cross-section, such as a nozzle, when turbulence is sheared by the mean flow, or when turbulence is subjected to a mean rotation. The general trends can be understood using vortex stretching concepts. For example, passing turbulence through an axisymmetric nozzle stretches the vortex filaments in the flow direction and tends to align them with the flow direction, *reducing* the turbulent fluctuations in the direction of flow but *increasing* the fluctuations transverse to the flow.

Because of the non-linearity of the governing equations, it is impossible to develop a rigorous theory of these processes. There are two alternative approaches to such a theory. The first is to use some sort of a *closure model* to produce a set of closed equations describing the evolution of statistical properties of the turbulence in response to the mean strain. The second approach is to simplify and then solve the exact equations for special cases. Both approaches are useful. In this chapter we examine *rapid distortion theory* (RDT), in which the exact equations for the fluctuation field are approximated in a way that is valid for very strong imposed mean strain rate, yielding linear equations amenable to exact solution.

It might be thought that the response to large strain rate could be calculated using the Reynolds stress transport equations (2.7.1), neglecting the terms that do not explicitly contain the mean velocity gradients. However, this analysis overpredicts the changes in the Reynolds stresses, because the pressure-strain term T_{ij} in (2.7.1) produces an immediate effect that reduces the impact of the production term P_{ij} by a factor of about 50%. The Poisson equation for the fluctuation pressure (2.5.3) shows that a sudden onset of mean velocity gradient *instantly* changes the fluctuation pressure field. The result is a sudden change of T_{ij} with the onset of applied S_{ij}, and this must be considered in the analysis. Turbulence modelers refer to the part of T_{ij} that changes suddenly with a sudden change in the mean deformation rate as the *rapid pressure strain* term. RDT plays a key role in understanding and modeling this term, and this chapter is intended to aid the use of RDT in this work.

The basic idea of RDT is that when $|S|q^2/\varepsilon \gg 1$ the time scale of the turbulence q^2/ε is long compared to that of the mean deformation, and so the turbulence does not have time to interact with itself. Thus, the non-linear terms in the governing equations (2.5.1)-(2.5.3) involving products of fluctuation quantities are neglected, and so the RDT equations are *linear* in the fluctuation quantities. The viscous terms are linear and can be included in the analysis, but are often neglected and will be here.

These equations contain the mean velocity gradients, which must be independent of position for homogeneous turbulence but may depend on time. The convective operators $\overline{D}$ contain the mean velocities, which must vary linearly with $\mathbf{x}$ in homogeneous turbulence. These coefficients prevent representation of the solution as periodic in the coordinates, and this hampers direct solution by Fourier methods. However, when transformed to coordinates marked on the mean flow at the start of the distortion, the variable coefficients are removed and the solution may be obtained by Fourier methods in the transformed system. This transformation is used in the numerical simulations of homogeneous turbulence (Rogallo 1981), where it permits the numerical solution to be *exact* for infinitely rapid distortions! The numerical simulations of the full equations carried out using this program are useful in helping assess the range of applicability of RDT, and it is rather surprising that, for some types of strain, RDT works remarkably well even at relatively low strain-rates (Lee and Reynolds 1985). Thus, RDT is becoming recognized as being very important and useful in turbulence analysis, modeling and simulation (Savill 1987).

4.2 The RDT equations

The most general mean velocity field in which homogeneous turbulence can exist is of the form

$$U_i = A_{ik}(t)x_k \tag{4.2.1a}$$

from which

$$U_{i,k} = A_{ik}(t). \tag{4.2.1b}$$

Note that (3.1.1) restricts the rotational history of the imposed mean deformation, but any mean strain rate history can be imposed.

Substituting (4.2.1) in (2.5.1), the inviscid RDT approximation for homogeneous turbulence is

$$\dot{u}_i' + A_{jk}x_k u_{i,j}' = -u_j' A_{i,j} - \frac{1}{\rho}p'_{,i}. \tag{4.2.2}$$

The continuity equation (2.3.4) also applies. We remind the reader that these equations hold if $\rho = \rho(t)$, so they can be applied in certain types of compressible flow situations.

Solution by Fourier methods is practical only if the coefficients in the equations are independent of $\mathbf{x}$. Therefore, it is necessary to transform the equations to remove the troublesome term on the left-hand side. The transformation is assumed to be

$$\xi_i = B_{ik}(t)x_k \qquad \tau = t. \tag{4.2.3}$$

Transforming (4.2.2) to the new coordinates, the left-hand side becomes

$$\frac{\partial u_i}{\partial \tau} + \frac{\partial u_i}{\partial \xi_n}\dot{B}_{nk}x_k + A_{jk}x_k\frac{\partial u_i}{\partial \xi_n}B_{nj}.$$

Setting the coefficient of x_k to zero to remove the variable coefficient,

$$\dot{B}_{nk} + A_{jk}B_{nj} = 0. \tag{4.2.4}$$

This defines the Rogallo transformation. The B_{ij} can be found by solving these linear equations, although a closed-form solution is not feasible. The transformation ties the new coordinate systems to the mean motion, with the new grid distorting and rotating as demanded by the mean flow. The Rogallo code for direct simulation of homogeneous turbulence operates in this coordinate system.

With this transformation the RDT momentum equations (4.2.2) become

$$\frac{\partial u_i'}{\partial \tau} = -u_j' A_{ij} - \frac{1}{\rho}\frac{\partial p'}{\partial \xi_k}B_{ki} \tag{4.2.5a}$$

and the continuity equation (2.3.4) becomes

$$\frac{\partial u_i'}{\partial \xi_k}B_{ki} = 0. \tag{4.2.5b}$$

The Poisson equation for the pressure fluctuation is obtained by taking the derivative of (4.2.5a) with respect to ξ_k and the derivative of (4.2.5b) with respect to τ and combining, using (4.2.4). Alternatively, one can simply transform (2.5.3). The result is

$$\frac{1}{\rho}\frac{\partial^2 p'}{\partial \xi_k \partial \xi_n}B_{ki}B_{ni} = -2B_{ki}A_{ij}\frac{\partial u_j'}{\partial \xi_k}. \tag{4.2.5c}$$

These linear equations can be solved to track the evolution of the Fourier coefficients of the velocity field in the *transformed* coordiates. The Reynolds stresses are integrals of this spectrum function, and the integrations may be carried out in the transformed coordinates. If the spectrum in the original coordinates is involved, the spectrum must be mapped back to $\mathbf{x}$ space using the coordinate transformation.

Closed-form solution of the RDT equations for a general problem is not possible. However, exact solutions for special cases can be obtained, in some cases in closed form and in others in terms of integrals. The general solution can be found as a power series in time. Some of these solutions that play useful roles in understanding turbulence and in turbulence modeling will now be discussed.

4.3 Response of turbulence to rapid rotation

RDT can be applied to study the effect of rapid rotation on turbulence in the absence of strain. Taking the rotation as clockwise about the x_3 axis, the mean velocity is

$$U_1 = \Gamma x_2 \qquad U_2 = -\Gamma x_1 \tag{4.3.1b}$$

and the coordinate transformation is (Fig. 4.3.1)

$$\xi_1 = x_1 \cos(\Gamma\tau) - x_2 \sin(\Gamma\tau) \tag{4.3.2a}$$

$$\xi_2 = x_2 \cos(\Gamma\tau) + x_1 \sin(\Gamma\tau) \tag{4.3.2b}$$

$$\xi_3 = x_3 \tag{4.3.2c}$$

$$\tau = t. \tag{4.3.2d}$$

Transforming, the RDT equations become

$$\frac{\partial u_1}{\partial \tau} = -\frac{1}{\rho}\left[\cos(\Gamma\tau)\frac{\partial p}{\partial \xi_1} + \sin(\Gamma\tau)\frac{\partial p}{\partial \xi_2}\right] - u_2\Gamma \tag{4.3.3a}$$

$$\frac{\partial u_2}{\partial \tau} = -\frac{1}{\rho}\left[-\sin(\Gamma\tau)\frac{\partial p}{\partial \xi_1} + \cos(\Gamma\tau)\frac{\partial p}{\partial \xi_2}\right] + u_1\Gamma \tag{4.3.3b}$$

$$\frac{\partial u_3}{\partial \tau} = -\frac{1}{\rho}\frac{\partial p}{\partial \xi_3}. \tag{4.3.3c}$$

The transformed continuity equation is

$$\frac{\partial u_1'}{\partial \xi_1}\cos(\Gamma\tau) + \frac{\partial u_1'}{\partial \xi_2}\sin(\Gamma\tau) - \frac{\partial u_2'}{\partial \xi_1}\sin(\Gamma\tau) + \frac{\partial u_2'}{\partial \xi_2}\cos(\Gamma\tau) + \frac{\partial u_3'}{\partial \xi_3} = 0. \tag{4.3.3d}$$

It is helpful to transform the velocity components to the rotating coordinate system. Denoting these velocities by v_i,

$$v_1 = u_1 \cos(\Gamma\tau) - u_2 \sin(\Gamma\tau) \tag{4.3.4a}$$

$$v_2 = u_2 \cos(\Gamma\tau) + u_1 \sin(\Gamma\tau) \tag{4.3.4b}$$

$$v_3 = u_3. \tag{4.3.4c}$$

Forming the equations for the new velocities form the old, one finds

$$\frac{\partial v_1}{\partial \tau} = -\frac{1}{\rho}\frac{\partial p}{\partial \xi_1} - 2v_2\Gamma \tag{4.3.5a}$$

$$\frac{\partial v_2}{\partial \tau} = -\frac{1}{\rho}\frac{\partial p}{\partial \xi_2} + 2v_1\Gamma \tag{4.3.5b}$$

$$\frac{\partial v_3}{\partial \tau} = -\frac{1}{\rho}\frac{\partial p}{\partial \xi_3} \tag{4.3.5c}$$

$$\frac{\partial v_i}{\partial \xi_i} = 0. \tag{4.3.5d}$$

The second terms on the right are of course the Coriolis terms.

Now we seek the solution for the evolution of the Fourier modes in the transformed space. Following the developments of section 3.3, we write

$$v_i' = \sum_{\underline{\kappa}} \hat{v}_i(\underline{\kappa}, t) e^{-i\kappa_n \xi_n} \tag{4.3.6a}$$

$$p' = \sum_{\underline{\kappa}} \hat{p}(\underline{\kappa}, t) e^{-i\kappa_n \xi_n} \tag{4.3.6b}$$

where $\underline{\kappa}$ is the wavenumber in the *transformed* coordinates Equating coefficients of like exponentials,

$$\frac{\partial \hat{v}_1}{\partial \tau} = \frac{i\kappa_1}{\rho}\hat{p} - 2\Gamma\hat{v}_2 \tag{4.3.7a}$$

$$\frac{\partial \hat{v}_2}{\partial \tau} = \frac{i\kappa_2}{\rho}\hat{p} + 2\Gamma\hat{v}_1 \tag{4.3.7b}$$

$$\frac{\partial \hat{v}_3}{\partial \tau} = \frac{i\kappa_3}{\rho}\hat{p} \tag{4.3.7c}$$

$$\kappa_i \hat{v}_i = 0. \tag{4.3.7d}$$

Applying the continuity equation (4.3.7d) to (4.3.7a-c),

$$\frac{1}{\rho}\hat{p} = \frac{2\Gamma(\hat{v}_2\kappa_1 - \hat{v}_1\kappa_2)}{i\kappa^2} \tag{4.3.8}$$

where $\kappa^2 = \kappa_1^2 + \kappa_2^2 + \kappa_3^2$. Substituting (4.3.8) in (4.3.7a-c), and seeking solutions of the form $\hat{v}_i(\underline{\kappa}, \tau) = a_i \exp(i\beta\tau)$, one obtains

$$i\beta a_1 - 2\Gamma\frac{\kappa_1}{\kappa^2}(a_2\kappa_1 - a_1\kappa_2) + 2\Gamma a_2 = 0 \tag{4.3.9a}$$

$$i\beta a_2 - 2\Gamma\frac{\kappa_2}{\kappa^2}(a_2\kappa_1 - a_1\kappa_2) - 2\Gamma a_1 = 0 \tag{4.3.9b}$$

$$i\beta a_3 - 2\Gamma\frac{\kappa_3}{\kappa^2}(a_2\kappa_1 - a_1\kappa_2) = 0. \tag{4.3.9c}$$

This linear equation system has non-trivial solutions only if the determinant of the coefficient matrix vanishes. This condition gives

$$\beta^2 = 4\Gamma^2\left(1 - \frac{\kappa_1^2 + \kappa_2^2}{\kappa^2}\right) = 4\Gamma^2\frac{\kappa_3^2}{\kappa^2} > 0. \tag{4.3.10}$$

Hence, except for modes with $\kappa_3 = 0$, the solutions are *undamped oscillations* in time at frequency $\beta(\underline{\kappa})$.

The $\kappa_3 = 0$ modes require special attention. They correspond to two-dimensional modes with their vorticity aligned with the rotation axis. The solution for these modes is

$$\hat{v}_1(\underline{\kappa}, \tau) = \hat{v}_1(\underline{\kappa}, 0) - C(\underline{\kappa})\kappa_2\tau \tag{4.3.11a}$$

$$\hat{v}_2(\underline{\kappa}, \tau) = \hat{v}_2(\underline{\kappa}, 0) + C(\underline{\kappa})\kappa_1\tau \tag{4.3.11b}$$

$$\hat{v}_3(\underline{\kappa}, \tau) = \hat{v}_3(\underline{\kappa}, 0) \tag{4.3.11c}$$

where

$$C = 2\Gamma\left(\frac{\kappa_1\hat{v}_1(\underline{\kappa}, 0) + \kappa_2\hat{v}_2(\underline{\kappa}, 0)}{\kappa^2}\right). \tag{4.3.11d}$$

But for $\kappa_3 = 0$ the numerator of C is zero by continuity, and hence the Fourier coefficients of these modes do not change under rapid rotation. Thus, these coefficients can also be regarded as undamped oscillations at frequency $\beta(\underline{\kappa})$.

The solution for the Fourier coefficients is therefore

$$\hat{v}_i = a_+ e^{i\beta\tau} + a_- e^{-i\beta\tau}. \tag{4.3.12}$$

$a_{1\pm}$ and $a_{2\pm}$ are related by (4.3.9a) or (4.3.9b),

$$\left(\pm i\frac{\kappa_3}{\kappa} + \frac{\kappa_1\kappa_2}{\kappa^2}\right)a_{1\pm} = \left(\frac{\kappa_1^2}{\kappa^2} - 1\right)a_{2\pm}. \tag{4.3.13}$$

The coefficients $a_{i\pm}$ are set by the initial values of the Fourier amplitudes,

$$\hat{v}_{i0} = a_{i+} + a_{i-} \tag{4.3.14}$$

where $\hat{v}_{i0}$ is the initial value of $\hat{v}_i(\underline{\kappa})$. Using (4.3.13) and (4.3.14), one finds

$$a_{1\pm} = \pm i\frac{\kappa}{2\kappa_3}\left[\left(\mp i\frac{\kappa_3}{\kappa} + \frac{\kappa_1\kappa_2}{\kappa^2}\right)\hat{v}_{10} + \left(1 - \frac{\kappa_1^2}{\kappa^2}\right)\hat{v}_{20}\right]. \tag{4.3.15}$$

Following section 3.4, the spectrum tensor E_{ij} (in the *rotating* coordinate system) is

$$E_{ij}(\underline{\kappa},\tau) = \left(\frac{L}{2\pi}\right)^3 < \hat{v}_i(\underline{\kappa},\tau)\hat{v}_j^*(\underline{\kappa},\tau) > . \tag{4.3.16}$$

Using the solution and a bit of algebra, one finds

$$E_{11}(\underline{\kappa},\tau) = \frac{\kappa^2}{4\kappa_3^2}\left\{2\left(\frac{\kappa_3^2}{\kappa^2}+\frac{\kappa_1^2\kappa_2^2}{\kappa^4}\right)E_{11}(\underline{\kappa},0) + 2\left(1-\frac{\kappa_1^2}{\kappa^2}\right)^2 E_{22}(\underline{\kappa},0) + \frac{\kappa_1\kappa_2}{\kappa^2}\left(1-\frac{\kappa_1^2}{\kappa^2}\right)\left(E_{12}(\underline{\kappa},0)+E_{21}(\underline{\kappa},0)\right)\right.$$

$$+2\left[\left(\frac{\kappa_3^2}{\kappa^2}-\frac{\kappa_1^2\kappa_2^2}{\kappa^4}\right)E_{11}(\underline{\kappa},0) - \left(1-\frac{\kappa_1^2}{\kappa^2}\right)^2 E_{22}(\underline{\kappa},0) - \frac{\kappa_1\kappa_2}{\kappa^2}\left(1-\frac{\kappa_1^2}{\kappa^2}\right)\left(E_{12}(\underline{\kappa},0)+E_{21}(\underline{\kappa},0)\right)\right]\cos(2\beta\tau)$$

$$\left.-2\left[\frac{\kappa_1\kappa_2\kappa_3}{\kappa^3}E_{11}(\underline{\kappa},0) + \frac{\kappa_3}{\kappa}\left(1-\frac{\kappa_1^2}{\kappa^2}\right)\left(E_{12}(\underline{\kappa},0)+E_{21}(\underline{\kappa},0)\right)\right]\sin(2\beta\tau)\right\}. \tag{4.3.17}$$

If the initial turbulence is isotropic, the initial spectrum is given by (3.7.14), and one finds that the coefficients of the sin and cos terms vanish; hence there is no change in the spectrum as viewed by an obsever in the rotating coordinate system. Since the spectrum is isotropic, the spectrum seen by a stationary observer is also unchanged. Thus, *rotation of itself will not distort the spectrum of isotropic turbulence.*

If thc initial spectrum is anisotropic, as for example produced by prior strain and associated rotation, the residual rotation will simply cause the spectrum to oscillate at a frequency $\omega = 2\beta(\underline{\kappa})$. The associated Reynolds stress (in the rotating frame), determined by integrating E_{11} over all $\underline{\kappa}$, will oscillate in a complicated manner that depends on the initial spectrum. However, using the symmetry property of the spectrum (3.4.13), the contribution of the $\sin(2\beta\tau)$ term to the integral is seen to vanish. Hence, relative to a rotating observer, the Reynolds stress oscillations can be expressed as an *even power series* in τ arising from the $\cos(2\beta\tau)$ term. Hence, the Reynolds stresses seen by a stationary observer would, to $O(t)$, appear to rotate in the manner described by the kinematic rotation terms, with deviations from this behavior being described by an *even* power series in time.

These are important results for turbulence modeling. Turbulence models, when reduced to the same rapid distortion approximations, should not show any effect of pure rotation (rotation without straining) on isotropic turbulence. Moreover, when applied to the pure rotation of anisotropic turbulence, the models should shown the kinematic rotation of the Reynolds stress described by (2.7.4), plus modifications by an *even* power series in time. This condition is very useful in setting coefficients in turbulence models, and we shall use it in Chapter 6.

4.4 Rapid isotropic compression or expansion

Consider next isotropic expansion (or compression) with

$$U_i = \Gamma x_i. \tag{4.4.1}$$

The RDT momentum equations are

$$\dot{u}_i' + \Gamma x u_{i,j}' = -\Gamma u_i' - \frac{1}{\rho(t)}p'_{,i}. \tag{4.4.2}$$

The density is given by the continuity equation,

$$\dot{\rho} = -3\rho\Gamma. \tag{4.4.3}$$

The RDT transformation is

$$\xi_i = x_i e^{-\Gamma t} \qquad \tau = t \tag{4.4.4}$$

and the transformed equations are

$$\frac{\partial u_i'}{\partial \tau} = -\Gamma u_i' - \frac{1}{\rho(t)}\frac{\partial p'}{\partial \xi_i}e^{-\Gamma t} \tag{4.4.6}$$

$$\frac{\partial u_i'}{\partial \xi_1} e^{-\Gamma t} = 0. \tag{4.4.7}$$

Multiplying (4.4.6) by u_i', the pressure term drops out by continuity (4.4.7). Averaging, we obtain the RDT approximation for the kinetic energy,

$$\frac{1}{2}\frac{dq^2}{d\tau} = -\Gamma q^2. \tag{4.4.8}$$

The solution is

$$q^2 = q_0^2 e^{-2\Gamma t} \tag{4.4.9}$$

where q_0^2 is the initial kinetic energy. Thus, the turbulence kinetic energy will decrease with expansion ($\Gamma > 0$) and increase with compression.

The evolution of the spectrum is obtained by solving the individual component equations. Fourier expansions are used as above. The pressure fluctuations (i.e. the rapid part) are zero by continuity, and all Fourier modes of the velocity vary as $exp(-\Gamma t)$. Thus, the spectrum retains its inital shape in the *stretched* coordinate system, and simply scales in magnitude with q^2. As a consequence the integral scale (3.4.15) varies in proportion to the strain,

$$\Lambda_f(t) = \Lambda_f(0) e^{\Gamma t}. \tag{4.4.10}$$

These results are useful in constructing turbulence models for compressible turbulence. Some of the turbulence models currently in use do not predict the proper behavior with compression, some even predicting an *increase* in length scale as turbulence is compressed!

4.5 Response of turbulence to rapid irrotational strain

RDT analysis for irrotational mean strain is neatly handled using the vorticity equation. Under the RDT approximations, with no mean rotation, (2.5.2) reduces to

$$\overline{D}\omega_i' = \omega_j' S_{ij} - \omega_i' S_{kk}. \tag{4.5.1}$$

We work in principal coordinates of S_{ij} and take

$$U_\alpha = \Gamma_\alpha(t) x_\alpha. \tag{4.5.2}$$

Recall that Greek indices are not summed. The RDT coordinate transformation is

$$\xi_\alpha = x_\alpha / e_\alpha \qquad\qquad \tau = t \tag{4.5.3a,b}$$

where

$$e_\alpha = \exp\left(\int_0^t \Gamma_\alpha(t')dt'\right) \tag{4.5.3c}$$

is the total strain in the α direction. The transformed vorticity equation is

$$\frac{\partial \omega_\alpha'}{\partial \tau} = \tilde{\Gamma}_\alpha \omega_\alpha' \tag{4.5.4a}$$

where

$$\tilde{\Gamma}_\alpha = \Gamma_\alpha - \Gamma_0 \tag{4.5.5a}$$

$$\Gamma_0 = \Gamma_1 + \Gamma_2 + \Gamma_3. \tag{4.5.5b}$$

The solution of (4.5.4) is

$$\omega_\alpha'(\mathbf{x}, \tau) = \omega_\alpha'(\mathbf{x}, 0)\tilde{e}_\alpha \tag{4.5.6}$$

where

$$\tilde{e}_\alpha = \exp\left(\int_0^t \tilde{\Gamma}_\alpha(t')dt'\right) \tag{4.5.7}$$

is a modified total strain in the α direction. This result clearly shows the essence of RDT; it computes the change in the turbulent state by considering the *rapid vortex streching* imposed by the mean field. The velocity field can be deduced from the vorticity field. In the transformed coordinates, the Poisson equation (1.9.5) for the velocity gives

$$\tilde{\nabla}^2 u_1' = \frac{\partial \omega_2'}{\partial \xi_3}\frac{1}{e_3} - \frac{\partial \omega_3'}{\partial \xi_2}\frac{1}{e_2} \tag{4.5.8a}$$

where the transformed Laplace operator is

$$\tilde{\nabla}^2 = \frac{1}{e_1^2}\frac{\partial^2}{\partial \xi_1^2} + \frac{1}{e_2^2}\frac{\partial^2}{\partial \xi_2^2} + \frac{1}{e_3^2}\frac{\partial^2}{\partial \xi_3^2}. \tag{4.5.8b}$$

The equations for ω_2' and ω_3' can be obtained by permuting the indices. The solution is obtained using Fourier expansions,

$$\omega_i'(\mathbf{x},\tau) = \sum_{\underline{\kappa}} \hat{\omega}_i(\underline{\kappa},\tau) e^{-i\kappa_n \xi_n} \tag{4.5.9a}$$

$$u_i'(\mathbf{x},\tau) = \sum_{\underline{\kappa}} \hat{u}_i(\underline{\kappa},\tau) e^{-i\kappa_n \xi_n} \tag{4.5.9b}$$

The solution for $\hat{u}_1$ is

$$\hat{u}_1 = \frac{i\left(\kappa_3\hat{\omega}_2/e_3 - \kappa_2\hat{\omega}_3/e_2\right)}{\frac{\kappa_1^2}{e_1^2} + \frac{\kappa_2^2}{e_2^2} + \frac{\kappa_3^2}{e_3^2}}. \tag{4.5.10}$$

The other components can be found by permutation of the indices.

The velocity spectrum function F_{ij} is related to the vorticity spectrum function H_{ij} by

$$E_{11}(\underline{\kappa},\tau) = \frac{\left(\frac{\kappa_3}{e_3}\right)^2 H_{22}(\underline{\kappa},0) + \left(\frac{\kappa_2}{e_2}\right)^2 H_{33}(\underline{\kappa},0) - 2\left(\frac{\kappa_2}{e_2}\right)\left(\frac{\kappa_3}{e_3}\right) H_{23}(\underline{\kappa},0)}{\left[\left(\frac{\kappa_1}{e_1}\right)^2 + \left(\frac{\kappa_2}{e_2}\right)^2 + \left(\frac{\kappa_3}{e_1}\right)^2\right]^2}. \tag{4.5.11}$$

From the solution for the vorticity evolution (4.6,6),

$$H_{\alpha\beta}(\underline{\kappa},\tau) = H_{\alpha\beta}(\underline{\kappa},0)\tilde{e}_\alpha \tilde{e}_\beta. \tag{4.5.12}$$

If we assume that the initial turbulence is isotropic, the initial vorticity spectrum is given by (3.7.23), with k replaced by κ. Using this spectrum and (4.5.12) in (4.5.11),

$$E_{11}(\underline{\kappa},\tau) = \frac{E(\kappa)}{4\pi\kappa^2}\frac{\left(\frac{\tilde{e}_2}{e_3}\right)^2\kappa_3^2(\kappa^2-\kappa_2^2) + \left(\frac{\tilde{e}_3}{e_2}\right)^2\kappa_2^2(\kappa^2-\kappa_3^2) + 2\left(\frac{\tilde{e}_2\tilde{e}_3}{e_2 e_3}\right)\kappa_2^2\kappa_3^2}{\left[\left(\frac{\kappa_1}{e_1}\right)^2 + \left(\frac{\kappa_2}{e_2}\right)^2 + \left(\frac{\kappa_3}{e_1}\right)^2\right]^2}. \tag{4.5.13}$$

The spectra of E_{22} and E_{33} can be found by permuting the indices.

The Reynolds stresses can now be calculated by integrating E_{ij} over all wavenumbers (see 3.4.6). The integrations are most easily carried out using spherical coordinates, and can be evaluated in closed form for a few very simple cases, such as isotropic compression. However, the general case of irrotational strain can be handled by power series expansion in the total strains. In (4.5.3c) we expand

$$e_\alpha = \exp(\alpha) = 1 + a_\alpha + \frac{1}{2}a_\alpha^2 + \ldots \tag{4.5.14}$$

The integrals are then expressed as power series in the a_α, and evaluated in spherical coordinates, where the angular integrations can be carried out analytically. The κ integration produces $q_0^2/3$, the initial isotropic value of R_{11}. Using this approach, the Reynolds stress R_{ij}, dissipation tensor D_{ij}, and vorticity $V_{11} = \overline{\omega_1'\omega_1'}$

were evaluated by the author and Moon Lee (Reynolds 1983) to $O(a^2)$. Subsequently Piomelli used the symbolic manipulation program MACSYMA to extend the Reynolds stress (the most important quantity for turbulence modeling) to $O(a^5)$ (Lee, Piomelli, and Reynolds 1986). The results are as follows (the other components can be found by permuting the indices):

$$R_{11} = q_0^2\left[\frac{1}{3} - \frac{1}{15}(2a_0 + 4a_1) + \frac{1}{105}(10a_0^2 + 12a_1^2 - 32a_2a_3) + \frac{1}{315}(-12a_0^3 + 48a_0a_2a_3 - 8a_1^3 + 48a_1a_2a_3)\right.$$

$$+\frac{1}{3465}(30a_0^4 + 32a_0^3a_1 - 48a_0^2a_1^2 - 128a_0^2a_2a_3 - 320a_0a_1a_2a_3 + 36a_1^4 - 32a_1^2a_2a_3 + 16a_2^2a_3^2)$$

$$+\frac{1}{225225}(-244a_0^5 - 1440a_0^4a_1 + 3360a_0^3a_1^2 - 4320a_0^2a_1^3 - 2488a_1^5 + 1200a_0^3a_2a_3 + 7600a_0^2a_1a_2a_3 + 4320a_0a_1^4$$

$$\left.-3440a_0a_1^2a_2a_3 - 880a_0a_2^2a_3^2 + 5200a_1^3a_2a_3 + 560a_1a_2^2a_3^2) + O(a^6)\right] \tag{4.5.15}$$

$$D_{11} = 2\varepsilon_0\left[\frac{1}{3} - \frac{2}{15}a_1 + \frac{1}{15}a_0 + O(a^2)\right] \tag{4.5.16}$$

$$V_{11} = \frac{\omega^2}{3}\left[1 + 2a_1 - a_0 + O(a^2)\right] \tag{4.5.17}$$

$$\varepsilon = \varepsilon_0\left[1 - \frac{1}{3}a_0 + O(a^2)\right] \tag{4.5.18}$$

$$b_{11} = -\frac{4}{15}a_1^* - \frac{4}{63}(a_1^{*2} + 2a_2^*a_3^*) + \frac{184}{1575}(a_1^{*3} - a_1^*a_2^*a_3^*) + \frac{124}{3465}(a_1^{*4} + 4a_1^{*2}a_2^*a_3^* - 2a_2^{*2}a_3^{*2})$$

$$+\frac{8}{23648625}(196819a_1^{*5} + 25189a_1^*a_2^{*2}a_3^{*2} - 479453a_1^{*3}a_2^*a_3^*) + O(a^{*6}) \tag{4.5.19}$$

where the Reynolds stress anisotropy tensor is

$$b_{ij} = \frac{R_{ij} - q^2\delta_{ij}/3}{q^2} \tag{4.5.20}$$

and the anisotropic strain components are

$$a_\alpha^* = a_\alpha - \frac{1}{3}a_0. \tag{4.5.21}$$

Note that the anisotropy tensor b_{ij} is depends only on the total anisotropic strain, and is independent of the strain-rate history. These results are useful in turbulence modeling where one seeks to develop models that will be consistent with RDT when the RDT approximations are applied to the model.

4.6 Combinations of strain and rotation

The general RDT problem for homogeneous turbulence involves combinations of strain and rotation, for which a general solution can be developed in symbolic form (Cambon 1981). Using the Fourier expansions (4.5.9) and a similar one for the pressure, (4.2.5c) is first solved to express the Fourier coefficients of the pressure in terms of those of the velocity,

$$\frac{1}{\rho}\hat{p} = -\frac{2i\kappa_k B_{ki}A_{ij}}{\kappa_n\kappa_m B_{mp}B_{np}}\hat{u}_j. \tag{4.6.1}$$

Then, the Fourier expansion of (4.2.5a) gives

$$\frac{\partial\hat{u}_i}{\partial\tau} = -A_{ij}\hat{u}_j + \frac{2\kappa_k B_{ki}\kappa_q B_{qp}}{\kappa_n\kappa_m B_{ms}B_{ns}}A_{pj}\hat{u}_j = H_{ij}\hat{u}_j. \tag{4.6.2}$$

Following Cambon, the solution can be expressed using Green's functions,

$$\hat{u}_i(\underline{\kappa},\tau) = G_{ik}(\underline{\kappa},\tau)\hat{u}_k(\underline{\kappa},0) \tag{4.6.3}$$

where the Green's functions are given by the solution of

$$\frac{\partial G_{ij}(\underline{\kappa},\tau)}{\partial \tau} = H_{ik}(\underline{\kappa},\tau)G_{kj}(\underline{\kappa},\tau) \qquad G_{ij}(\underline{\kappa},0) = \delta_{ij}. \tag{4.6.4}$$

This allows the spectrum tensor E_{ij} to be expressed in terms of the initial spectrum,

$$E_{ij}(\underline{\kappa},\tau) = G_{ip}(\underline{\kappa},\tau)G^*_{jq}(\underline{\kappa},\tau)E_{pq}(\underline{\kappa},0). \tag{4.6.5}$$

The Reynolds stresses are then simply integrals of the spectrum function over all $\underline{\kappa}$.

This method of solution is instructive for looking at the structure of the solution, but the calculations for the Reynolds stresses require approximate evaluation of the integrals, for example by power series expansions. Moreover, when the principal axes of the strain rate vary with time the Green's functions are not easily obtained, except perhaps as power series in time. If one is going to resort to series solution, a direct solution by power series in time is simpler. We will develop this here for future reference.

A *superscript summation convention* aids the analysis. We denote a series by

$$A = \sum_{n=0}^{\infty} A^{(n)}t^n = A^{(n)}t^n. \tag{4.6.6}$$

Any repeated superscript or power is summed over all possible values. The delimiters on the superscripts establish the range, with ( ) establishing a lowest value of 0 and [ ] establishing a lowest value of unity. Muliplication of two series and sorting out of powers of t is then very easily accomplished. For example, simply replacing n by $r-m$ in the product below collects the coefficient of t^r,

$$AB = A^{(n)}t^n B^{(m)}t^m = A^{(r-m)}B^{(m)}t^r. \tag{4.6.7}$$

Here the delimiters correctly establish that the m summation in the coefficient of t^r is from 0 to r. The leading coefficients can also be extracted,

$$A^{(r-m)}B^{(m)} = A^{(r)}B^{(0)} + A^{(0)}B^{(r)} + A^{[r-m]}B^{[m]} \tag{4.6.8}$$

where the m sum at the end now ranges from 1 to $r-1$.

We treat a general case of arbitrary strain and initial rotation as applied to initially isotropic turbulence, and express the velocity gradient tensor A_{ik} (see 4.2.1) as

$$A_{ik}(t) = S_{ik}(t) + \frac{1}{2}\epsilon_{kiq}\Omega_q(t). \tag{4.6.9}$$

The strain-rate history described by $S_{ik}(t)$ and the initial rotation described by $\Omega_i(0)$ will be arbitrary, and the rotation history is governed by (3.1.1).

Expanding,

$$\begin{aligned} S_{ik} &= S^{(n)}_{ik}t^n & \Omega_q &= \Omega^{(n)}_q t^n \\ A_{ik} &= A^{(n)}_{ik}t^n & B_{ik} &= B^{(n)}_{ik}t^n \\ \hat{u}_i &= \hat{u}^{(n)}_i t^n & \hat{p} &= \hat{p}^{(n)}t^n. \end{aligned} \tag{4.6.10}$$

The coefficients then are generated recursively. From (3.1.1)

$$(r+1)\Omega_i^{(r+1)} = \Omega_j^{(r)}S_{ij}^{(r-q)} - \Omega_i^{(r)}S_{jj}^{(r-q)}. \tag{4.6.11}$$

From (4.6.11)

$$A_{ik}^{(r)} = S_{ik}^{(r)} + \frac{1}{2}\epsilon_{kiq}\Omega_q^{(r)}. \tag{4.6.12}$$

From (4.2.4)

$$(r+1)B_{nk}^{(r+1)} = -A_{jk}^{(r-q)}B_{nj}^{(q)} \qquad B_{nk}^{(0)} = \delta_{nk}. \tag{4.6.13a,b}$$

The Fourier representation (in stretched space) of (4.2.5a) gives

$$(r+1)\hat{u}_i^{(r+1)} = -\hat{u}_j^{(r-q)}A_{ij}^{(q)} + \frac{1}{\rho}i\kappa_k\hat{p}^{(r-q)}B_{ki}^{(q)}. \tag{4.6.14}$$

The continuity condition (4.2.5b) gives

$$\kappa_k\hat{u}_i^{(r-q)}B_{ki}^{(q)} = 0. \tag{4.6.15}$$

The Fourier representation of the Poisson equation (4.2.5c) gives

$$-\frac{1}{\rho}\kappa_k\kappa_n\hat{p}^{(q-r)}B_{ki}^{(r-s)}B_{ni}^{(s)} = 2i\kappa_k B_{ki}^{(q-r)}A_{ij}^{(r-s)}\hat{u}_j^{(s)}. \tag{4.6.16}$$

Extracting the leading pressure term given by $r = 0$,using (4.6.15b),

$$-\frac{1}{\rho}\kappa^2\hat{p}^{(q)} = \frac{1}{\rho}\kappa_k\kappa_m\hat{p}^{(r-q)}1^{[r]}B_{ki}^{(q-s)}B_{mi}^{(s)} + 2i\kappa_k B_{ki}^{(q-r)}A_{ij}^{(r-s)}\hat{u}_j^{(s)} \tag{4.6.17}$$

where the notation $1^{[r]}$ forces $r > 0$ in the sum.

The procedure is now very simple. At each order r, one finds the rotation term from from (4.6.11), the velocity gradient term from (4.6.12), the transformation term from (4.6.13), the pressure term from (4.6.17), and the velocity terms from (4.6.14). The spectrum tensor is expressed as a similar series expansion, and its terms are generated and integrated in spherical coordinates to calculate the Reynolds stresses, much as in the previous section. This is a natural task for a symbolic manipulator like MACSYMA. The result would enable the determination of all unknown coefficients in the model for the rapid pressure strain term (see Chapter 6); we are attempting to carry out this evaluation.

4.7 Two-dimensional turbulence

RDT of two-dimensional turbulence is useful for testing the range of performance of turbulence models. Stanford student Laura Pauley carried out an RDT analysis of initially axisymmetric two-dimensional turbulence for three-dimensional irrotational strain along the principal axes of b_{ij}, with $b_{22} = -1/3$. Her results are

$$R_{11} = \frac{q_0^2}{2}\left\{1 + [a_1 + 2\tilde{a}_2 + a_3] + \left[\frac{1}{2}(a_1^2 + a_3^2) + a_1a_3 + 2\tilde{a}_2(a_1 + \tilde{a}_2 + a_3)\right]\right.$$

$$\left. + \left[-\frac{11}{24}a_1^3 - \frac{5}{8}a_1^2a_3 - \frac{11}{8}a_1a_3^2 - \frac{101}{24}a_3^3 + \tilde{a}_2(a_1^2 + a_3^2 + 2a_1a_3) + 2\tilde{a}_2^2\left(a_1 + \frac{2}{3}\tilde{a}_2 + a_3\right)\right] + O(a^4)\right\} \tag{4.7.1}$$

$$b_{11} = \frac{1}{6}\left[1 + \frac{45}{8}(a_1^3 - a_3^3) + \frac{9}{8}(a_1^2a_3 - a_1a_3^2) + O(a^4)\right] \tag{4.7.2}$$

where the total strain in the i^{th} direction is $e_i = \exp(a_i)$, $\tilde{a}_2 = a_2 - a_0$ and $a_0 = a_1 + a_2 + a_3$. Note that strain aligned with the vorticity does not affect the anisotropy, and that changes in anisotropy do not occur until third order. It would be instructive and useful to extend this analysis to more general 2-D cases including rotation and strain not aligned with the principal axes of b_{ij}.

5. MODELING SCALE EVOLUTION IN HOMOGENEOUS TURBULENCE

5.1 Introduction

This chapter and the next are devoted to one-point models of homogeneous turbulence. Here we deal with modeling the evolution of the length and time scales, assuming that whatever must be known about the tensor character of the turbulence can be generated by an anisotropy model. Anisotropy modeling is addressed in the subsequent chapter.

The turbulent kinetic energy equation provides the equation for the turbulence velocity scale q^2. For homogeneous turbulence (2.6.2) becomes

$$(\dot{q^2}) = 2(P - \varepsilon). \tag{5.1.1}$$

If the other model scale variable is ε, this equation is closed. Alternatively, if one choses to use a time scale variable τ instead, a model relating ε to τ is required. There are many clues that the use of a time scale as the second scale parameter would offer advantages in modeling more general flows. Where it becomes desirable to think along these lines we will use the large-eddy time scale identified in Chapter 3,

$$\tau = \frac{q^2}{\varepsilon}. \tag{5.1.2}$$

Following the most popular current trend, we shall start by using a model equation for ε as our second equation. In homogeneous turbulence (see 3.6.4) $\varepsilon = \nu\omega^2$, and so the ω^2 equation (2.8.12) yields the ε (care must be taken to account for the density change when introducing ν). For homogeneous turbulence with $\rho = \rho(t)$ and $\mu =$ constant the result is

$$\dot{\varepsilon} = 2\nu\overline{\omega_i'\omega_j'}S_{ij}^* - \frac{1}{3}\varepsilon S_{kk} + 2\Omega_j\overline{s_{ij}'\omega_i'} + 2\nu\overline{\omega_i'\omega_j's_{ij}'} - 2\nu^2\overline{\omega_{i,j}'\omega_{i,j}'} \tag{5.1.3}$$

where

$$S_{ij}^* = S_{ij} - \frac{1}{3}S_{kk}\delta_{ij} \tag{5.1.4}$$

is the anisotropic strain rate. The last two terms provide the means by which ε changes in isotropic turbulence. In addition, we see that incompressible strain, isotropic volume change, and rotation will also modify the evolution of ε. We shall address these issues separately.

5.2 Decay of isotropic turbulence

With no production the energy equation gives

$$\dot{q^2} = -2\varepsilon \tag{5.2.1}$$

Assuming that one can make a model using only q^2 and ε as variables, the form of the ε equation for isotropic turbulence can be deduced by dimensional analysis,

$$\dot{\varepsilon} = -C_{\varepsilon 0}\frac{\varepsilon^2}{q^2} \tag{5.2.2}$$

where the coefficient $C_{\varepsilon 0}$ can depend on the turbulence Reynolds number (see 3.2.2) $R_T = q^4/(\nu\varepsilon)$. This is the form used by all models of this type.

Insight is obtained by recognizing that the right hand side of (5.2.1) comes from the difference of the last two terms in (5.1.3). The first of these is the turbulent vortex stretching term, which is related to the derivative skewness by (3.10.9). The last term can be written as

$$2\nu^2\overline{\omega_{i,j}'\omega_{i,j}'} = 2\nu^2\int_0^\infty k^4E(k)dk \tag{5.2.3}$$

which shows that it is dominated by the smallest scales of motion and hence should scale on the Kolmogorov variables. It can be estimated using the model spectrum of Fig 3.9.4. Using these two estimates for isotropic

turbulence, put in terms that resemble the model equation (5.2.1), one finds that both terms scale as $\sqrt{R_T}$, and

$$\dot{\epsilon} = \sqrt{R_T}\left[-\gamma\frac{35}{2}\left(\frac{1}{15}\right)^{3/2} - \frac{3\alpha}{10}\left(\frac{4}{3\alpha}\right)^{5/2}\right]\frac{\epsilon^2}{q^2}. \tag{5.2.4}$$

Experiments clearly indicate that a constant coefficient $C_{\epsilon 0}$ does a very adequate job at high Reynolds numbers, which means that the *difference* in the two terms within the brackets in (5.2.4) must decrease as $1/\sqrt{R_T}$. Both terms are very large and they are nearly in balance (an estimate of the skewness can be made from this balance). It would be unwise to model these two large terms separately when we only need their difference, and for this reason the two are lumped together in (5.2.2).

The value of $C_{\epsilon 0}$ can be determined by fitting the energy decay rate for isotropic turbulence to that measured experimentally, and this is what most modelers have done. The exact solution of the q^2 and ϵ model equations is

$$q^2 = q_0^2(1 + t/a)^{-n} \qquad \epsilon = \epsilon_0(1 + t/a)^{-(n+1)} \tag{5.2.5a, b}$$

$$a = \frac{q_0^2}{2\epsilon_0} \qquad n = \frac{2}{(C_{\epsilon 0} - 2)} \tag{5.2.5c, d}$$

The subscripts 0 denote initial values. The best experiments suggest n should be in the range 1.1-1.3. At low Reynolds numbers, where the turbulence is in its *final period*, $n = 5/2$ is found theoretically and confirmed experimentally.

The model spectrum (3.9.4) can be used to find n (Reynolds 1976) by assuming that the spectrum is permanent below k_L, i.e. that the low wavenumber spectrum parameter A is constant. Expressing ϵ in terms of q^2 and A using (3.9.5) and (3.9.6), then using this in (5.2.1) to find the q^2 history, one obtains (5.2.4a) with $n = (2m + 2)/(m + 3)$. This clearly supportes the idea that the low wavenumber part of the spectrum affects the energy decay rate. The k^4 spectrum ($m = 4$) gives $n = 10/7$, which is really too high to fit the best experiments very well. However, the k^2 spectrum, with $m = 2$, gives $n = 6/5$, in quite good agreement with experiments. In a finite-Fourier series representation, the assignment of the same energy to each low wavenumber Fourier mode would make E_{ii} independent of $\mathbf{k}$ and hence $E(k)$ vary like k^2, and so k^2 turbulence can be thought of as being *equipartitioned* at low wavenumbers.

With $n = 6/5$ as suggested by both the experiments and the k^2 spectrum, $C_{\epsilon 0} = 11/3$, and this is the value that we prefer. It is very close to the value of 3.84 used by many $k - \epsilon$ modelers.

5.3 Isotropic compression

For isotropic turbulence, $R_{ij} = q^2\delta_{ij}/3$. Denoting $S_{kk} = 3\Gamma$ (see 4.4.1), and assuming isotropic volume change with $\rho = \rho(t)$, the energy equation (2.6.2) reduces to

$$\dot{q^2} = -2\Gamma q^2 - 2\epsilon. \tag{5.3.1}$$

The ϵ must be modified to account for the change in volume. The exact ϵ equation (5.1.3) suggests that this modification might be

$$\dot{\epsilon} = -C_{\epsilon 0}\frac{\epsilon^2}{q^2} - \epsilon\Gamma. \tag{5.3.2}$$

For very large Γ the solutions to the above equations are

$$q^2 = q_0^2 e^{-2\Gamma t} \tag{5.3.3a}$$

$$\epsilon = \epsilon_0 e^{-\Gamma t} \tag{5.3.3b}$$

The energy development matches RDT (4.4.9). If we assume that the integral scale is proportional to q^3/ϵ, the large-eddy length scale, then according to (5.3.3) the length scale varies as $\exp(-2\Gamma t)$. This says that expanding the flow volume will *reduce* the length scale, which should be disturbing to anyone and is not in agreement with RDT. Nevertheless, this modification of the ϵ equation was used for some time in i.c. engine modeling before the problem was noted (Reynolds 1980).

The RDT analysis suggests instead that the ϵ equation for this problem should be

$$\dot{\epsilon} = -C_{\epsilon 0}\frac{\epsilon^2}{q^2} - \frac{4}{3}\epsilon S_{kk} \tag{5.3.4}$$

For rapid volume change this produces

$$\epsilon = \epsilon_0 e^{-4\Gamma t} \tag{5.3.5}$$

for which the length scale varies in proportion to the strain, i.e. as $\exp(\Gamma t)$.

This example points out the pitfalls of using the exact equation for ϵ as the basis for its model equation. To paraphrase Saffman, one should model the *Physics* and not the *equations*.

5.4 Rotation

Experiments and numerical simulations show that rotation does not appreciably alter the anisotropy of isotropic turbulence. RDT (section 4.6) showed that rotation does not affect much of the spectrum at all, but does tend to produce a slow growth in the energy of the two-dimensional component of the turbulence aligned with the axis of rotation. The simulations (Bardina et al 1985) reflect this growth as a change in the integral scales, with the scale in the direction of the rotation axis becoming longer than the other two as time passes. Rotation also reduces the dissipation rate, apparently by inhibiting the energy transfer cascade.

Most turbulence models in use today show *no* effect of pure rotation on ϵ, a weakness that has been slow to receive correction. Bardina found that his large-eddy simulations and Wiegland and Nagib's (1978) experimental data could both be predicted extremely well using a simple modification of the ϵ equation,

$$\dot{\epsilon} = -\frac{11}{3}\frac{\epsilon^2}{q^2} - C_{\epsilon\Omega}\epsilon\Omega \tag{5.4.1a}$$

where Ω is the rms rotation rate

$$\Omega = \sqrt{\Omega_{ij}\Omega_{ij}}. \tag{5.4.1b}$$

Bardina found that $C_{\epsilon\Omega} = 0.15/\sqrt{2}$ worked well, and we adopt this value.

The imposition of a mean strain-rate provides a source of turbulent kinetic energy through the turbulence production term (2.6.3). We assume that the anisotropy part of the turbulence model will produce R_{ij} values given q^2 and ϵ, hence P need not be modeled. Thus, no modeling for the q^2 equation is required for homogeneous turbulence.

The associated changes in the dynamics of ϵ must be incorporated in the ϵ model equation. To date the most effective means for doing this is to add a term proportional to P,

$$\dot{\epsilon} = -C_{\epsilon 0}\frac{\epsilon^2}{q^2} - C_{\epsilon\Omega}\epsilon\Omega + C_{\epsilon P}\frac{P\epsilon}{q^2} \tag{5.4.1}$$

An estimate of $C_{\epsilon P}$ can be made using the homogeneous shear flow data of Tavoularis and Corrsin (1981). Homogeneous shear flow apparently reaches an equilibrium structure in which the Reynolds stresses all scale with the turbulent kinetic energy. The energy and dissipation rate both increase with time in a manner that keeps the turbulence time scale very nearly constant at a value set by the mean shearing rate $\Gamma = dU_1/dx_2$. The equation for τ, derived from (5.1.2) using (5.1.1) and (5.4.1), is

$$\dot{\tau} = (C_{\epsilon 0} - 2) + C_{\epsilon\Omega}\Omega\tau - (C_{\epsilon P} - 2)\frac{P}{\epsilon}. \tag{5.4.2}$$

The experiments gave $\Gamma q^2/\epsilon = 12.7$, corresponding to $\Omega\tau = 8.98$, and $P/\epsilon = 1.8$, Using $C_{\epsilon 0} = 11/3$ and $C_{\epsilon\Omega} = 0.15/\sqrt{2}$, a constant value of τ requires $C_{\epsilon P} = 3.45$. This is somewhat higher than the value that Bardina recommended, which was based on his large eddy simulations of strained flows.

Most $k-\epsilon$ models used today do not include the $C_{\epsilon\Omega}$ term. For plane shear flows the rotation term and the production terms have the same form, and when these terms are into a single term expressed as in the form of the production term the resulting combined coefficient based on the above coefficients is about 3.0, which is very close to the value of 2.88 used in many $k-\epsilon$ models.

5.5 Proposal for a simple $k-\tau$ model

Compared to the ϵ equation (5.4.1), the τ equation (5.4.2) is impressive in its simplicity. When one examines models for inhomogeneous turbulence, q^2/ϵ frequently appears, suggesting that the time scale might be preferable to ϵ as the second model variable. The choice should be based on the ease with which the model extends to new situations. The diffusion terms required for inhomogeneous flows are particularly useful in evaluating various proposals.

For example, consider what happens to the terms in the ϵ equation near a solid boundary. The ϵ^2/q^2 term goes to infinity, but the $P\epsilon/q^2$ term goes to zero. Consequently, a great deal of effort has been spent inventing near-wall patches for these terms. One does not excape these simply by changing variables, unless a slight modification is made. In contrast, Wilcox (1986), who uses a reciprocal time scale in place of ϵ, achieves reasonable near-wall solutions, even in the viscous region, with *no* near-wall modifications of his model equation.

Two-equation models have been criticized because the length scales are anisotropic in anisotropic turbulence but the model assumes isotropy of length scale. The success that two-equation models enjoy would seem remarkable in the light of this objection. But suppose it is really *time scale* information that is carried by ϵ, and that the anisotropy of length scales is reflected by anisotropy of R_{ij}.

Another clue is provided by the case of isotropic volume change, for which the τ equation is

$$\dot{\tau} = (C_{\epsilon 0} - 2) - \frac{4}{3} S_{kk} \tau. \tag{5.5.1}$$

Note the appearance of the strain rate term.

It is suggested that it might be better to replace the production term in the τ equation by a term proportional to the rms strain rate. Some additional simplicity of form is obtained by using the kinetic energy $k = q^2/2$ and redefining the time scale and turbulent Reynolds number by

$$\tilde{\tau} = k/\epsilon \qquad \tilde{R}_T = k\tilde{\tau}/\nu \tag{5.5.2a, b}$$

The model equation proposed is

$$\dot{\tilde{\tau}} = C_{\tilde{\tau}0} + C_{\tau\Omega}\Omega\tilde{\tau} - C_{\tau S^*} S^* \tilde{\tau} - \frac{4}{3} S_{kk} \tilde{\tau}. \tag{5.5.3}$$

Here S^* is the rms anisotropic strain rate

$$S^* = \sqrt{S^*_{ij} S^*_{ij}} \tag{5.5.4a}$$

determined from the anisotropic strain rate tensor

$$S^*_{ij} = S_{ij} - \frac{1}{3} S_{kk} \delta_{ij}. \tag{5.5.4b}$$

Note that none of these terms is ill-behaved at the wall, and so there is hope that the near-wall modifications can be much simpler. The constants for this model, evaluated in the same manner as those in the ϵ equation, are

$$C_{\tilde{\tau}0} = 5/6 \qquad C_{\tau\Omega} = 0.11 \qquad C_{\tau S^*} = 0.60. \tag{5.5.5a, b, c}$$

Exploration of this idea is encouraged.

6. MODELING ANISOTROPY IN HOMOGENEOUS TURBULENCE

6.1 Description of anisotropy

The scale equations developed in the previous chapter are closed only for isotropic turbulence. In general, the Reynolds stress tensor must also be determined by the model. The *Reynolds stress anisotropy tensor*

$$b_{ij} = \frac{R_{ij} - \frac{1}{3}q^2\delta_{ij}}{q^2} \tag{6.1.1}$$

is a very convenient way to describe the deviations from isotropy. This chapter deals with b_{ij} and its modeling, which must be done with great care if unrealistic predictions are to be avoided.

The anisotropy tensor has some important properties that need to be kept firmly in mind. By definition it is *trace free*,

$$b_{ii} = 0. \tag{6.1.2}$$

It is often convenient to think of b_{ij} in its principal coordinates, where only diagonal elements are non-zero. By (6.2.1) the sum of these principal values is zero, so only *two* are independent. This means that the anisotropy can be characterized by two independent invariants,

$$\mathrm{II} = -b_{ij}b_{ji}/2 \qquad \mathrm{III} = b_{ij}b_{jk}b_{ki}/3. \tag{6.1.3a,b}$$

If the turbulence is *two-dimensional*, meaning that one (principal-axis) velocity component is always zero, by the definition (recall Greek indices are not summed)

$$b_{\alpha\alpha} = -1/3 \qquad \text{if} \qquad R_{\alpha\alpha} = 0. \tag{6.1.4}$$

And, if all of the energy becomes concentrated in one component,

$$b_{\alpha\alpha} = 2/3 \qquad \text{if} \qquad R_{\alpha\alpha} = q^2. \tag{6.1.5}$$

This is called *one-dimensional turbulence*. Note that the one non-zero velocity component could be a function of the other two coordinates, say $u_1'(x_2, x_3, t)$, so that the flow would resemble a honeycomb of opposing jets.

Thus, the possible values of the two independent principal $b_{\alpha\alpha}$, say b_{11} and b_{22}, must lie within the triangle on Fig 6.1.1. The vertices correspond to the three possible states of one-dimensional turbulence, and the sides to states of two-dimensional turbulence. The isotropic state is the origin. The diagonal lines, along which two principal components are the same, are states of *axisymmetric turbulence*.

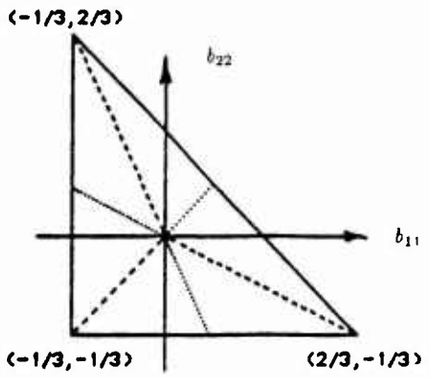

Figure 6.1.1 Range of possible principal values of the anisotropy tensor

Note that one can either move along an axisymmetric line away from isotropy to a two-dimensional state (edge) or to a one-dimensional state (vertex). These limiting cases may seem extreme. However, turbulence near a wall is two-dimensional (the normal component vanishes), and turbulence in a strongly sheared layer moves remarkably far towards one-dimensionality.

In homogeneous turbulence, the move towards a two-dimensional state is made by straining the turbulence in one direction and contracting it equally in the other two. This stretches vortex filaments in the direction of positive strain, aligning these filaments with the flow and thereby reducing the fluctuations in the direction of positive strain. This is what happens to turbulence when it is passed through an *axisymmetric contraction.*

The move towards a one-dimensional state is achieved by straining the flow equally in two orthogonal directions, and contracting it in the third, as one could do in an axisymmetric diffuser (using boundary layer suction to prevent separation). The vortex cores are stretched out to form sheets (pancakes) and the limiting one-dimensional case corresponds to a honeycomb of two-dimensional vorticity. We will call this type of deformation *axisymmetric expansion.*

An equivalent and less specific way to characterize the anisotropy is through the *anisotropy invariant map* introduced by Lumley. For axisymmetric turbulence we write the anisotropy tensor in principal coordinates as

$$b_{ij} = \begin{pmatrix} a & 0 & 0 \\ 0 & a & 0 \\ 0 & 0 & -2a \end{pmatrix}. \tag{6.1.6}$$

Then

$$\mathrm{II} = -3a^2 \qquad \mathrm{III} = -2a^3. \tag{6.1.7}$$

Along lines where $a < 0$ so that the component along the axis is more energetic than the other two (axisymmetric expansion),

$$\mathrm{III} = +2\left(\frac{-\mathrm{II}}{3}\right)^{3/2} \tag{6.1.7a}$$

while if $a > 0$ so that the axis component is less energetic (axisymmetric contraction)

$$\mathrm{III} = -2\left(\frac{-\mathrm{II}}{3}\right)^{3/2}. \tag{6.1.7a, b}$$

The two-dimensional boundaries can be studied in principal coordinates, writing

$$b_{ij} = \begin{pmatrix} -\frac{1}{3} & 0 & 0 \\ 0 & \frac{a+1}{6} & 0 \\ 0 & 0 & \frac{a-1}{6} \end{pmatrix}. \tag{6.1.8}$$

Then

$$\mathrm{II} = -\frac{1}{12}\left(1 + \frac{a^2}{3}\right) \qquad \mathrm{III} = \frac{a^2 - 1}{108} \tag{6.1.9a, b}$$

so that it for two-dimensional turbulence

$$G = \frac{1}{9} + \mathrm{II} + 3\mathrm{III} = 0. \tag{6.1.10}$$

Using these results, the range of possible turbulence states is shown in the invariant map of Fig. (6.1.2). The origin is the isotropic state, the upper boundary is the locus of two-dimensional states, the two sides are the two types of axisymmetric states, and the upper vertex is the one-dimensional state. The anisotropy invariant map is a very useful way to characterize the state of turbulence in modeling, simulations, and experiments.

Two tensors that can be formed from the anisotropy tensor are its square,

$$b^2_{ij} = b_{ik}b_{kj} \tag{6.1.11}$$

and its cube,

$$b_{ij}^3 = b_{in}b_{nm}b_{mj}. \tag{6.1.12}$$

The *Cayley-Hamilton theorem* of linear algebra says that a matrix satisfies its own characteristic equation, which in this instance means that

$$b_{ij}^3 + \mathrm{II}b_{ij} - \mathrm{III}\delta_{ij} = 0 \tag{6.1.13a}$$

or alternatively

$$b_{ij}^3 = \frac{1}{2}b_{kk}^2 b_{ij} + \frac{1}{3}b_{kk}^3\delta_{ij}. \tag{6.1.13b}$$

Hence, b_{ij}^3, and all higher powers of the tensor, are linearly dependent on the lower powers and hence do not contain new tensorial structure beyond that in b_{ij}^2, b_{ij}, and δ_{ij}. As we shall see, this is very important in turbulence modeling. Readers not familiar with this important theorem may find it instructive to verify (6.3.13b) by writing b_{ij} in its principal coordinates, carrying out the products using the trace-free condition to express one of the principal values in terms of the other two.

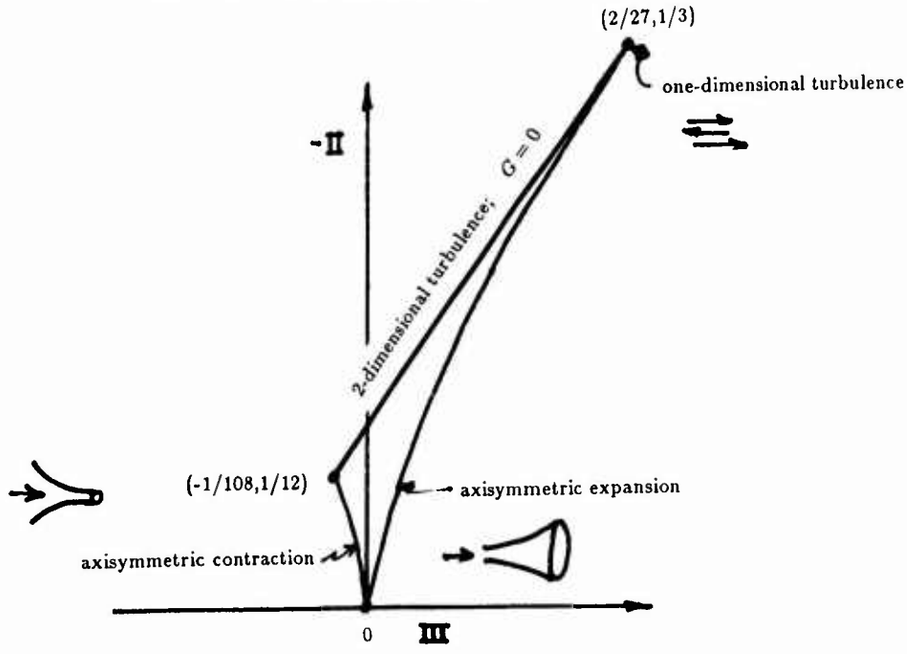

Figure 6.1.2 Anisotropy invariant map

6.2 Evolution equation for the anisotropy tensor

Using the evolution equation for R_{ij} (2.7.1) and the definition of b_{ij}, the equation for evolution of b_{ij} in homogeneous turbulence with $\rho = \rho(t)$ can be written as

$$\dot{b}_{ij} = -\frac{2}{3}S_{ij}^* - (b_{ik}S_{kj}^* + b_{jk}S_{ki}^* - \frac{2}{3}b_{nm}S_{nm}^*\delta_{ij}) + 2b_{nm}S_{nm}^*b_{ij}$$

$$+(b_{ik}\Omega_{kj} + b_{jk}\Omega_{ki}) + \frac{1}{q^2}[T_{ij} - (D_{ij} - \frac{1}{3}D_{kk}\delta_{ij})] + 2\frac{\epsilon}{q^2}b_{ij} \tag{6.2.1}$$

Here S^*_{ij} is the anisotropic strain rate tensor defined by (5.5.4). Note that only anisotropic strain produces Reynolds stress anisotropy, and that the right hand side is properly trace-free. The terms containing the mean rotation tensor Ω_{ij} represent a kinematic rotation of the anisotropy tensor. When used in conjunction with q^2 and ε equations, models for the pressure-strain term T_{ij} and the anisotropy of the dissipation tensor D_{ij} must be provided.

There is a class of turbulence models called *algebraic two-equation models* in which it is assumed that the turbulence structure has reached an equilibrium state determined by a balance of the terms on the right hand side of (6.2.1). For example, the standard $k-\varepsilon$ model uses an algebraic equation equivalent to

$$b_{ij} = -\frac{C_\mu}{4}\frac{q^2}{\varepsilon}S_{ij} \tag{6.2.2}$$

with $C_\mu = 0.09$. A problem should be immediately apparent. The sudden imposition of a strong strain could easily produce b_{ij} states lying outside of the anisotropy invariant map. This is a very serious potential problem when such models are applied in new flows.

Another weakenss of this model is that it assumes that the principal axes of stress and strain-rate are aligned. This is not true in the most important engineering flow, namely shear flow. However, the constant C_μ has been set to give the right anisotropy of the shearing stress. For example, in the homogeneous shear flow experiment of Tavoularis and Corrsin discussed in section (5.4), $b_{12} = -0.149$ is predicted by (6.2.2), in excellent agreement with the measurements. However, the model predicts $b_{11} = 0$, whereas the experiments show $b_{11} = 0.196$, so the normal stresses are badly in error. However, they do not play a significant role in determining the mean velocity field, and so this error usually of little consequence.

Algebraic models assume that the turbulence structure responds instantly to changes in the imposed mean strain. This is reasonable for computing the slow evolution of mean fields, but not satisfactory if the strain rates are large, i.e. if $S^*q^2/\varepsilon \gg 0$, where S^* is the rms anisotropic strain rate. And algebraic models predict instant restoration of isotropy after the removal of an applied mean strain-rate. Hence, if one wants to have realistic predictions of the Reynolds stresses in these cases, a model of the b_{ij} evolution equation be solved in parallel with the q^2 and ε equations.

In the balance of this chapter we review the formal methods that have been applied in attempts to develop rational models to close the b_{ij} evolution equation. Then, at the end we will present a much simpler model that achieves some of the objectives of the more complicated models at much less expense. This new model might be useful for engineering analysis.

6.3 Decomposition of the pressure-strain term

The Poisson equation for the fluctuation pressure (2.6.1) has two terms on the right that act as sources for pressure fluctuations. The source involving the mean velocity gradients will change instantly when the gradients change, resulting in an instant change in the fluctuating pressure field and hence an instant change in the pressure-strain term T_{ij}. The source involving only the turbulence will change only as the turbulence adjustes to its new consitions. This suggests that the pressure fluctuations be split into *rapid* and *slow* parts,

$$p' = p^{(1)} + p^{(2)} \tag{6.3.1a}$$

where the rapid term is the solution of

$$\frac{1}{\rho}p^{(1)}{}_{,ii} = -2u'_{j,i}\,U_{i,j} \tag{6.3.1b}$$

and the slow term is the solution of

$$\frac{1}{\rho}p^{(2)}{}_{,ii} = -2u'_{j,i}\,u'_{i,j} + 2\overline{u'_{j,i}\,u'_{i,j}}. \tag{6.3.1c}$$

The resulting contributions to the pressure-strain term (2.7.5) will be denoted by $T^{(1)}_{ij}$ and $T^{(2)}_{ij}$, respectively.

Eqn. (3.6.1b) is linear and has constant coefficients in homogeneous turbulence, and so can be solved by Fourier methods. We follow the approach of Chapter 3, and write

$$p^{(1)} = \sum_{\mathbf{k}} \hat{p}(\mathbf{k}) e^{-i\mathbf{k}\cdot\mathbf{x}} \qquad u_i' = \sum_{\mathbf{k}} \hat{u}_i(\mathbf{k}) e^{-i\mathbf{k}\cdot\mathbf{x}}. \tag{6.3.2a,b}$$

The time-dependence of the coefficients is not explicitly expressed because we are solving the Poisson equation at one instant of time. The solution of (6.3.1b) is then

$$\frac{1}{\rho}\hat{p}(\mathbf{k}) = -2U_{p,j}\frac{ik_p}{k^2}\hat{u}_j(\mathbf{k}). \tag{6.3.3}$$

Multiplying the pressure fluctuation series by the the velocity gradient series, using the conjugate symmetry properties of the Fourier modes, averaging over the box of Fig. 3.3.1, then taking the limit as done in section 3.3, one finds

$$\frac{1}{\rho}\overline{p^{(1)}u_{i,q}'} = 2U_{p,j}\,M_{ijpq} \tag{6.3.4}$$

where

$$M_{ijpq} = \int \frac{k_p k_q}{k^2} E_{ij}(\mathbf{k}) d^3\mathbf{k}. \tag{6.3.5}$$

The rapid pressure-strain term is the sum of two such terms,

$$T_{iq}^{(1)} = 2U_{p,j}\,(M_{ijpq} + M_{qjpi}). \tag{6.3.6}$$

Modeling of the rapid pressure strain term therefore becomes a task of modeling M_{ijpq}, which we address in the next section.

6.4 Modeling the M_{ijpq} tensor

The M_{ijpq} tensor has been modeled in various ways, all relatively simple, usually with one constant being adjusted to fit data for the predictions of a selection of flows. Here we introduce a very different approach; we arge that the anisotropy model, when applied in circumstances for which rapid distortion theory would apply, should give results consistent with RDT. The RDT form of the *model* equation includes only the rapid pressure strain term, the production term, and the mean rotation term in (6.2.1), exactly the same terms used in RDT theory. The solution above for the rapid pressure field is exactly the same as used in RDT. Therefore, in principle it should be possible to determine all of the coefficients in the rapid pressure strain model (i.e. in M_{ijpq}) so as to make the anisotropy predicted by the model equation under RDT approximations *exactly* the same as that predicted by RDT theory, for an *arbitrary* rapid deformation.

Following Shih and Lumley (1985), we begin by writing the general expression for a tensor $\tilde{M}_{ijpq} = M_{ijpq}/q^2$ that is assumed to be a function of the tensor b_{ij}, with the symmetries in indices required by the definition. This is

$$\begin{aligned}\tilde{M}_{ijpq} = {} & C_1\delta_{ij}\delta_{pq} + C_2(\delta_{ip}\delta_{jq} + \delta_{iq}\delta_{jp}) + C_3\delta_{ij}b_{pq} + C_4\delta_{pq}b_{ij} + C_5(\delta_{ip}b_{jq} + \delta_{iq}b_{jp} + \delta_{jp}b_{iq} + \delta_{jq}b_{ip}) \\ & + C_6\delta_{ij}b_{pq}^2 + C_7\delta_{pq}b_{ij}^2 + C_8(\delta_{ip}b_{jq}^2 + \delta_{iq}b_{jp}^2 + \delta_{jp}b_{iq}^2 + \delta_{jq}b_{ip}^2) + C_9 b_{ij}b_{pq} + C_{10}(b_{ip}b_{jq} + b_{iq}b_{jp}) \\ & + C_{11}b_{ij}b_{pq}^2 + C_{12}b_{pq}b_{ij}^2 + C_{13}(b_{ip}b_{jq}^2 + b_{iq}b_{jp}^2 + b_{jp}b_{iq}^2 + b_{jq}b_{ip}^2) + C_{14}b_{ij}^2b_{pq}^2 + C_{15}(b_{ip}^2b_{jq}^2 + b_{iq}^2b_{jp}^2).\end{aligned} \tag{6.4.1}$$

Because of the Cayley-Hamilton theorem, higher powers of b_{ij} are not required. The coefficients $C_1 - C_{15}$ may be function of the invariants II and III, and of other scalars, such as R_T.

The continuity (2.3.4) equation requires $\tilde{M}_{ijiq} = 0$. When this condition is applied to (6.4.1), an equation containing δ_{jq}, b_{jq}, and b_{jq}^2 is obtained. Since these are independent tensors, the coefficient of each must vanish. This produces three equations,

$$C_1 + 4C_2 + b_{kk}^2C_8 + \frac{1}{3}b_{kk}^3(C_{11} + C_{12} + 2C_{13}) = 0 \tag{6.4.2a}$$

$$C_3 + C_4 + 5C_5 + \frac{1}{2}b_{kk}^2(C_{11} + C_{12} + 4C_{13}) + \frac{1}{3}b_{kk}^3(C_{14} + C_{15}) = 0 \tag{6.4.2b}$$

$$C_6 + C_7 + 5C_8 + C_9 + C_{10} + \frac{1}{2}b_{kk}^2(C_{14} + 3C_{15}) = 0. \tag{6.4.2c}$$

From its definition, $M_{ijpq} = R_{ij}$, so $\tilde{M}_{ijpq} = b_{ij} + \delta_{ij}/3$. In the same way, this condition gives three additional constraints,

$$3C_1 + 2C_2 + b_{kk}^2 C_6 + \frac{4}{3}b_{kk}^3 C_{13} = \frac{1}{3} \tag{6.4.3a}$$

$$3C_4 + 4C_5 + b_{kk}^2(C_{11} + 2C_{13}) + \frac{2}{3}b_{kk}^3 C_{15} = 1 \tag{6.4.3b}$$

$$3C_7 + 4C_8 + 2C_{10} + b_{kk}^2(C_{14} + C_{15}) = 0. \tag{6.4.3c}$$

These six conditions reduce the number of undetermined coefficients to nine, and give

$$C_1 = \frac{2}{15} + b_{kk}^2\left(\frac{5}{3}C_8 + \frac{2}{5}C_9 + \frac{2}{15}C_{10}\right) + b_{kk}^3\left(\frac{1}{15}C_{11} + \frac{1}{15}C_{12} - \frac{2}{5}C_{13}\right)$$
$$+(b_{kk}^2)^2\left(\frac{1}{15}C_{14} + \frac{7}{5}C_{15}\right) \tag{6.4.4a}$$

$$C_2 = -\frac{1}{30} + b_{kk}^2\left(-\frac{2}{3}C_8 - \frac{1}{10}C_9 - \frac{1}{30}C_{10}\right) + b_{kk}^3\left(-\frac{1}{10}C_{11} - \frac{1}{10}C_{12} - \frac{1}{15}C_{13}\right)$$
$$+(b_{kk}^2)^2\left(-\frac{1}{60}C_{14} - \frac{7}{20}C_{15}\right) \tag{6.4.4b}$$

$$C_3 = -\frac{1}{3} - \frac{11}{3}C_5 + b_{kk}^2\left(-\frac{1}{3}C_{11} - \frac{1}{2}C_{12} - \frac{4}{3}C_{13}\right) + b_{kk}^3\left(-\frac{1}{3}C_{14} - \frac{1}{9}C_{15}\right) \tag{6.4.4c}$$

$$C_4 = \frac{1}{3} - \frac{4}{3}C_5 + b_{kk}^2\left(-\frac{1}{3}C_{11} - \frac{2}{3}C_{13}\right) + b_{kk}^3\left(-\frac{2}{9}C_{15}\right) \tag{6.4.4d}$$

$$C_6 = -\frac{11}{3}C_8 - C_9 - \frac{1}{3}C_{10} + b_{kk}^2\left(-\frac{1}{6}C_{14} - \frac{7}{6}C_{15}\right) \tag{6.4.4e}$$

$$C_7 = -\frac{4}{3}C_8 - \frac{2}{3}C_{10} + b_{kk}^2\left(-\frac{1}{3}C_{14} - \frac{1}{3}C_{15}\right) \tag{6.4.4f}$$

Once the coefficients are evaluated, $T_{ij}^{(1)}$ can be determined. The result, written in terms of the *anisotropic strain rate tensor* (5.5.4) and the rotation tensor, is

$$\frac{T_{ij}^{(1)}}{2q^2} = 2(C_1 + C_2)S_{ij}^* + (C_3 + C_4 + 2C_5)\left(S_{ik}^* b_{kj} + S_{jk}^* b_{ki} - \frac{2}{3}S_{nm}^* b_{mn}\delta_{ij}\right)$$
$$+(C_6 + C_7 + 2C_8)\left(S_{ik}^* b_{kj}^2 + S_{jk}^* b_{ki}^2 - \frac{2}{3}S_{nm}^* b_{mn}^2\delta_{ij}\right) + 2(C_9 + C_{10})S_{pq}^*\left(b_{iq}b_{jp} - \frac{1}{3}b_{pq}^2\delta_{ij}\right) + 2C_{10}S_{pq}^* b_{qp}b_{ij}$$
$$+(C_{11} + C_{12} + 2C_{13})S_{pq}^*\left(b_{iq}b_{pj}^2 + b_{jq}b_{pi}^2 - \frac{2}{3}b_{mn}^3\delta_{ij}\right) + 2C_{13}S_{pq}^* b_{qp}^2 b_{ij} + 2C_{13}S_{pq}^* b_{qp}\left(b_{ij}^2 - \frac{1}{3}b_{nn}^2\delta_{ij}\right)$$
$$+2(C_{14} + C_{15})S_{pq}^*\left(b_{ip}^2 b_{jq} - \frac{1}{3}b_{np}^2 b_{nq}^2\delta_{ij}\right) + 2C_{15}S_{pq}^* b_{pq}^2(b_{ij}^2 - \frac{1}{3}b_{nn}^2\delta_{ij})$$
$$+(C_3 - C_4)(\Omega_{ki}b_{kj} + \Omega_{kj}b_{ki}) + (C_6 - C_7)(\Omega_{ki}b_{kj}^2 + \Omega_{kj}b_{ki}^2) + (C_{11} - C_{12})\Omega_{pq}(b_{iq}b_{pj}^2 + b_{jq}b_{pi}^2). \tag{6.4.5}$$

Realizability has been of much concern in modeling the pressure-strain term and other terms in the b_{ij} equation. The principal values b_{aa} can not be less than $-1/3$, and any model that would carry a principal value below this amount (i.e. outside the bounds of the invariant map) then produces *unrealizable turbulence* (nonsense). Truncated approximations to the series above have this danger, although the model

just described, with the infinite set of coefficients, would be realizable because RDT solutions are realizable. In order to guarantee realizabilty one can enforce certain conditions. There are various ways to develop these conditions. Shih and Lumley (1985) get them by requiring that the T_{aa} terms must not drive b_{aa} out of bounds. This requires

$$U_{p,j}\, M_{ajpa} = 0 \qquad \text{when} \quad b_{aa} = -1/3 \tag{6.4.6}$$

which produces three additional constraints,

$$C_1+C_2-\frac{1}{3}(C_3+C_4+2C_5)+\frac{1}{9}(C_6+C_7+2C_8+C_9+C_{10})-\frac{1}{27}(C_{11}+C_{12}+2C_{13})+\frac{1}{81}(C_{14}+C_{15}) = 0 \tag{6.4.7a}$$

$$C_5 - \frac{1}{3}C_{10} + \frac{1}{9}C_{13} = 0 \tag{6.4.7b}$$

$$C_8 - \frac{1}{3}C_{13} + \frac{1}{9}C_{15} = 0. \tag{6.4.7c}$$

We believe it is preferable to impose the realizability conditions directly on the modeled tensor M_{ijpq}. When the velocity component u'_a is everywhere zero then $\hat{u}_a = 0$ and consequently $M_{ajpq} = 0$. In the principal coordinates of b_{ij} this requires

$$M_{1111} = 0 \qquad M_{1122} - M_{1133} = 0 \qquad M_{1212} = 0 \qquad \text{when} \quad b_{11} = -1/3 \tag{6.4.8a,b,c}$$

Using the fact that $b^3_{kk} = -1/9 + b^2_{kk}/2$ on the two-dimensional line, (6.4.8a-c) give

$$C_1 + 2C_2 - \frac{1}{3}(C_3 + C_4 + 4C_5) + \frac{1}{9}(C_6 + C_7 + 4C_8 + C_9 + 2C_{10}) - \frac{1}{27}(C_{11} + C_{12} + 4C_{13}) + \frac{1}{81}(C_{14} + 2C_{15}) = 0 \tag{6.4.9a}$$

$$\frac{1}{3}C_3 + \frac{1}{9}(C_6 - C_9) - \frac{1}{27}(C_{11} - C_{12}) + \frac{1}{81}C_{14} = 0 \tag{6.4.9b}$$

$$\frac{1}{6}C_5 + \frac{1}{18}(C_8 - C_{10}) + \frac{1}{162}C_{15} = 0 \tag{6.4.9c}$$

$$C_2 - \frac{1}{6}C_5 + \left(\frac{1}{18} + \frac{1}{2}b^2_{kk}\right)C_8 - \frac{1}{18}C_{10} + \left(\frac{1}{27} - \frac{1}{6}b^2_{kk}\right)C_{13} + \left(-\frac{1}{162} + \frac{1}{18}b^2_{kk}\right)C_{15} = 0. \tag{6.4.9d}$$

When equations (6.4.4) are used to express the lower coefficients, (6.4.9d) is $-1/2$ (6.4.9a), and so only three independent conditions are obtained,

$$\frac{1}{15} + \frac{1}{3}C_5 + \left(-\frac{1}{9} + \frac{1}{3}b^2_{kk}\right)C_8 + \frac{1}{5}b^2_{kk}C_9 + \left(\frac{1}{9} + \frac{1}{15}b^2_{kk}\right)C_{10} + \left(-\frac{1}{45} + \frac{1}{10}b^2_{kk}\right)(C_{11} + C_{12})$$
$$+\left(-\frac{4}{45} + \frac{2}{5}b^2_{kk}\right)C_{13} + \frac{1}{30}(b^2_{kk})^2C_{14} + \left(\frac{1}{81} - \frac{1}{9}b^2_{kk} + \frac{7}{10}(b^2_{kk})^2\right)C_{15} = 0 \tag{6.4.10a}$$

$$-\frac{1}{9} - \frac{11}{9}C_5 - \frac{11}{27}C_8 - \frac{2}{9}C_9 - \frac{1}{27}C_{10} - \left(\frac{1}{27} + \frac{1}{18}b^2_{kk}\right)C_{11} + \left(\frac{1}{27} - \frac{1}{6}b^2_{kk}\right)C_{12}$$
$$-\frac{4}{9}b^2_{kk}C_{13} + \left(\frac{2}{81} - \frac{2}{27}b^2_{kk}\right)C_{14} + \left(\frac{1}{243} - \frac{4}{27}b^2_{kk}\right)C_{15} = 0 \tag{6.4.10b}$$

$$\frac{1}{6}C_5 + \frac{1}{18}(C_8 - C_{10}) + \frac{1}{162}C_{15} = 0 \tag{6.4.10c}$$

When these are satisfied, the Shih-Lumley conditions will also be satisfied. It is important to realize that these realizability constraints apply only when the turbulence is two-dimensional, i.e. only on the line $G = 0$ that forms the top boundary of the invariant map.

The equations above suggest that the coefficients will depend on the invariants and not simply be constants. We might expand each coefficient as a power series in the invariants,

$$C_n = C_n^{(0)} + b^2_{kk}C_n^{(2)} + b^3_{kk}C_n^{(3)} + (b^2_{kk})^2C_n^{(4)} + b^2_{kk}b^3_{kk}C_n^{(5)} + (b^3_{kk})^2C_n^{(6)} + \ldots \tag{6.4.11}$$

We see that the first approximations to the isotropic coefficients C_1 and C_2 are already known, and the first approximations to the linear coefficients C_3-C_5 are determined by the first approximation to C_5.

Most turbulence models presently in use include only the terms in M_{ijpq} through C_5 (the linear terms), employing constant values for the coefficients. But with C_6-$C_{15} = 0$ no single value of C_5 can satisfy all three realizability conditions (6.4.10), so these linear models do not satisfy realizability.

The simplest set of coefficients satisfying realizability is obtained by truncating M_{ijpq} to $O(\mathrm{b}^2)$ and assuming all coefficients are constants. The truncation gives

$$C_{11} = C_{12} = C_{13} = C_{14} = C_{15} = 0. \tag{6.4.12a}$$

From (6.4.4a,b), the coefficients C_1 and C_2 will be constants only if $C_8 = 0$ and $C_{10} = -3C_9$. Then, the realizability conditions give

$$C_1 = 2/15 \qquad C_2 = -1/30 \qquad C_3 = 1/30 \qquad C_4 = 7/15$$
$$C_5 = -1/10 \qquad C_7 = 2/10 \qquad C_9 = 1/10 \qquad C_{10} = -3/10 \tag{6.4.12b}$$

These are the coefficients determined in a slightly different manner by Shih and Lumley (1986). Under the rapid distortion approximations, the time-series solution of the model equations resulting from (6.4.12) match RDT of isotropic turbulence only to $O(1)$. The model also predicts that anisotropic turbulence subjected to pure rotation would undergo anisotropy changes, in excess of those caused by the kinematic rotation terms, of $O(t)$, whereas RDT indicates that this excess change must be an *even* power series in t (see section 4.3) and hence should not appear until $O(t^2)$. It would seem desirable to obtain a better match to RDT.

Under rapid pure rotation of anisotropic turbulence, (6.4.5) will produce an $O(t)$ change in b_{ij} in excess of that produced by the kinematic rotation terms unless $(C_3^{(0)} - C_4^{(0)}) = 0$. This condition gives

$$C_5^{(0)} = -2/7 \qquad C_3^{(0)} = C_4^{(0)} = 5/7. \tag{6.4.13}$$

With these values, the RDT-equivalent model predicitions also agrees with RDT to $O(t)$ *for all irrotational strains* (Reynolds 1983). Le Penven and Gence (1983) carried the analysis to one additional order in t for the case of irrotational strain at a constant strain rate, and found that the coefficients could indeed be matched to $O(t^2)$. Hence, it seems clear that (6.4.13) gives the rational choices for the first approximations to the linear coefficients. However, with $C_5 = -2/7$ the realizability conditions can not be satisfied by a truncation of M_{ijpq} to $O(\mathrm{b}^2)$, and one must include higher-order terms to effect realizability.

It seems clear that continued matching with RDT would determine all of the coefficients, and since RDT predicts realizable turbulence the resulting model would guarantee realizability. The RDT required for a complete matching must be sufficiently general to allow all coefficients to be determined. The arbitrary irrotational strain analysis given in section (4.5) is not sufficient because there the principal axes of S_{ij} were fixed and hence the principal axes of S_{ij} and b_{ij} always remained aligned. An RDT for of isotropic turbulence with arbitrary initial rotation rate and arbitrary strain rate history is required (see section 4.6). It should be possible to select the constants in the coefficient expansions (4.6.10) to match RDT to any arbitrary order in a time-series solution of the RDT-approximate model equations, and then to use the realizability conditions to truncate the expansions, maintaining full realizability. Thus, in principal the rapid pressure strain model should be determined completely by RDT analysis, with no adjustable constants matched to experiments. We are attempting to complete this task.

Another approach that may be fruitful is to use RDT for initially axisymmetric *two-dimensional* turbulence, in conjunction with the realizability constraints, to develop expressions for the coefficients that must hold along the two-dimensional line $G = 0$. The results of section 4.7 should be useful in this regard. These coefficients might then be expanded in power series in G in order to determine appropriate values for three-dimensional turbulence, perhaps by matching to RDT. Many interesting analyses of this nature remain to be done in turbulence modeling.

6.5 Modeling the slow terms

The negative of the slow pressure-strain term and the dissipation anisotropy term are modeled together in (6.2.1) as

$$T_{ij}^{(2)} - (D_{ij} - D_{kk}\delta_{ij}/3) = -\epsilon\phi_{ij}. \tag{6.5.1}$$

Assuming that it is possible to model ϕ_{ij} in terms of b_{ij}, a premise that is not supported very well by direct numerical simulations, the most general form must be

$$\phi_{ij} = (\alpha + 2)b_{ij} + \beta(b_{ij}^2 + \frac{2}{3}\mathrm{II}\delta_{ij}) \tag{6.5.2}$$

where the coefficients α and β could be functions of the invariants II and III and possibly of other scalars, such as R_T. Under these assumptions, one can in principle evaluate the coefficients by reference to experiments and simulations on the *return to isotropy* following removal of mean strain rate. In this case (6.2.1) reduces to

$$\dot{b}_{ij} = -\frac{\varepsilon}{q^2}(\phi_{ij} - 2b_{ij}) = -\frac{\varepsilon}{q^2}\left[\alpha b_{ij} + \beta(b_{ij}^2 - \frac{1}{3}b_{kk}^2\delta_{ij})\right]. \tag{6.5.3}$$

If the anisotropy is weak, α controls the return and must be positive if there is to be a return.

Using (6.5.3), the evolution of the state point on the invariant map is described by the two equations

$$\frac{d\mathrm{II}}{dt} = -\frac{\varepsilon}{q^2}(2\alpha\mathrm{II} - 3\beta\mathrm{III}) \tag{6.5.4}$$

$$\frac{d\mathrm{III}}{dt} = -\frac{\varepsilon}{q^2}(3\alpha\mathrm{III} + \frac{2}{3}\beta\mathrm{II}^2) \tag{6.5.5}$$

so that the trajectory on the map is described by

$$\frac{d\mathrm{II}}{d\mathrm{III}} = \frac{2\alpha\mathrm{II} - 3\beta\mathrm{III}}{3\alpha\mathrm{III} + \frac{2}{3}\beta\mathrm{II}^2}. \tag{6.5.6}$$

Therefore, if the underlying premise of the model is correct, the trajectories must be unique and the ratio $\gamma(\mathrm{II}, \mathrm{III}) = \alpha/\beta$ can be determined by the local trajectory.

There have not been many experiments on the return to isotropy. Those that do exist often show very strange behavior. Direct numerical simulations of Lee and Reynolds (1985) using the Rogallo code in a 128^3 mesh attempted to address these questions in the hope of evaluating the parameters. Turbulence that had been strained by axisymmetric contraction relaxed smoothly to isotropy along the axisymmetric line as expected. But turbulence that had been strained by axisymmetric expansion showed very strange behavior, in some cases moving further *away* from isotropy before starting the return. Turbulence strained by complex combinations that produced states near the middle of the anisotropy map did not show convincingly unique trajectories. A sample of the trajectories following removal of plane strain are shown in Fig. 6.5.1. The points to the left have been strained most rapidly, and the initial states are predicted very well by RDT. The lowermost points are in general agreement with the one experiment on the relaxation from plane strain by Tucker and A. Reynolds (1968). Note that one point begins its "return" by going substantially far in the wrong direction. It seems impossible to incorporate this wierd behavior within the structure of (6.5.2).

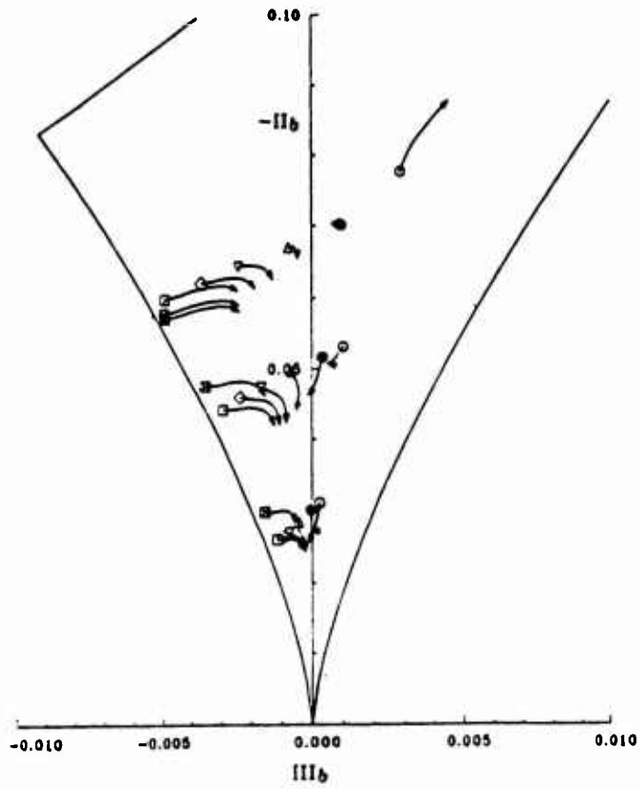

Figure 6.5.1 Trajectories of the return to isotropy from plane strain (simulations)

The simulations cast doubt on the basic idea of modeling these terms using only the b_{ij} tensor. But the simulations did show that the return of the small-scales to isotropy, as reflected by the anisotropy in the vorticity and disssipation tensors, was quite well behaved and easily modeled. This suggests some directions for future modeling research.

These simulations, as well of those of Rogallo for homogeneous shear flow, suggest very strongly that

$$\phi_{ij} \to 2b_{ij} \qquad \text{as} \quad |b| \to 0. \tag{6.5.7}$$

This means that there should be no linear return to isotropy. Careful examination of the very nearly isotropic data of Comte-Bellot and Corrsin (1966) seems to support this behavior.

Choi (1983) perfomed experiments on the return to isotropy from the right side of the invariant map, and did seem to observe more consistent behavior. A fit to his data developed by the Cornell group and reported by Shih and Lumley (1986) is

$$\alpha = 12.44(9G)^2(1-9G)^{3/4} \qquad \beta = 0. \tag{6.5.8}$$

The G factors provide a sort of realizability, and there is no linear return to isotropy.

A criticism that might be raised about this model is that it does not allow two-dimensional turbulence to remain two-dimensional, relaxing to an axisymmetric state. It is possible to construct a model that does by using the realizability condition. When $u'_\alpha = 0$ everywhere, then $D_{\alpha\alpha} = 0$, $T_{\alpha\alpha} = 0$, and hence $\phi_{\alpha\alpha} = 2b_{\alpha\alpha}$, which will sustain $b_{\alpha\alpha} = -1/3$. Thus, the realizability condition gives

$$\alpha = 3\beta\left(\frac{1}{9} + \frac{2}{3}\mathrm{II}\right) \qquad \text{when} \quad G = 0. \tag{6.5.9}$$

Since this constraint only need be true for $G = 0$, we can add functions of G without destroying realizability. A linear term suffices, with its coefficient chosen to remove the linear return to isotropy when $G = 1/9$ and $\mathrm{II} = 0$ and to make β vanish for small anisotropy,

$$\alpha = \left(\frac{1}{3} + 2\mathrm{II} - 3G\right)\beta_0 \tag{6.5.10a}$$

$$\beta = \beta_0(1 - 9G). \tag{6.5.10b}$$

The model is then

$$\dot{b}_{ij} = -\frac{\varepsilon}{q^2}\left[\left(\frac{1}{3} + 2\mathrm{II} - 3G\right)\beta_0 b_{ij} + \beta_0(1 - 9G)\left(b_{ij}^2 + \frac{2}{3}\mathrm{II}\delta_{ij}\right)\right]. \tag{6.5.11}$$

With this model, for nearly isotropic turbulence (6.5.4) becomes

$$\alpha \approx -\beta_0 \mathrm{II} \tag{6.5.12}$$

while for small anisotropy (6.5.8) gives

$$\alpha \approx 12.44(-9\mathrm{II})^{3/4}. \tag{6.5.13}$$

Matching at $-\mathrm{II} = 0.05$ suggests $\beta_0 \approx 10$. This modified model satisfies realizability, restores axisymmetry in two-dimensional turbulence, displays no linear return to isotroy, and gives return rates of the right order of magnitude.

However, one might suspect that the slightest little three-dimensionality would explode the turbulence into a three-dimensional field, so perhaps it is unreasonable to insist on maintaining two-dimensionality in the model. Undecided issues likes this provide fruitful grounds for new research, and we are now exploring questions like these using direct turbulence simulation.

6.6 A simple anisotropy model

The gap between the eddy-viscosity models used in the simplest $k-\epsilon$ models and those discussed above is immense. There is a need for a much simpler model that would protect engineering calculations from the dangers of unrealizable turbulence, provide some indications of the trends in anisotropy for unusual flow situations, and handle dynamic changes on roughly the right time scale, but without such calculational complexity. The beginnings of such an idea are presented here.

We start with the idea that a large positive strain rate in one direction tends to stretch vortex filaments in that direction, aligning them with the flow, thereby intensifying the perpendicular fluctuation components and reducing those along the axis. In the limit of very strong strain rate, the energy in the axial fluctuations axial will approach zero. The anisotropy model must prevent negative values. And, we know that only the it anisotropic component of strain produces anisotropy in the turbulence. A simple algebraic model with this character is

$$b_{ij} = \frac{-S^*_{ij}\tau}{A_0 + A_S S^* \tau}. \tag{6.6.1}$$

In order for realizability to be maintained, b_{aa} should approach $-1/3$ as $S^*_{aa} \to \infty$, for *any* combinations of other S^*_{ij}. This requires that the coefficient A_S depend on the type of strain.

In the principal coordinates of S^*_{ij}, we take S^*_{11} as having a large positive value Γ, and write the strain-rate tensor as

$$S^*_{ij} = \Gamma \begin{pmatrix} 1 & 0 & 0 \\ 0 & -\frac{1+a}{2} & 0 \\ 0 & 0 & -\frac{1-a}{2} \end{pmatrix}. \tag{6.6.2}$$

Note that $a = 0$ gives axisymmetric contraction, $a = 1$ gives plane strain, and $a = 3$ gives axisymmetric expansion. Then

$$S^* = \Gamma\sqrt{1 + \frac{(1+a)^2}{4} + \frac{(1-a)^2}{4}} = \Gamma\sqrt{\frac{3+a^2}{2}} \tag{6.6.3}$$

For large positive Γ our model must yield

$$b_{11} \to -\frac{1}{3} = -\frac{\Gamma\tau}{A_S S^* \tau} \tag{6.6.4}$$

and this requires that

$$A_S = \sqrt{\frac{18}{3+a^2}}. \tag{6.6.5}$$

We need a way to represent a for an arbitrary orientation of the coordinates. The structure of S^*_{ij} is characterized by

$$W = \frac{S^*_{ij} S^*_{jk} S^*_{ki}}{(S^*)^3} \tag{6.6.6}$$

which for (6.6.2) is

$$W = \frac{3(1-a^2)/4}{|(3+a^2)/2|^{3/2}}. \tag{6.6.7}$$

W ranges from $-1/\sqrt{6}$ for axisymmetric expansion to $1/\sqrt{6}$ for axisymmetric contraction. Plane strain and shear flow correspond to $W = 0$. Using (6.6.5) to express a in terms of A_S, and then in turn expressing W in terms of A_S, we find

$$W = \frac{A_S^3}{9} - \frac{A_S}{2} \tag{6.6.8}$$

This allows us to determine A_S from a known W. The relationship between them is shown in Fig. 6.6.1.

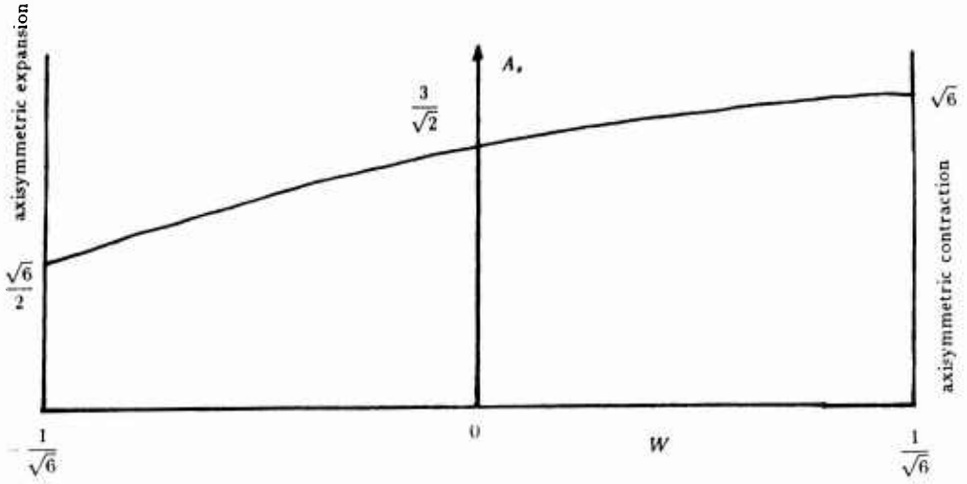

Figure 6.6.1 Variation of the model parameter with strain type

The constant A_0 should be chosen to produce the proper level of shear stress in shear flow, for that is the most important engineering flow. Shear flow can be represented as a combination of rotation and irrotational strain. Denoting $U_{1,2} = \Gamma$,

$$S_{ij} = \begin{pmatrix} 0 & \frac{\Gamma}{2} & 0 \\ \frac{\Gamma}{2} & 0 & 0 \\ 0 & 0 & 0 \end{pmatrix} \qquad \Omega_{ij} = \begin{pmatrix} 0 & \frac{\Gamma}{2} & 0 \\ -\frac{\Gamma}{2} & 0 & 0 \\ 0 & 0 & 0 \end{pmatrix}. \tag{6.6.9a,b}$$

Hence, for shear flow $W = 0$, $A_S = 3/\sqrt{2}$, and $S = \Gamma/\sqrt{2}$. With these values, $A_0 = 23$ produces $b_{12} = -0.15$ at $\Gamma\tau = 12.7$, corresponding to the homogeneous shear flow experiments of Tavoularis and Corrsin.

We now have an anisotropy model that is always realizable for all types of strain, and has the right general trend of b_{ij} with S_{ij}, but assumes that a state of structural equilibrium has been attained. In order to handle transients, we propose an evolution equation for b_{ij} that would give (6.6.1) as its equilibrium solution,

$$\dot{b}_{ij} = -C_1\left[(A_0 + A_S S^* \tau) b_{ij} + S^*_{ij}\tau\right]/\tau \tag{6.6.10}$$

By choosing $C_1 = 4/15$, the model will agree with the initial phase of rapid distortion of isotropic turbulence, and the rate of return to isotropy is of the right general magnitude for linear approximations. Note that the model correctly predicts no change in the ansiotropy of isotropic turbulence under pure rotation.

For many engineering problems the main objective of the turbulence model is to reveal important trends This simple anisotropy model would make the important stresses change in the right general way, without becoming unrealizable, and therefore it should be an attractive alternative for use in simple two-equation turbulence models. Preliminary studies by students in the author's turbulence class support this conjecture.

7. NUMERICAL SIMULATIONS OF TUBULENCE

7.1 Introduction

Over the past decade, two important types of numerical simulations have become important. The earlier work concentrated on *large eddy simulations* (LES), in which simple models are used for the small-scale turbulence and a realization of the large-scale turbulence is computed. The underlying idea is that the structure of large eddies differ greatly from flow to flow (which is why universal models are elusive), whereas the small eddies are more universal and therefore easier to model. Large eddy simulations have provided important information for turbulence modeling, and there is now great interest in the development of large eddy simulations as a tool for engineering analysis. A prominent program in this direction exists in France at the EDF.

It was argued that, since the ratio of the largest to the smallest scales of turbulence varies as $R_T^{3/4}$ (see 3.2.4), it would never be practical to do a significant simulation of all the important turbulent scales. However, valid *direct simulations* of turbulent flows at R_T of the order of 100-300 have become possible. This is the range of *turbulence* Reynolds numbers in turbulent shear flows with Reynolds numbers, based on the layer thickness and the driving mean velocity difference, of about 1000, and a number of direct simulations of channel flows and boundary layer flows at these low Reynolds numbers have now been attained. These direct simulations provide an important new tool for studying turbulence, particularly because they yield essentally any data that one might desire. Already they have contributed important new insight into turbulent structure and have aided advances in turbulence modeling, as well as new understanding of transition physics.

In this chapter we will review the fundamentals and current status of this very fast-moving area of research, drawing primarily from the experience of the large group working in this area at the NASA/Ames Research Center and Stanford University. At present this group involves about ten NASA scientists, three Stanford Professors, a dozen or so graduate students, and some post-doctoral scholars and other visitors, with the work being coordinated by the joint NASA/Stanford Center for Turbulence Research. Some of the exciting new things going on in this group will be outlined, with details being left for the authors to report for themselves.

7.2 Fundamentals of large eddy simulation

In LES one needs a way to define the large-scale components of the fields. and filtering is usually used. The *filtered field* $\overline{f}$ is defined by

$$\overline{f}(\mathbf{x},t) = \int G(\mathbf{x},\mathbf{x}';\Delta) f(\mathbf{x}',t) d^3\mathbf{x}'. \tag{7.2.1}$$

Here G is a filter function, which determines exactly what fraction of the motion is defined as being large scale, and Δ is a filter parameter that implements this choice. The filter function must be normalized such that

$$\int G(\mathbf{x},\mathbf{x}';\Delta) d^3\mathbf{x}' = 1 \tag{7.2.2}$$

for all $\mathbf{x}$. The *residual field* f' is then what is left over after filtering,

$$f(\mathbf{x},t) = \overline{f}(\mathbf{x},t) + f'(\mathbf{x},t). \tag{7.2.3}$$

The filtered residual field is *not* zero since

$$\overline{\overline{f}} \neq \overline{f} \qquad \overline{f'} \neq 0. \tag{7.2.4}$$

Filtering (7.2.3),

$$\overline{f} = \overline{\overline{f}} + \overline{f'} \tag{7.2.5a}$$

so the filtered residual field can be expressed in terms of the singly and doubly-filtered resolved fields,

$$\overline{f'} = \overline{\overline{f}} - \overline{f}. \tag{7.2.5b}$$

This proves very useful in modeling the residual turbulence.

In homogeneous turbulence the filter must be of the form $G(\mathbf{x}-\mathbf{x}';\Delta)$. Then

$$\overline{f}(\mathbf{x},t)=\int G(\mathbf{x}-\mathbf{x}';\Delta)f(\mathbf{x}',t)d^3\mathbf{x}'$$

has the Fourier transform

$$\hat{\overline{f}}(\mathbf{k},t)=\hat{G}(k;\Delta)\hat{f}(\mathbf{k},t) \tag{7.2.6}$$

where the k argument of G is the *magnitude* of the k vector. Several filters ahve been explored. The *sharp cut-off filter*

$$\hat{G}=\begin{cases}C & \text{if } |k_i-k_i'|\le k_c\\ 0 & \text{otherwise}\end{cases} \tag{7.2.7}$$

make a clean separation of large and small scales in spectral space, but the Gibbs phenomena in the inverse Fourier transform make the physical-space interpretation undesirable. Smoother behavior can be obtained with the Gaussian filter,

$$G(\mathbf{x}-\mathbf{x}';\Delta)=Ae^{-6(x_i-x_i')(x_i-x_i')/\Delta^2} \tag{7.2.8}$$

where A is a constant determined by the normalization and depends on the number of directions in which the filter is applied. The Fourier transform of the Gaussian filter is also Gaussian,

$$\hat{G}(\mathbf{k};\Delta)=Be^{-k^2\Delta^2/24}. \tag{7.2.9}$$

Filtering is more of a problem for inhomogeneous flows . The most satisfying approach is to use an appropriate set of expansion functions in the inhomogeneous directions and then to define the filtered value as the *n-term* approximation. However, most work has instead used finite-difference methods in the inhomogeneous directions with the Gaussian filter in the homogeneous directions, and taken whatever implicit filtering is provided by the difference scheme. This is not very satisfying because it leaves the computed field ill defined, and does not provide a systematic way for estimation of the energy content in the residual field. This is one of the unsatisfying loose ends in LES that needs to be cleaned up by some good research.

The evolution equations for the filtred field are derived by filtering the Navier-Stoles equations, so it is important that the filtering definition commute with differentiations with respect to both time and space. The Gaussian filter has this property, and so homogeneous turbulence really can be done properly with LES using the Gaussian filter. If $\rho=\rho(t)$ then the filtered continuity equation is

$$\dot{\rho}+\rho\overline{u}_i=0. \tag{7.2.10}$$

Subtracting this from the full equation,

$$u_{i,i}'=0 \tag{7.2.11}$$

so the residual field is divergence-free, and if $\rho=$ *constant* the filtered field is divergence-free. Filtering the momentum equations, assuming μ is constant and again allowing $\rho=\rho(t)$, the equation for the filtered velocity field is

$$\dot{\overline{u}}_i+(\overline{u_iu_j})_{,j}=-\frac{1}{\rho}\overline{p}_{,i}+\nu\overline{u}_{i,jj}. \tag{7.2.12}$$

Representing the velocity as the sum of filtered and residual components,

$$\overline{u_iu_j}=\overline{\overline{u}_i\overline{u}_j}+R_{ij} \tag{7.2.13}$$

where the residual stress terms are

$$R_{ij}=\overline{\overline{u}_iu_j'}+\overline{u_i'\overline{u}_j}+\overline{u_i'u_j'}. \tag{7.2.14}$$

In LES one needs to model R_{ij}. Given this model, and a suitable computer, and a few little details like boundary and initial conditions, *single realizations* of turbulence fields can be generated. In homogeneous turbulence this appears to be sufficient, because volume averages over a single realization seem to provide good representations for ensemble averages.

The term $\overline{\overline{u}_i\overline{u}_j}$ does not need to be modeled because it can be computed directly by filtering the product of the filtered velocities. This is easily done in Fourier space, and we handle this term this way now. Our earlier representation of this in terms of $\overline{u}_i\overline{u}_j + L_{ij}$, where L_{ij} was the Leonard stress, is now abandoned.

It may be noted that we have not made any mention of numerical methods and have avoided use of the term *sub-grid scale turbulence*. We believe that it is important to cast the LES equations in a way that is independent of the numerical method, and would lend itself to purely theoretical analysis. However, in reality the filter width that is taken is related to the computational grid employed. The results depend upon the ratio of filter width to mesh width, and the best results are obtained when the filter width is twice the mesh width.

7.3 Modeling the residual stresses in large eddy simulation

One can not afford a very complex model for the residual stresses in LES. Almost all of the work to date has been done with simple algebraic models, although there have been some explorations with simple one-equation turbulence models.

It is useful to separate R_{ij} into isotropic and anisotropic parts, as is done with viscous stresses,

$$R_{ij} = \frac{1}{3}R_{kk}\delta_{ij} + T_{ij}. \tag{7.3.1}$$

The isotropic term is absorbed with the filtered pressure by writing

$$P^* = \frac{1}{\rho}\overline{p} + \frac{1}{3}R_{kk} \tag{7.3.2}$$

and then P^* replaces $\overline{p}/\rho$ and T_{ij} replaces R_{ij} in (7.2.12).

An important element of most LES calculations is the *Smagorinski* model, which assumes that the residual T_{ij} is a linear function of the anisotropic strain rate imposed by the filtered field

$$T_{ij} = -2\nu_T\overline{S}_{ij} \tag{7.3.3}$$

where ν_T is an eddy viscosity of the residual field. If it is assumed that the length scale of the dominant residual eddies is the filter width, and that the time scale is that set by the strain rate of the filtered field, then

$$\nu_T = (C_S\Delta)^2\sqrt{\overline{S}_{mn}\overline{S}_{mn}}. \tag{7.3.4}$$

The coeffient in this model can in principle be evaluated by performing direct numerical simulations on a fine mesh (say 128^3), then filtering this data to a coarse mesh (say 8^3) to define the filtered and residual fields, and then comparing the model with the residual field from the coarse filtering. Clark et. al. (1979) were the first to emply this technique, which is now known as a *Clark test*. For isotropic turbulence the results are moderately encouraging, and do not show much dependence on Reynolds number, a value of about 0.12 being typical. However, when this test is applied in strained and sheared flows, essentially no correlation is found between the model and the data. The model simply is inadequate under these more interesting circumstances.

An important advance in residual stress modeling was made by Bardina (1985), who first proposed to model

$$R_{ij} = C_B\left(\overline{u}_i\overline{u}_j - \overline{\overline{u}}_i\overline{\overline{u}}_j\right). \tag{7.3.5}$$

The basic idea was to characterize the stresses of the residual scales as being similar to that of the smallest resolvable motions, so Bardina called this the *scale similarity model*. By itself it was not adequate either, because it does not dissipate sufficient energy. But it does provide energy transfer from high to low wavenumbers, and effect that is missing in the Smagorinsky model. When used in combination with the Smagorinsky model (the Bardina *mixed model*) remarkably good results are obtained in the Clark tests, with the same values of the constant yielding correlations between predicted and actual stresses of the order of 70% for shear flow, irrotational strain, and unstrained flow!.

The value of the constant C_B can actually be deduced from a simple theoretical argument. If one transform to new coordinates moving linearly with respect to the original ones,

$$x_i^* = x_i - c_i t \qquad t^* = t \qquad u_i^* = u_i + c_i \tag{7.3.6a,b}$$

the equations of motion of course do not change because they are invariant under such (Galelean) transformations. However, individial terms in the equations do change when transformed. For the filtering operation,

$$\overline{u^*}_i = \overline{u}_i + c_i \qquad u^{*\prime}_i = u'_i \tag{7.3.7a,b,c}$$

so that R_{ij} transforms to

$$R_{ij} = \overline{\overline{u^*}_i u^{*\prime}_j} + \overline{u^{*\prime}_i \overline{u^*}_j} + \overline{u^{*\prime}_i u^{*\prime}_j} + c_i \overline{u^{*\prime}_j} + c_j \overline{u^{*\prime}_i} = R^*_{ij} + c_i \overline{u'_j} + c_j \overline{u'_i}. \tag{7.3.8}$$

The terms modeling R_{ij} should transform in the same way; the Smagorinsky model is invariant under the transformation, and hence can not possibly represent all of R_{ij}. The added terms of the Bardina model (7.3.5) transform to

$$R_{ij} = C_B\left[\overline{u^*}_i \overline{u^*}_j - \overline{\overline{u^*}_i \overline{u^*}_j} + c_i(\overline{u^*}_j - \overline{\overline{u^*}}_j) + c_j(\overline{u^*}_i - \overline{\overline{u^*}}_i)\right]. \tag{7.3.9}$$

Using (7.2.3) and (7.3.7b), this becomes

$$R_{ij} = R^*_{ij} + C_B\left(c_i \overline{u'_j} + c_j \overline{u'_i}\right). \tag{7.3.10}$$

Comparing (7.3.8) and (7.3.10), it is evident that $C_B = 1$. Bardina was unaware of this result at the time he did his numerical work, on the basis of which he recommended a value of 1.05!

In recent work yet to be published, Piomelli has been reexamining LES residual modeling using the recent direct simulation of channel flow as the basis for Clark tests, also carrying out LES simulations with various models. This work has shed some new light on LES modeling, which can be summarized as follows. In coarse mesh calculations (say 16^3) no real difference is observed between using just the Smagorinsky model and the Bardina mixed model, and the results in general reflect the coarseness of the grid. However, at 64^3 calculations there are important differences. The calculations are filtering has been in planes parallel to the wall only, because as yet we do not really have any good way to do explicit filtering in directions of inhomogeneity. Piomelli finds that the choice of filter function is important in determining the performance of the residual turbulence model. The filter makes its appearance in the calculations when the term $\overline{u_i}\,\overline{u_j}$ is calculated by filtering the product of the computed filtered components. If the Gaussian filter is used with the Bardina mixed model, *very good* results are obtained. If the Gaussian filter is used with the Smagorinsky model, very *poor* results are obtained. But if the Smagorinski model is used with the sharp cut-off filter, *fair* results are obtained.

The inference from this work is that the sharp cut-off filter defines a clear length scale for the residual turbulence, whereas the Gaussian filter spreads the residual scales out over a broader range. The Bardina model accounts for the different scales in the residual field generated by the Gaussian filter. On the other hand, only one length scale is carried by the Smagorinsky model, and therefore this model can not account for all the scales filtered by the Gaussian filter.

One might argue that the turbulence time scale in the Smagorinsky viscosity should be a scale appropriate to the residual field. In isotropic turbulence the strain rate of the resolved field sets this scale, but in inhomogeneous flows with strong mean strain rate it may be better to extract the time scale from the high wavenumber end of the resolved field, as in the Bardina model. One possible approach is to use the velocity scale in this range,

$$\nu_T = C\Delta\sqrt{(\overline{u}_k - \overline{\overline{u}}_k)(\overline{u}_k - \overline{\overline{u}}_k)}. \tag{7.3.11}$$

Another approach would be to use the strain rate,

$$\nu_T = C_1\Delta^2\sqrt{(\overline{S}_{mn} - \overline{\overline{S}}_{mn})(\overline{S}_{nm} - \overline{\overline{S}}_{nm})}. \tag{7.3.12}$$

In LES one probably does not want to attempt to resolve the wall region of boundary layers, and so some appropriate wall conditions are needed. For high Reynolds numbers, it is through this condition that the viscosity will enter the problem. The main thrust of Piomelli's work has been to assess various proposals for these conditions. At this writing about all we can say is that nothing that we or anyone else has suggested shows up very will in Clark tests against the direct simulations of channel flow. However, we are hopeful that a satisfactory working model for the residual wall stress will be found, and this probably will draw upon new knowledge about the structure of the wall region that is currently being extracted from the direct simulations.

7.4 Insights from direct simulations of homogeneous turbulence

Boundary conditions are a problem in turbulence simulations. The problem is avoided in homogeneous turbulence by use of *periodic* boundary conditions. The resulting turbulence is somewhat artificial in that the motion on opposite sides of the computational domain is fully correlated, which of course would not be the case in a real turbulence field. One must select a computational domain large enough that the statistical correlations at separations of *half* the computational domain are small, and when this is done the statistical results up to this separation seem to be quite like those of real turbulence.

A large number of homogeneous turbulence simulations have been carried out by the Ames/Stanford group, almost all using the Rogallo code. This program uses the coordinate transformation (4.2.4), and as a result achieves remarkable robustness in runs with very strong deformation. For a recent description of the code see Lee and Reynolds (1985). Simulations now include homogeneous shear flow at a variety of shear rates, many cases including scalar transport, a variety of irrotational strain flows, return to isotropy following various strains, some rotation cases. Special codes have handled a funny type of homogeneous compressible shear flow and some flow compression cases. Meshes ranging from 64^3 to 256^3 have been used, although the 128^3 cases are now the most abundant.

In a direct simulation one must capture both the energy at large scales and the dissipation at small scales, and this limits the calculations to relatively low Reynolds numbers. One can usually tell when not enough small-scales have been captured by a pile-up of energy at the high wavenumebr end of the spectrum. The the model spectrum (3.9.4) can be used to estimate the fraction of energy left out of a calculation at any given R_T. Typical 128^3 calculations miss less than 1% of the turbulence energy at $R_T = 50$, a typical range for these simulations.

The initial turbulence field must be constructed in a divergence-free manner, and this is easily done with the Fourier representation. The spectrum can be shaped initially and scaled to contain the proper energy for a target R_T. For details see Lee and Reynolds (1985).

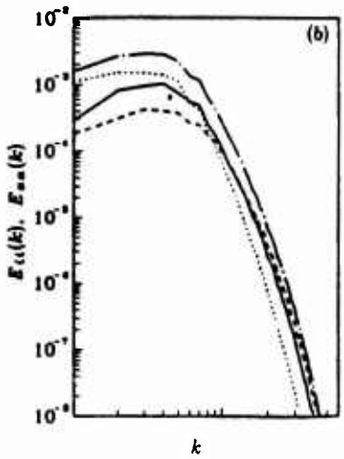

Figure 7.4.1 Spectra for relaxation from plane strain

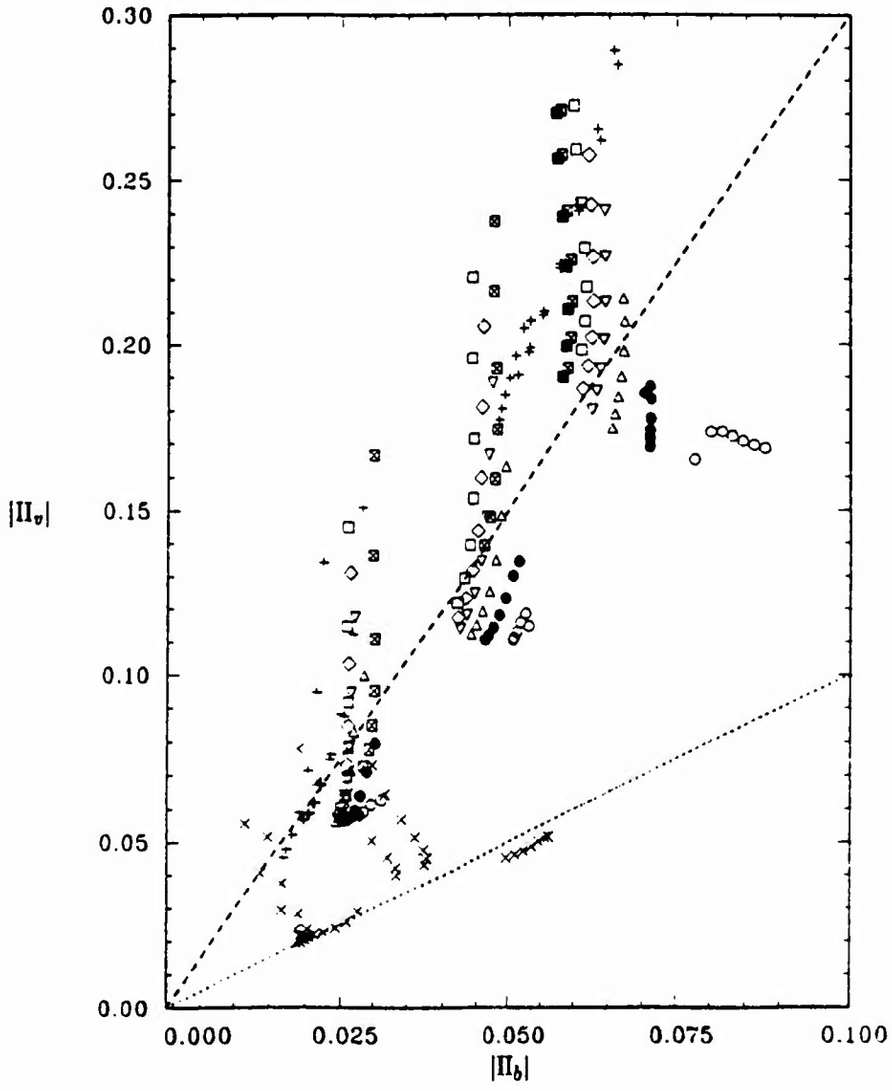

Figure 7.4.2 Anisotropies during relaxation from various strains

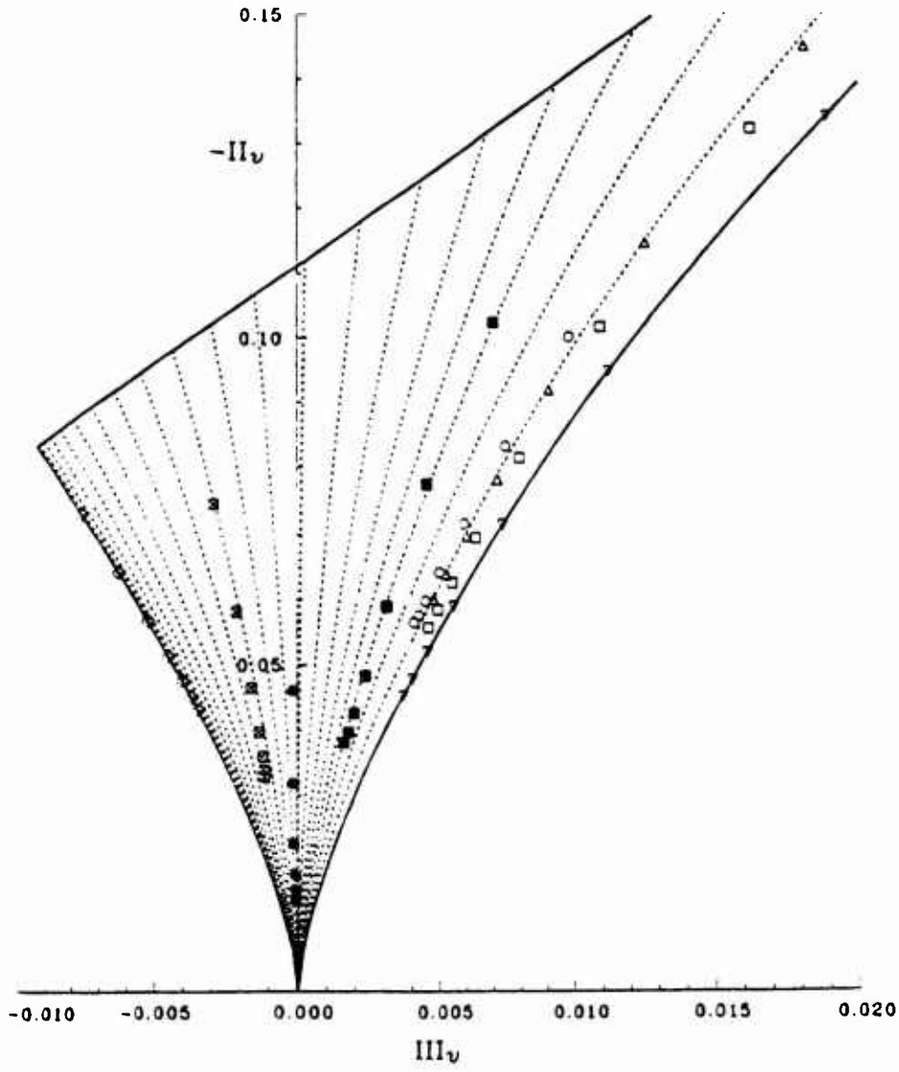

Figure 7.4.3 Vorticity relaxation trajectories

All of these calculations show a remarkable amount of small-scale anisotropy. For example, Fig.7.4.1 shows one of Lee's spectra during relaxation from plane strain, with the different lines representing different components. Note that the anisotropy persists throughout the $-5/3$ range of the spectrum. We investigated this issue of small scale anisotropy by extending the measures of anisotropy discussed in Chapter 6 to the vorticity and dissipatin fields. The *vorticity tensor* is defined as

$$V_{ij} = \overline{\omega_i' \omega_j'} \tag{7.4.1}$$

and the *vorticity anisotropy tensor* is

$$v_{ij} = \frac{V_{ij} - \omega^2 \delta_{ij}/3}{\omega^2}. \tag{7.4.2}$$

The dissipation anisotropy tensor is defined by

$$d_{ij} = \frac{D_{ij} - D_{kk}^2 \delta_{ij}/3}{D_{kk}}. \tag{7.4.3}$$

These two anisotropy tensors are characterised by their second and third invariants, defined the same way as those for the Reynolds stress anisotropy tensor b_{ij} (see 6.1.3). Their anisotropy invariant maps are the same form as those for b_{ij} explained in section 6.1. The boundary lines are the same for the b_{ij} and d_{ij} invariant maps, but on the vorticity invariant map the two axisymmetric side boundaries are reversed, and the uppermost point corresponding to *one-dimensional vorticity* corresponds to the *two-dimensional velocity* field.

Fig. (7.4.2) shows the second invariants of vorticity and velocity during relaxation to isotropy from a variety of different strain types. The trajectories on this diagram are generally down and then to the left. Upon the removal of mean strain rate, the vorticity anisotropy relaxes quickly to a point, and then relaxes slowly, *locked on* to the anisotropy of the Reynolds stress!. Moreover, essentially all of the points showed *more* anisotropy of the vorticity thatn of the Reynolds stress! These are astonishing observations to anyone who has grown up with the idea that the small scales become isotropic quickly, compared to the slow relaxation of the scale anisotropy.

It is also very interesting that the relationship between the two invariants in the lock-on phase returning from axisymmetric expansion is quite different than that when returning from axisymmetric contraction. This suggests that there may be two types of competing structures in turbulence, the noodles formed by axisymmetric contraction and the pancakes formed by axisymmetric expansion, and that perhaps better turbulence models could be made by treating these structures separately.

We have mentioned that the trajectories for return to isotropy on the Reynolds stress invariant map are not well behaved, which casts doubt on the viability of modeling the slow pressure strain and dissipation anisotropy terms in terms of b_{ij}. However, those on the vorticity map are extremely well behaved. Figure (7.4.3) shows these trajectories, which are well fit by the simple model

$$\dot{v}_{ij} = -\alpha \frac{q^2}{\varepsilon} v_{ij} \tag{7.4.4}$$

where α depends on both the invariants of b_{ij} and v_{ij}. The dissipation anisotropy trajectories are quite different, but they too are very well behaved and can be modeled quite neatly. For details see Lee and Reynolds (1985).

Upon reflection, the requirement that the vorticity field be anisotropic is obvious from the Biot-Savart law; if the vorticity spectrum were isotropic, the Reynolds stress spectrum would be isotropic. It may be that explicit consideration of this anisotropy in turbulence modeling could have some advantages. We have been exploring some possibilities.

In another recent study, Rogers (1986) has examined the structure of homogeneous turbulent shear flow. His studies reveal that hairpin vortices of the type found in wall boundary layers are also found in homogeneous turbulence. However, in homogeneous turbulence there are both "up" and "down" hairpins, while in a boundary layer one sees only one kind. He also found evidence of some transverse vortices believed to be associated with the weak orientation of vorticity caused by mean rotation (see section 4.6).

Lee has extended Rogers work to (high) shear rates and Reynolds numbers comparable with the viscous region of turbulent boundary layers. Remarkably, he finds long longitudinal *streaks* that familiar objects in the wall region, with transverse spacings that scale on the turbulent stress and viscosity in exactly the same way as in wall boundary layers. This work suggests that it is the high shear rate, and not the wall, that produces the streaks! This would be good news for modelers, because it would mean that models based on homogeneous turbulence might have far more to do with boundary layer flows than one might think.

Rogers also studied scalar transport in homogeneous shear flow at three different Prandtl numbers. There are three interesting situations corresponding to an (imposed) means scalar gradient in each direction. He calculated the scalar fields for all three cases at the same time for a set of common hydrodynamic simulations. A surprising result, actually seen in experiments by Tavoularis and Corrsin, is that some *cross-gradient* scalar fluxes are *larger* than the flux in the direction of the mean gradient!.

Rogers used his insight about the hairpin vortex structures and the transverse vortices to explain the mechanism by which these cross-gradient transports can develop. He then went on to model the scalar flux in two ways, using his simulation data both as a guide in the modeling and as the basis for coefficient evaluation. The models deal with an anisotropic diffusion tensor D_{ij}, defined by

$$h_i = \overline{u_i' \theta'} = -D_{ij} \Theta_{,j} \tag{7.4.5}$$

where θ' is the scalar fluctuation and $\Theta_{,j}$ is a mean scalar gradient. The diffusivity tensor could be calculated from his measurements, and is found to be inherently non-symmetric. However, he did find that it became antisymmetric in a coordinate system that is aligned with the principal axes of the Reynolds stress. This led him to model the diffusion tensor in the form

$$D_{ij} = C_1 \delta_{ij} + C_2 R_{ij} + C_3 \Omega_{ij}. \tag{7.4.6a,b}$$

He was able to correlate his coefficients with Reynolds and Prandtl numbers to within about 20%.

Rogers made another model assuming that the scalar flux is aligned with the sum of the mean gradient terms in its own transport equation, and thereby obtained a model of comparable accuracy with only one free coefficient. This model is

$$\frac{1}{\tau} C_D h_i + h_j U_{i,j} + R_{ij} \Theta_{,j} = 0 \qquad C_D = 16.1 \left(1 + \frac{1.17}{Pr}\right)^{0.152} \left(1 + \frac{131}{\sqrt{R_T}}\right)^{-0.535} \tag{7.4.7a,b}$$

where $\tau = q^2/\epsilon$ and $R_T = q^4/(\nu\epsilon)$. This result should be of immediate use in turbulence modeling for both homogeneous and inhomogeneous flows. Rogers has recently checked this model against direct simulations of turbulent channel flow at $Pr = 1$ and found that it is remarkably accurate for the flux in the direction of the mean temperature gradient and within about 20% for the flux perpendicular to the mean temperature gradient.

7.5 Direct simulations of spatially-developing flows

Some of the most exciting work at present are the boundary layer simulations of Spalart. He is using a clever stretching of the coordinate system that enables him to use periodic inflow-outflow conditions in a growing boundary layer, and has already produced results about the structure of boundary layers in pressure gradients of much interest to experimentalists.

In order to simulate more general turbulent flows, inflow and outflow conditions are needed. The outflow problem is simpler and we have had a reasonable solution for some time. The inflow problem is harder, but we have recently made some excellent progress.

Lowery (1986) simulated the spatially-developing mixing layer, including scalar transport. He found that a soft convective outflow condition,

$$\frac{\partial}{\partial t} + U_c \frac{\partial}{\partial x} = 0 \tag{7.5.1}$$

applied to the velocity components and scalar worked quite well, with minumum upstream influence. The convection velocity U_c was taken as the average of the two free stream speeds. At the inlet he forced the flow with a combination of fundamental and two subharmonics of a dominant instability of the inlet layer

(tanh profile). because the layer was forced, it responded like a forced layer, with parings occuring cyclicly at frosen locations. And, the layer grows not linearly, as do natural layers, but by leaps and bounds, as do forced mixing layers in the laboratory.

It has been asked if the mixing layer is *absolutely* unstable, in which case if the forcing is stopped after large disturbances have developed downstream the layer should continue to remain. When Lowery terminated forcing, the initial region of the layer relaminarized, suggesting that the instability was *convective*, but midway down the flow the turbulence never went away, and by the exit the flow was quite turbulent. His calculation did not include the splitter plate, which undoubtedly plays a role in promoting absolute instability, so the matter is not really resolved. Lowery also studied the growth of three-dimensional disturbances in the layer, finding that they grew to scales and structures characteristic of the braid region of the mixing layer.

Ongoing extensions of our mixing layer simulation work by Sandham involve the use of random jitter of the forcing to simulate more natural turbulent inflow condition. This produces the linear growth seen in natural experimental layers, at growth rates in excellent agreement with experiemnts. The resulting statistical quantitiers, including the scalar pdf, are much more like those measured for natural layers. It now seems that this will be quite an acceptable method for generating relativelty simple yet effective inflow conditons for direct numerical simulations of turbulence.

Current work is concentrating on extensions to compressible mixing layers, the goal being to use these direct simulations as the basis for building better turbulence models for supersonic flows, including combustion, both for use in LES and in simpler turbulence models. There is a growing group at Ames, involving Rogers, Moser and others, beginning to work very seriously on turbulent combustion simulations. It seems safe to forecast that a decade from now the capabilities for know much more about the modeling and simulation of these and flows of technical interest will be considerably advanced, and students who have mastered these notes should be ready to begin the exciting work ahead in this area.

REFERENCES

Bardina, J., Ferziger, J.H., and Rogallo, R.S. 1985 Effect of rotation on isotropic turbulence; computation and modelling, J. Fluid Mechanics, **154**, p 321.

Cambon, C. and Jeandel, D. 1981 Approach of non-isotropic turbulence submitted to mean velocity gradients, Proc. Third Symposium on Turbulent Shear Flows, Davis, California, p 17.7.

Choi, K-S 1983 A study of the return to isotropy of homogeneous turbulence, Ph.D. Thesis, Cornell University, Ithaca, New York

Clark, R.A., Ferziger, J.H. and Reynolds, W.C. 1979 Evaluation of subgrid-scale models using an accurately simulated turbulent flow, J. Fluid Mech. **91**, p 1.

Comte-Bellot, G. and Corrsin, S. 1966 The use of a contraction to improve the isotropy of grid generated turbulence, J. Fluid Mech **25**, p81.

Gence, J.N. and Mathieu, J. 1980 The return to isotropy of turbulence having been submitted to two successive plane strains, J. Fluid Mech. **101**, p555.

Lee, M.J., Piomelli, U., and Reynolds,W.C. 1986 Useful formulas in the rapid distortion theory of homogeneous turbulence, Phys. Fluids **29**, p3471.

Lee, M.J. and Reynolds, W.C. 1985 Numerical experiments on the structure of homogeneous turbulence, Report TF-24, Department of Mechancial Engineering, Stanford University.

Le Penven, L. and Gence, J.N 1983 Une methods de construction systematique de la relation de fermeture liant la partie lineaire de la correlation pression-deformation au tensor de Reynolds dans une turbulence homogene soumise a une deformation uniforme, C.R. Acad Sc., Paris t. 297, Serie II, p 309.

Lowery, P.S and Reynolds, W.C. 1986 Numerical simulation of a spatially-developing, forced, plane mixing layer, Report TF-26, Department of Mechanical Engineering, Stanford University.

Reynolds, W.C. 1976 Computatation of turbulent flows, Ann. Rev. Fluid Mech. **8**, p183.

Reynolds, W.C. 1983 Physical concepts, analytical foundations, and new directions in turbulence modeling and simulation; in Turbulence Models and Their Applications, Publication 56, Editions Eyrolles, Paris, France.

Reynolds, W.C., and Perkins, H.C.1977 , Engineering Thermodynamics, Second Edition, McGraw Hill Book Company, New York.

Rogers, M.M., Moin,P., and Reynolds, W.C. 1986 The structure and modeling of the hydrodynamic and passive scalar fields in homogeneous turbulent shear flow, Report TF-25, Department of Mechanical Engineering, Stanford University.

Savill, A.M. 1987 Recent Developments in Rapid Distortion Theory, Ann. Rev. Fluid Mechanics, **19**, p531.

Shih, T-H and Lumley 1985 Modeling of pressure correlation terms in Reynolds stress and scalar flux equations, Report FDA-85-3, Fluid Dynamics and Aerodynamics Program, Cornell University, Ithaca, New York

Tavoularis, S. and Corrsin, S. 1981 Experiments in nearly homogeneous turbulence with a uniform mean temperature gradient, J. Fluid Mech., **104**, p311 and p349.

Tucker, H.J. and Reynolds, A.J. 1968 The distortion of turbulence by irrotational plane strain, J. Fluid Mechanics, **32**, p657.

Wiegland, R.A. and Nagib, H.M. 1978 Grid generated turbulence with and without rotation about the streamwise direction, IIT Fluid and Heat Transfer Report R78-1, Illinois Inst. of Technology, Chicago, Ill.

Wilcox, D.C. 1986 Multiscale model for turbulent flows, AIAA paper 86-0029; see also User's guide to program EDDYBL, DCW Industries.